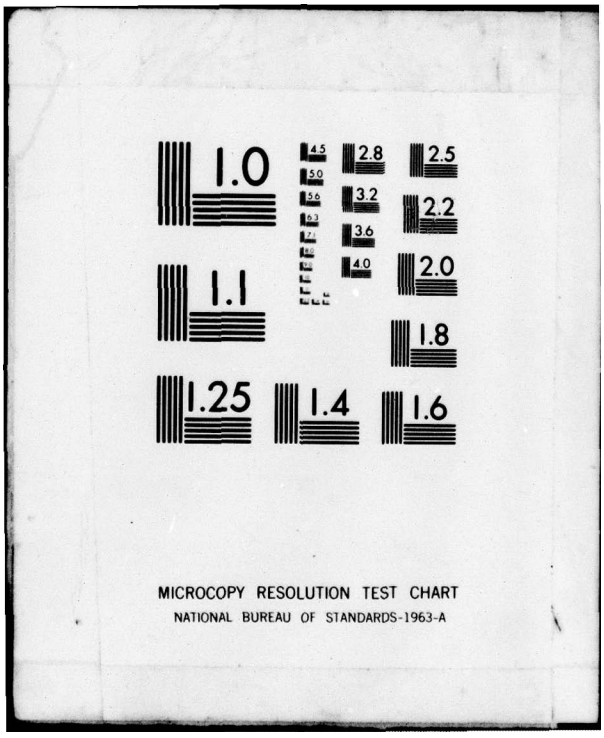
AD-A074 621 SANDIA CORP ALBUQUERQUE N MEX F/G 18/3
DAMAGING AIR SHOCKS AT LARGE DISTANCES FROM EXPLOSIONS.(U)
APR 52 E F COX, H J PLAGGE, J W REED
UNCLASSIFIED AEC-WT-303 NL




1.0
1.1
1.25
1.4
1.6
1.8
2.0
2.2
2.5
2.8
3.2
3.6
4.0
4.5
5.0
5.6
6.3
MICROCOPY RESOLUTION TEST CHART
NATIONAL BUREAU OF STANDARDS-1963-A

AD A074621

DATA PROCESSING SHEET

PHOTOGRAPH THIS SHEET

II
LEVEL

1
INVENTORY

DDC ACCESSION NUMBER
AD A074621

AEC WT-303
DOCUMENT IDENTIFICATION

DISTRIBUTION STATEMENT A
Approved for public release;
Distribution Unlimited
DISTRIBUTION STATEMENT

Accession For
NTIS GRA&I
DDC TAB
Unannounced
Justification
By Per Htr. on file
Distribution/
Availability Codes
Dist. | Avail and/or special
A
DISTRIBUTION STAMP

DDC
RECEIVED
OCT 3 1979
D
DATE ACCESSIONED

79 10 01 125
DATE RECEIVED IN DDC

PHOTOGRAPH THIS SHEET

AND RETURN TO DDA-2

WT - 303

COPY 93

AEC Schedules 'Small' Explosions At Nevada Site

LAS VEGAS, Nev., Aug. 9 (AP) —A new series of small explosions at the Indian Springs Testing Ground will begin after Aug. 15, the Atomic Energy Commission said today.

The commission's statement did not say the blasts would be of atomic origin. Spokesmen refused to elaborate. The statement referred only to "small amounts of high explosives."

Purpose of the explosions is to "obtain detailed data for anticipating atmospheric conditions during test operations," the commission said, "and to study the effect of temperature inversion and upper air winds on blast waves."

Observers recalled that a great cloud of yellow smoke formed over the testing ground following the blasts last February. This was said to be due to temperature inversion, an atmospheric condition which kept the cloud from rising and drifting away. Apparent aim of the new tests is to find a way to avoid setting off major blasts on days when temperature inversion can be expected.

The commission said teams with delicate instruments would be stationed at seven locations as far as 100 miles away in Utah and Nevada to record the effects of the detonations. The teams will be at St. George, Utah, and Las Vegas, Tonopah, Beatty, Indian Springs, Boulder City and Caliente, Nev.

It is "improbable," the commission said, that residents of these towns will feel, see or hear the explosions. Travelers on highways near the site may hear the blasts and see smoke clouds, the commission said.

The commission said the tests would last several months with the recording teams in operation "all winter."

RESTRICTED

DAMAGING AIR SHOCKS AT LARGE DISTANCES FROM EXPLOSIONS

E. F. Cox, Department 5110
H. J. Plagge, Section 5242-3
Capt. J. W. Reed, USAF, Section 5242-3

April 24, 1952

RESTRICTED DATA

This document contains restricted data as defined in the Atomic Energy Act of 1954. Its transmittal or the disclosure of its contents in any manner to an unauthorized person is prohibited.

This material contains information affecting the National Defense of the United States within the meaning of the Espionage Laws, Title 18, U.S.C., Secs. 793 and 794, the transmission or revelation of which in any manner to an unauthorized person is prohibited by law.

This document is the property of Sandia Corporation and is on loan to the recipient. It must be returned to the Sandia Corporation Technical Library upon request or when no longer needed.

SANDIA CORPORATION

SECURITY INFORMATION RESTRICTED

CONTENTS

	Page
Summary	7
Shock Waves Become Sound Waves	8
Where Sound Energy Goes	10
Calculable Conditions	15
Blast Energy Concentration on the Ground	29
Blast Damage and Pressure	31
Ozonosphere Signals	50
Ionosphere E-Layer Signals	58
The Microbarograph	60
Appendix A	67
Appendix B	71

DECLASSIFIED

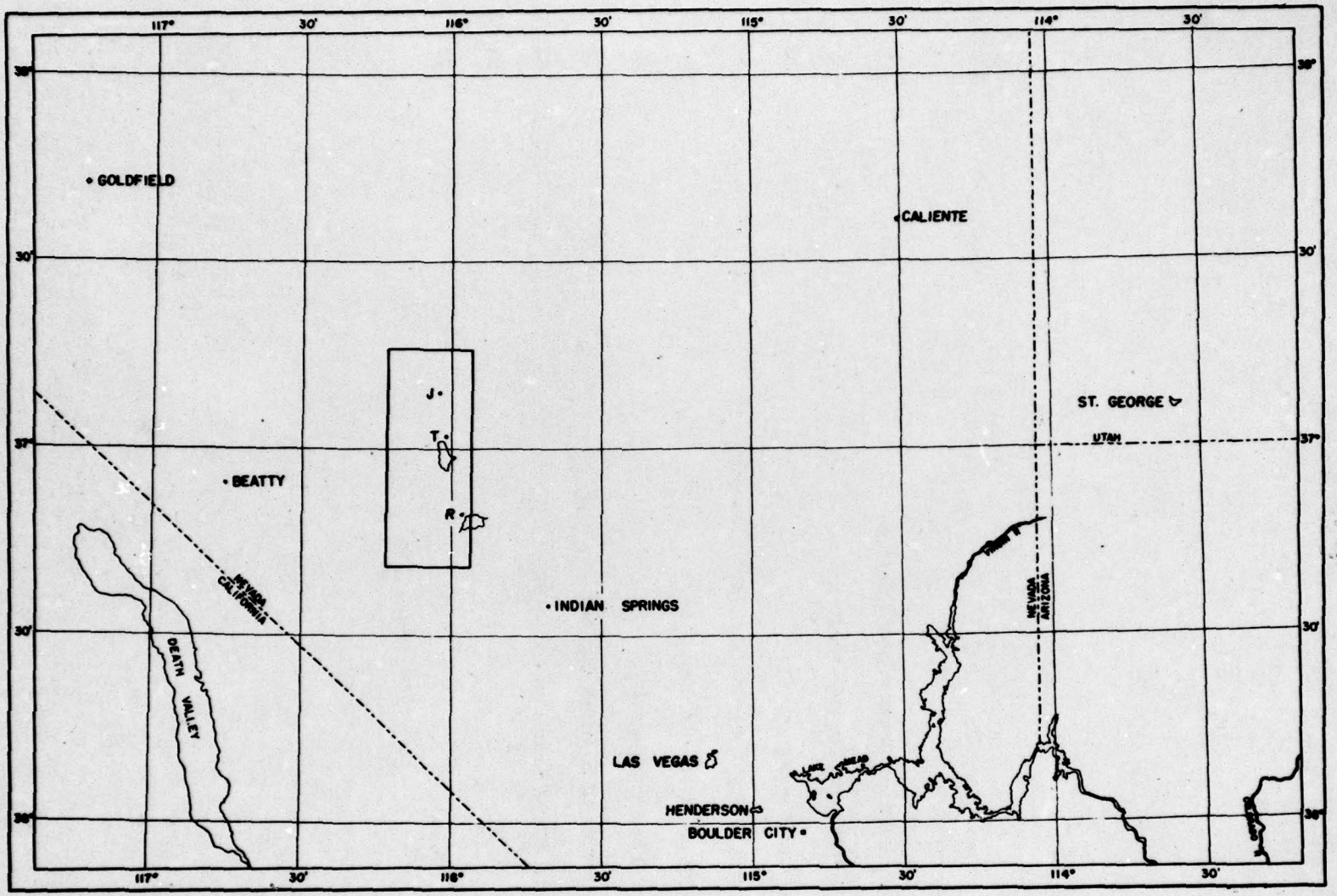


Fig. 1

TABLE I

Distances (miles) and bearings from shot points to microbarograph stations

Station	Code	Shot point T3	Shot area T7	Shot point R	Shot area J
Indian Springs	ISP				
Distance (miles)		37.3	40.0	24.1	44.0
Bearing (degrees)		330° 07'	332° 14'	319° 15'	333° 28'
Beatty	BTY				
Distance (miles)		41.6	42.3	43.7	42.7
Bearing (degrees)		76° 36'	72° 30'	95° 54'	67° 06'
Las Vegas	LSV				
Distance (miles)		76.6	79.1	64.1	82.9
Bearing (degrees)		321° 28'	323° 19'	315° 41'	323° 53'
Goldfield	GLF				
Distance (miles)		80.4	78.6	91.4	75.7
Bearing (degrees)		124° 0'	122° 11'	130° 14'	120° 07'
Henderson	HEN				
Distance (miles)		87.9	90.3	75.6	94.0
Bearing (degrees)		319° 0'	320° 51'	313° 41'	321° 17'
Caliente	CAL				
Distance (miles)		91.3	90.1	95.8	89.5
Bearing (degrees)		245° 13'	247° 01'	236° 52'	249° 34'
Boulder City	BLC				
Distance (miles)		99.1	101.5	86.9	105.1
Bearing (degrees)		318° 14'	320° 05	313° 32'	320° 20'
St. George	SGU				
Distance (miles)		135.1	135.1	133.6	136.1
Bearing (degrees)		268° 55'	269° 54'	262° 49'	271° 46'
Las Vegas (before Oct 1)	LSV				
Distance (miles)		79.3		66.9	85.5
Bearing (degrees)		321° 23'		315° 40'	

UNCLASSIFIED
UNCLASSIFIED
DECLASSIFIED

[redacted]
UNCLASSIFIED

ACKNOWLEDGMENTS

Many persons of the Sandia Laboratory, Los Alamos Scientific Laboratory, and the military services participated to some extent in the experiments reported. It is impossible to say that any one part of the work was more or less important than any other part since final results were an integration of several types of activities.

The authors wish to express their gratitude to Dr. J. C. Clark, Dr. G. L. Felt, Dr. W. E. Ogle, and Mr. B. C. Lyon, Dr. A. C. Graves, and Mr. C. L. Tyler for their encouragement and support during the series of experiments.

For meteorological predictions and data we are indebted to the USAF Air Weather Service. Specifically we wish to thank Lt. Col. E. H. Karstens, who was in charge of AWS operations at the AEC Test Site; Maj. S. A. Bird, Capt. L. E. Worthley, and M/Sgt. R. H. Gordon for the weather predictions supplied to us from Nellis Air Force Base and the AEC Test Site; Dr. G. P. Cressman for wind predictions; and the entire RAOB team for work directed by M/ Sgt. Bruce W. Blount.

Personnel operating the eight microbarograph stations were changed on several occasions during the course of experiments. We wish to thank each of these men for their work, especially when we recall the odd and long hours during which many of the shots were conducted: N. Bolinger, ET/2 M. N. Cavey, A. M. Cobb, M. B. Covington, P. S. Dubroff, J. L. McDaniels, H. B. Moody, T/Sgt. J. W. Samuelson, R. Thompson, ET/1 B. L. Ward, L. Witt, and R. M. Yearout.

The explosive handlers and those in charge of communications and transportation were all located at the AEC Test Site. We acknowledge here the splendid work of SFC H. W. Johnson, M/Sgt. J. R. Green, SFC D. E. Gobble, SFC E. Oeller, SFC J. W. Clay. Mr. N. Bolinger acted as roving repairman for the microbarograph equipment, and had it not been for his tireless efforts in overhauling equipment, the experiment would have ended early.

All the Sandia Laboratory field operations were under the direction of Mr. H. E. Lenander, Manager of the Sandia Laboratory Proving Ground Department (5230), and Mr. R. S. Millican, Supervisor of the Weapon Effects Instrumentation Division (5233). A considerable part of the planning stage was conducted by Mr. L. J. Vortman, Supervisor of the Planning Division (5231). We wish to express special appreciation for the excellent cooperation and work of Mr. R. B. Bunker, Supervisor of the Special Measurements Section (5233-4), who had direct charge of all microbarometric field work.

For analysis of the hundreds of rolls of microbarograph records we greatly appreciate the work of Mrs. Mary J. Andersen. For computing and plotting the many sound ray paths, only a few of which are shown in this report, we thank Mr. A. T. Marrs, Capt. Vernon E. Windell, USAF, and M/Sgt. Gale E. Walton, USAF, of the Meteorological Section of Sandia Laboratory.

UNCLASSIFIED [redacted]

DAMAGING AIR SHOCKS AT LARGE DISTANCES FROM EXPLOSIONS

Summary. -- For determining striking locations of slightly damaging shock pressures from atomic weapon tests, ordinary acoustical laws of refraction and reflection may be employed when distances of interest exceed a few miles. Paths of blast energy propagation are computable from meteorological forecasts or soundings but are limited in accuracy and in altitude by present-day meteorological instruments. Since fundamental wave-lengths of the blast waves 35 to 135 miles from atomic weapon bursts are about 4 kilofeet, energy propagation is affected only trivially by commonplace terrain features, even small ranges of mountains.

Mathematical expressions from which blast-energy striking distances and distributions may be calculated from meteorological predictions are presented for eight simplified situations. A new tabular system for computing sound-ray paths from meteorological observations is derived (Appendix A). These derivations are applied to all Operation Buster and Jangle shots, as well as some TNT shots, to demonstrate benefits and weaknesses of the methods. In general excellent results are achieved in predicting where the blast will strike, but only moderate success has come from our attempts to predict how strong the shock will be on a specific locality and how severe the damage will be. Part of the difficulty stems from the fact that damaging shocks may travel through the ozonosphere, far above heights attainable by present-day meteorological sounding equipment, in their route from source to receiver. Only by comparing measured pressures from a TNT shot fired near intended ground zero shortly prior to an intended atomic weapon shot, with statistical values already obtained and presented in this report, is it possible to estimate locations where ozonosphere-borne shocks may cause damage.

Although there is no evidence that they have ever produced damage, shock signals which traveled part of their paths through the ionosphere E-layer are discussed and demonstrated. Further, an explanation is given for the multiple 'booms' heard at the Control Point on the occasions of the Buster Charlie and Easy Shots.

* * * * * * *

Atomic bombs burst at the Atomic Energy Commission's Nevada Test Site early in February 1951 caused considerable damage in two nearby inhabited areas, Indian Springs (24 miles away) and Las Vegas (66 miles away). Damage consisted mainly of broken windows and cracked plaster. In one instance a door broke its stops, tore loose from its hinges, and landed in the yard.

Costs of repairing these damages were insignificant compared with other costs related to a full-scale test operation. Yet the possibility that some person might be seriously injured by shattering glass made it imperative, or at least highly desirable, that the Test Organization devote serious attention to the situation lest this continental test site be lost to the

Atomic Energy Commission for future operations. Tests can be conducted much more economically at the Nevada Test Site than at the Pacific Proving Grounds; continued use of this continental site is highly desirable from both the logistic and the economic point of view.

In July 1951, at the request of Dr. J. C. Clark, Deputy Test Director for Operations Buster and Jangle, the authors of this report obtained meteorological data from the temporary Control Point at the Nevada Test Site for the dates of February 2 and 6, 1951, when considerable damage was done by the bombs burst in the Frenchman Flat area. On February 6 the shock broke numerous windows at Indian Springs and a few windows in Las Vegas, although residents of Las Vegas reported the noise less intense than that of February 2. Treatment of the problem by simple acoustical methods brought forth good explanations of the happenings on both dates. Acoustical methods therefore looked promising enough for continued use in efforts to protect inhabited locales from air-shock damage during future operations.

Predictions, supplied by the writers to the Test Director prior to each shot of the Buster and Jangle series, albeit they have been more qualitative than quantitative, bear out the original contention that paths of damaging air blast waves can be reasonably well predicted by acoustic means, and inhabited areas in the vicinity of the Nevada Test Site can be protected by delaying shots if necessary until meteorological conditions are favorable.

Shock Waves Become Sound Waves

At some finite distance from an explosion, whatever its size, the shock wave or waves generated by the explosion become sound waves. Until definitions of the terms involved are precise, the distance at which this phenomenon occurs is indeterminable. Sound or acoustic waves are generally understood to be waves involving pressure perturbations which are small compared with the ambient pressure of the medium carrying the perturbations, whereas a shock wave is a wave in which the perturbation pressure is a significant fraction, proper or improper, of the ambient pressure. Until the words 'small' and 'significant' are numerically defined, it will be impossible to state when one is dealing with a shock wave or with a sound wave.

Another characteristic sometimes used to differentiate between shock waves and sound waves is the rise time of the first pressure perturbation. For a sound wave of repetitive frequency ν, the rise time of pressure from ambient to peak value would be $1/4\nu$. On the other hand, a shock wave is often considered as essentially an abrupt discontinuity in pressure and has a rise time of the order of microseconds or a fraction of a microsecond.

Theoretical studies[1] have attempted to determine the thickness of a shock front, and these studies agree on at least two points:

The computed thickness of a shock front should not be less than one molecular mean free path; shock fronts are less abrupt for weak shocks than for strong ones.

Becker's formula for the thickness, $\mathcal{E}$, of a shock front (Equation 36a in Becker's paper[1]), reduced to a simple form applicable for very weak shocks traveling through air at standard atmospheric pressure, becomes

$$\mathcal{E} = \frac{3.5 \times 10^{-5}}{\Delta} \text{ cm}, \qquad (1)$$

where Δ is the perturbation pressure expressed in bars*. Thus the thickness of a shock front related to a shock wave having a pressure rise of one millibar would be 0.35 mm, equivalent to the rise distance of an ultrasonic wave having a frequency of 237 kilocycles per second. It would appear therefore that increasing finite thickness of a shock front as the shock pressure level decreases is not alone sufficient to explain transformation of the shock wave into an acoustic wave.

E. E. Stokes[2] pointed out that for spherical waves in which the entire disturbance is contained in an expanding shell of constant thickness, the wave form must eventually become balanced with respect to rarefaction and condensation even though initially the entire disturbance was compression. Conservation of energy requires that the wave amplitude diminish inversely as the radial distance from the source. However, since the volume of the shell increases as the square of the radius, the wave form can not continue to consist of condensation alone; this would violate the conservation of matter as regards the excess mass of air in the condensation wave. A rarefaction wave must be formed in the process of propagation of a condensation wave to furnish the material required to maintain a condensation wave at the level imposed by the energy in the wave. This phenomenon appears to give rise to an N-shaped wave† which, from the numerical values shown in Fig. 2 of the paper by DuMond et al, shows more promise of explaining the presence of the frequencies found in the current series of measurements than does the theory of a finite shock front. The whole phenomenon of decay of a shock wave into an acoustic wave requires future investigation.

As the next section of this report will show, the speeds of sound waves are all-important in governing where they go, and it would seem reasonable to presume that similar, although more complex physical laws would apply to shock waves, especially weak ones. The speed, σ, of a shock in air, derived from the Rankine-Hugoniot relations, relates to the speed of the sound, c, and to the ratio, β, of the perturbation pressure, p, to the ambient pressure, P ($\beta \equiv p/P$), according to the equation

$$\sigma = c\,(1 + 0.857\,\beta)^{1/2}. \qquad (2)$$

For small overpressures this becomes

$$\sigma = c\,(1 + 0.428\,\beta). \qquad (3)$$

Thus a shock of one psi (1/15 atmosphere) travels only three per cent faster than sound, and ordinary laws of acoustics must be applicable without much modification to such shocks and to weaker ones.

---

*In this report the term 'bar' denotes a pressure of 10^6 dynes/cm^2. Standard atmospheric pressure is 1.013 bars. One millibar is 1000 dynes/cm^2 and is equal to 2.12 pounds per square foot. One microbar is 1 dyne/cm^2. One microbar is an exceedingly small unit when related to tactile sense datum since it amounts to only 0.3 ounce per square yard; yet acoustically a pressure of one microbar is relatively large and amounts to a sound pressure level of 42 decibels over the commonly accepted threshold of hearing, 0.0002 microbar.

†So far as the authors can find, the earliest report on an N-shaped wave is that of L. D. Landau in a paper briefly abstracted in J. Phys. Acad. Sci., USSR, 6, 229 (1942). It is further discussed by J. W. M. DuMond et al in J. Acoust. Soc. Amer., 18, 97 (1946), and by Courant and Friedrichs in Supersonic Flow and Shock Waves, Section 75, Interscience Publications, Inc., New York, 1948. See also Merritt, M. L., Some Measurements of Terrain Effects on Blast Waves, WT-301, February 12, 1952.

Where Sound Energy Goes

Sound waves have long been known to follow familiar physical laws of reflection, refraction, and diffraction. As far as the present problem is concerned, perturbation pressures required to do significant damage are so large that diffraction can be neglected.

In one sense reflection of waves is of great importance; in another sense it is unimportant for this problem. Reflection of significant amounts of sound energy can occur only when the sound-wave front strikes a boundary separating two media wherein densities and sound velocities are radically different. The air-to-earth transition is therefore an almost perfect reflector. Further, since this study deals with waves whose periods are usually between 0.2 and 5 seconds, wave lengths in air lie between 0.06 and 1.6 kilometers; hence only very high hills are likely to interfere with essentially specular reflection.

On the other hand, insignificant reflection would result from clouds or other meteorological discontinuities above the earth. Lord Rayleigh[3] gives two examples of interest here:

> "Sound is traveling in air at 0°C and strikes an abrupt "boundary" beyond which the medium is air at T°C. For normal incidence, the reflected intensity of sound is only $8.3 \times 10^{-7} \times T^2$ times the incident intensity.
>
> "For the case of a sound wave traveling in dry air at 10°C, and striking normally a boundary separating this dry air from air at the same temperature but saturated with moisture, the reflected sound intensity would be only 1/ 774,000 times as strong as the incident sound."

In the foregoing examples by Rayleigh transitions between the two media have been abrupt and not at all like those found in nature, which are usually quite gradual. It is apparent therefore that amounts of energy significant to this problem can not be reflected from natural meteorological transitions.

Having thus dispensed with both diffraction and reflection, only refraction (bending) of sound rays is left to explain damaging concentrations of blast energy at large distances.

Sound-ray paths through media wherein sound velocity is a variable obey Fermat's principle of least time,

$$\int \frac{ds}{V} \text{ must be minimal.} \tag{4}$$

Here ds is an increment of path length and V is sound velocity along increment ds. A less general but usually more applicable form of Fermat's principle is Snell's law, which states that for a stationary medium having parallel boundary layers,

$$c \sec \Theta = \text{an invariant along any ray path.} \tag{5}$$

Here c is the speed of the sound and Θ is the angle, in the plane formed by the ray and the boundary normal, between the ray and the boundary surface.

Sound speed in a nonmoving gas according to Laplace's equation is

$$c = (\gamma P/\rho)^{1/2} = (\gamma R K / M)^{1/2} \tag{6}$$

where R is the gas constant, γ is the ratio of specific heats of the gas, M is its molecular weight, and P, ρ, and K are, respectively, ambient gas pressure, density, and absolute temperature. For dry air this becomes

$$c = 20.068\ (273 + T^{o})^{1/2}\ \text{meter/sec}, \tag{7}$$

or

$$c = 64.839\ (273 + T^{o})^{1/2}\ \text{ft/sec}, \tag{8}$$

where T is expressed in degrees Centigrade in both instances. The above formulas may be corrected for humidity by using 'virtual temperature' since by definition the virtual temperature of a parcel of air is that temperature of dry air necessary for its density be the same as that of moist air under the same pressure.*

Studies of sound propagation through the natural atmosphere can not afford, in general, to ignore motion of the conducting medium, ie, wind. A quotation from Rayleigh[4] is appropriate. "From Fermat's law of least time, it follows that the course of a ray in a moving, but otherwise, homogeneous medium, is the same as it would be in a medium, of which all parts are at rest, if the velocity of propagation be increased at every point between by the component of the wind-velocity in the direction of the ray. If the wind be horizontal and does not vary in the same horizontal plane, the course of a ray, whose direction is everywhere but slightly inclined to that of the wind, may be calculated on the same principle as that applied... to the case of a variable temperature, the normal velocity of propagation at any point being increased, or diminished, by the local wind-velocity according as the motion of the sound is to leeward or to windward."

For atmospheres having only horizontal winds an accurate statement of Snell's law is

$$c \sec \Theta + u = A, \tag{9}$$

where Θ is the inclination of the sound ray from the horizontal; u is the component of wind velocity in the direction under consideration; and A, invariant for any selected sound ray, is the velocity of the intersection of the wave front with the horizontal. For the small angles involved in sound paths through the atmosphere,

$$\sec \Theta = 1 + \frac{\Theta^2}{2}. \tag{10}$$

Substituting this expansion for sec Θ into equation 9 gives

$$\Theta^2 = \frac{2\,[A - (c + u)]}{c} = \frac{2\,[A - V]}{c}. \quad (\text{Note: } V \equiv c + u) \tag{11}$$

Wind velocity seldom exceeds ten per cent of sound velocity at any troposphere altitude. According to equation 9, A must be nearly the same size as c and equation 9 can be rewritten thus:

$$c + u \cos \Theta = A \cos \Theta \approx c + u = V. \tag{12}$$

---

*Present work in the dry Nevada desert has certainly not required corrections related only to high values of relative humidity.

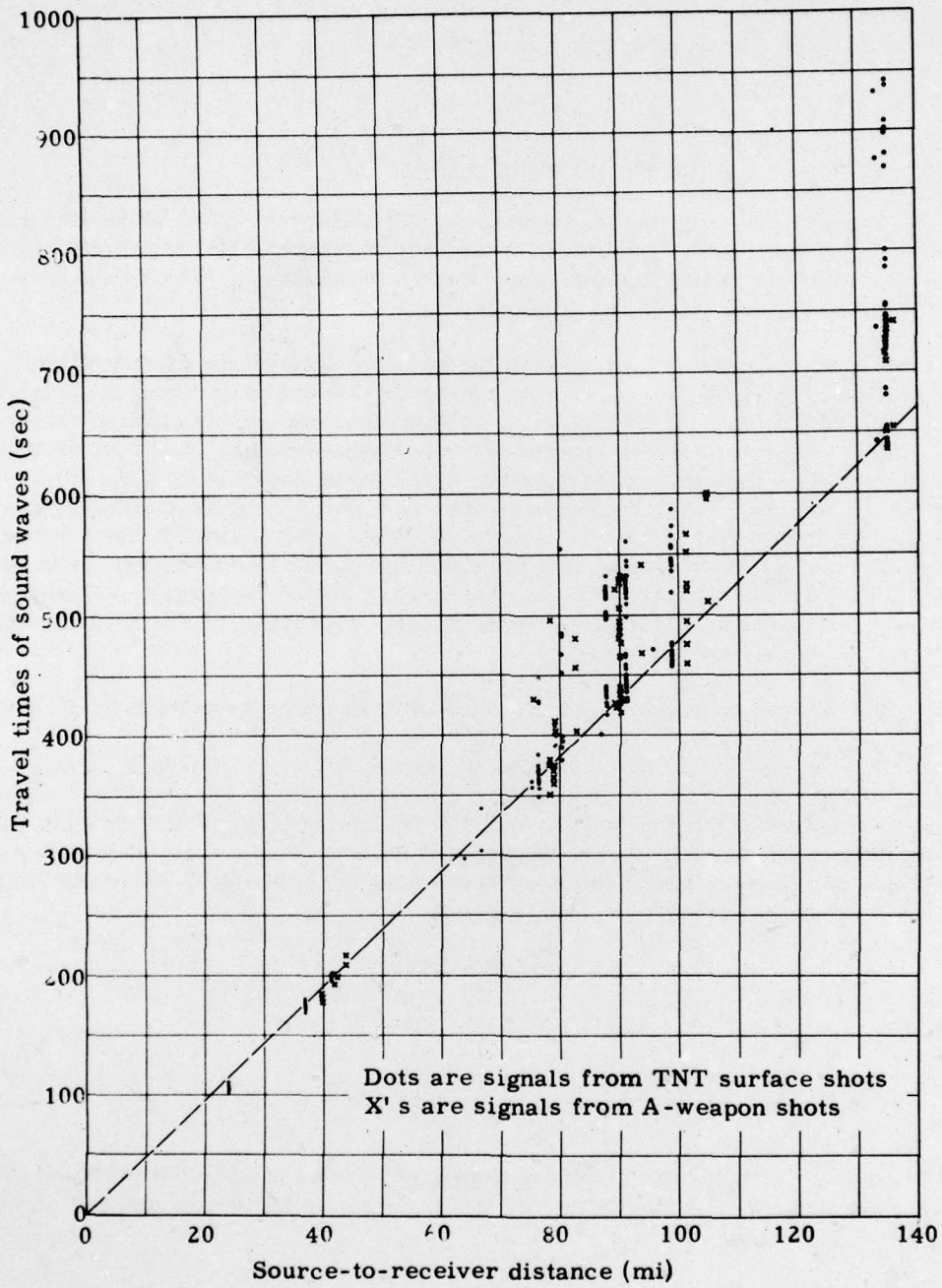

1000
900
800
700
600
500
400
300
200
100
0
Travel times of sound waves (sec)
0
20
40
60
80
100
120
140
Source-to-receiver distance (mi)
Dots are signals from TNT surface shots
X's are signals from A-weapon shots

Fig. 2

An approximate expression for Snell's law is therefore

$$V \sec \Theta = A, \tag{13}$$

which is the simple form recommended by Rayleigh[4].

A relatively complete treatment of the problem of tracing sound rays in its most general three-dimensional aspect was prepared by Fujiwhara[5] in an attempt to explain observations of explosive sounds from eruptions of the volcano Asama in central Japan between 1909 and 1913. He made the assumptions that only air temperature and wind affect the velocity of sound and that air temperature and wind vary only with height. The problem becomes almost hopelessly complex if it is attempted also to introduce any horizontal changes of temperature or wind vectors.

The present work, making use of the same assumptions as did Fujiwhara, employs so far as possible the 'refraction law' (equations 11 or 13). To apply this law to atmospheric transmission, temperature as a function of altitude must be known to determine c, and wind vector velocities must be known to determine u in the different directions of interest. Meteorological observations (RAOB) are used to obtain data having as much accuracy as these soundings are able to give.

Meteorological balloons have a very finite ceiling. So far as is known, no meteorological balloon has ever supplied data from an altitude exceeding 130 kilofeet. Radiosonde observations (RAOB) made by the Air Weather Service of the U.S. Air Force operating at the AEC Control Point were generally successful in obtaining data up to 40 or 50 kilofeet. During the present series of experiments all sound signals returned to earth by refraction within the troposphere were bent back from altitudes of less than 25 kilofeet. For tropospheric refraction studies, it is unnecessary to obtain meteorological data at altitudes greater than 30 kilofeet except in rare instances.

Sounds can be refracted to earth only from atmospheric layers wherein the velocity of sound exceeds that at earth level. It is also a requirement for a sound wave returning to earth from a particular layer that the velocity within that layer exceed the velocity within any layer between it and the earth. If one observes sounds which are returned to the earth and are not explicable in terms of known meteorological data of the troposphere, and if the time taken for these sounds to reach a point on the earth is far greater than that which would be required for a sound signal to travel directly between the source and the receiver, then these signals must be assumed to have been refracted to earth by atmospheric layers, exterior to the tropopause, wherein sound velocity exceeds measured values within the troposphere.

Sound waves which have remained within the troposphere during their entire route from emitter to receiver are readily distinguished by their transit times. Table I and Fig. 1 show locations and distances of eight microbarograph stations with respect to several shot points within the AEC Restricted Area. During the series of shots reported here each microbarograph satisfactorily recorded a number of signals, ie, very distinct signals against low background noises. Indian Springs (approximately 35 miles away) and St. George (approximately 135 miles away) obtained the largest numbers of excellent records, while Beatty (approximately 42 miles away) obtained the fewest. Figure 2 relates travel times of the sound waves with distances between blast points and microbarograph stations. The heavy dashed line that connects the data points representing average minimum travel time to each station represents a sound speed of 1,103 fps; this line passes through the origin of coordinates. Since this typical speed relates directly by equation 8 to a temperature of 12.5°C, which is about average for the low troposphere in Nevada for September-November, we conclude that any

signal arriving within a few (<20) seconds of the time predicted by this dashed line has traveled entirely within the troposphere. Signals arriving later, data points well above the dashed line, came back to earth from strata above the tropopause. These signals will be discussed in later sections entitled Ozonosphere Signals and Ionosphere Signals.

Calculable Conditions

Every large airport and Air Force base employs a forecaster who will upon request supply a prediction of temperature versus altitude and vector wind velocities versus altitude for a stated location and hour. His forecasts may be good or bad representations of atmospheric conditions, as verified by RAOB. In general a forecast made more than six hours in advance can hardly be considered an accurate enough representation of conditions as they will exist over a specified area at a specified time to warrant elaborate calculations of a number of sound ray paths. So that paths and concentrations of blast energy might be predicted by quick methods compatible with the accuracies of forecasts made more than three hours in advance of a shot, several simple cases have been derived, and for each a graph is drawn depicting sound speed c on the X-axis versus altitude h on the Y-axis. At each altitude for which the vector wind is predicted by the forecaster the component of wind velocity in each direction of interest is added algebraically to the c curve. Thus a graph showing sound speed ($V \equiv c + u$) versus altitude h is obtained for each direction of interest.* Each graph is then approximated by one of the following cases, given in order of increasing complexity.

Case 1 - Explosion on the Ground. -- The simplest possible case is when the sound velocity, V_0, at the earth's surface is larger than V at any higher altitude (Fig. 3). This situation can exist only when the initial gradient of V next to the ground is negative. From an explosion on the ground all sound rays starting in the direction under consideration are bent upward initially, and since $V_h < V_0$ for all altitudes h, no positive gradient succeeds in bending any ray completely back to the horizontal.

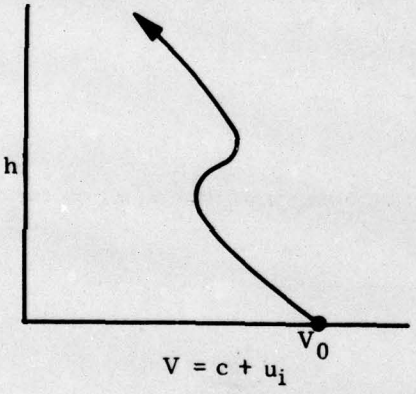


Fig. 3

If $V_h = V_0$ at some altitude h, the ray whose initial angle with the ground is zero degrees is just bent back to horizontal. Theoretically this one ray travels up and down between earth and the atmospheric layer in which $V_h = V_0$, but since a single ray carries no energy, the case is trivial.

It is concluded therefore that for a case like this one, no sound energy is bent back to earth in the direction of interest.

---

*For the work at the Nevada Test Site the wind vectors were resolved to an azimuth of 45° (northeast) in the general direction of Caliente; to an azimuth of 135° (southeast) in the general direction of Indian Springs, Las Vegas, Henderson, and Boulder City; to an azimuth of 250° in the direction of Beatty; and to an azimuth of 315° (northwest) in the general direction of Goldfield. Sometimes an azimuth of 90° (east) in the direction of St. George, and sometimes an azimuth of 180° in the general direction of the Control Point and Camp 3 were considered.

Case 2 - Explosion on the Ground. -- The case illustrated in Fig. 4 has a constant positive gradient up to altitude h_1, at which height $V = V_1$. Above h_1, $V_h \leq V_1$ so that no sound energy is refracted back to earth from altitudes $h > h_1$.

In traversing a vertical increment dh a sound ray making an angle Θ with the horizontal goes forward an incremental horizontal distance which is equal to $\cot \Theta \cdot dh$. When it reaches the top or apex of its path, where $\Theta = 0^o$ since the ray is horizontal at its top, it has gone forward a distance

$$x = \int_{\Theta = \Theta_0}^{\Theta = 0^o} \cot \Theta \cdot dh, \qquad (14)$$

where Θ_0 is the starting angle of the ray.

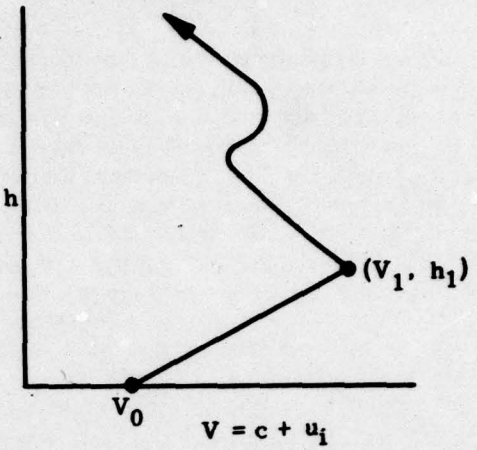


Fig. 4

The basic assumption has been to the effect that V, hence Θ, changes with altitude only and not with horizontal distance. Every sound ray path is therefore symmetrical about its apex and reaches earth at a distance R from the source given by

$$R = 2 \int_{\Theta = \Theta_0}^{\Theta = 0^o} \cot \Theta \cdot dh. \qquad (15)$$

Integration can be performed by relating Θ to h using a combination of the equation for the positive gradient section of Fig. 4,

$$V = V_0 + \left(\frac{V_1 - V_0}{h_1} \right) h, \qquad (16)$$

and equation 13 ($V \sec \Theta = V_0 \sec \Theta_0$).

Hence

$$dh = \frac{-h_1 V_0 \sin \Theta \cdot d\Theta}{(V_1 - V_0) \cos \Theta_0}, \qquad (17)$$

and

$$R = \frac{2 h_1 V_0 \tan \Theta_0}{V_1 - V_0} \approx \frac{2 h_1 V_0 \Theta_0}{V_1 - V_0}. \qquad (18)$$

Thus a ray leaving the source at 0^o lands immediately; the higher the starting angle, Θ_0, the farther away the ray lands.* The limit is reached by the ray whose starting angle permits the ray to become horizontal ($\Theta = 0^o$) at altitude h_1 where $V = V_1$. From equation 13

$$(\Theta_0)_{\text{limit}} = \text{arc cos} \frac{V_0}{V_1}, \qquad (19)$$

*Equation 18 shows that for small angles ($\tan \Theta_0 \approx \sin \Theta_0$) ray paths are segments of circles all having the same radius of curvature, $h_1 V_0 / (V_1 - V_0)$. Accurately the radius of curvature is $hV_0 \sec \Theta / (V_1 - V_0)$, which is minimum when the ray is horizontal.

hence

$$R_{max} = \frac{2\,h_1 V_0}{V_1 - V_0} \cdot \frac{(V_1^2 - V_0^2)^{1/2}}{V_0}$$

$$= 2\,h_1 \sqrt{\frac{V_1 + V_0}{V_1 - V_0}}\,. \qquad (20)$$

The blast energy dumped to the ground between $R_{min} = 0$ and R_{max} was initially contained within the angle between 0^o and arc cos (V_0/V_1). For a series of experiments all using the same weight of explosives fired at the same point, arc cos (V_0/V_1) then gives a rough measure of the amount of energy being returned to the earth.

Each locale in this direction of interest has impinging on it an infinite number of sound rays since each ray reflects from the ground and repeats its path over and over again (Fig. 5).

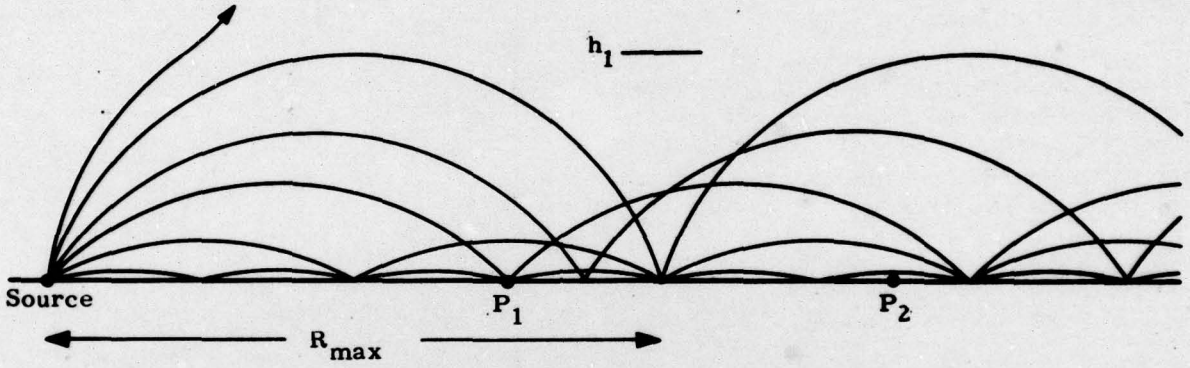


Fig. 5

To a close approximation, consistent with Rayleigh's expression of Snell's law as given in equation 13, sounds traveling from the source to any point via all ray paths reach the point at the same time. Over any path the transit time

$$\tau = 2 \int_{\Theta = \Theta_0}^{\Theta = 0} \frac{dh}{(c + u \cos \Theta) \sin \Theta} \approx 2 \int_{\Theta = \Theta_0}^{\Theta = 0} \frac{dh}{V \cdot \sin \Theta}\,. \qquad (21)$$

Following substitution from equations 13 and 17 this integral becomes

$$\tau = \frac{2\,h_1 \Theta_0}{V_1 - V_0} \qquad (22)$$

as a first-power expansion in Θ_0. In combination with equation 18, this says that

$$\tau = \frac{R}{V_1}, \qquad (23)$$

independent of the path.

Actually travel times are not quite independent of ray paths. The general situation is complicated, but for constant winds, ie, u independent of h, treatment of the problem by use of the accurate expression (equation 9) leads to

$$\tau = \frac{R \sec \Theta_0}{A} = \frac{R}{c_0 + u_0 \cos \Theta_0} . \tag{24}$$

If no wind is blowing, transit times are completely independent of path. If winds are present, ie, $u_0 \neq 0$, the higher apex paths require longer travel times if the wind is in the direction of interest and shorter times if the wind is against the direction of interest. Thus for this case a single sound pulse, which can travel from source to receiver via an infinite number of paths all requiring slightly different travel times, will usually be heard as a rumble.

Case 3 - Explosion on the Ground. -- The situation shown in Fig. 6 leads to a skip distance or region of silence near the source and a 'focus' of energy out beyond the region of silence.

All sound rays leaving the source in this direction of interest are initially bent upward; since $V_2 > V_0$, some of them are returned to earth. Again by the original assumption, paths are symmetrical about their apexes, and landing distances are given by

$$R = 2 \int_{\substack{h = h_1 \\ h = 0}} \cot \Theta \cdot dh + 2 \int_{\substack{h_2 \geq h \geq h_p \\ h = h_1}} \cot \Theta \cdot dh. \tag{25}$$

Here h_p is the altitude at which $V = V_0$.

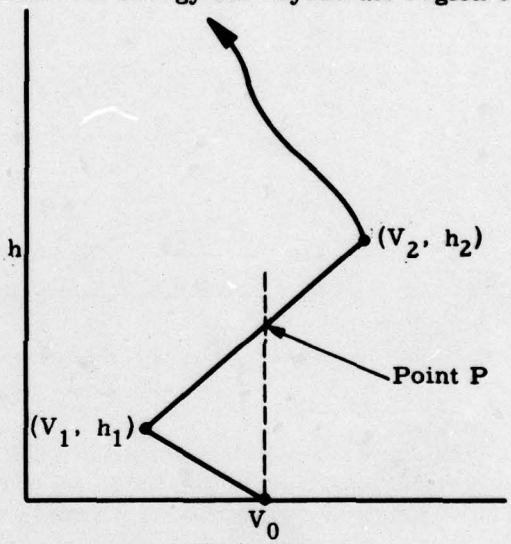


Fig. 6

The two rays which bound the 'focus' on the ground are of particular interest. However, to learn which two rays form the boundaries of the noise zone it is necessary to calculate two angles or three landing distances and compare the two angles or the three landing distances to determine which are truly the maximum and minimum landing distances.

One ray of possible interest is that which leaves the source at grazing incidence with the ground. It travels only as high as h_p. Its landing distance, which is determined from equation 25, is

$$R_1 = 2 \left[\frac{h_1}{V_0 - V_1} + \frac{h_2 - h_1}{V_2 - V_1} \right] \sqrt{(V_0 - V_1)(V_0 + V_1)}. \tag{26}$$

The second ray of interest is that which has its apex at altitude h_2. Its landing distance is

$$R_2 = 2 \left\{ \left[\frac{h_1}{V_0 - V_1} + \frac{h_2 - h_1}{V_2 - V_1} \right] \sqrt{(V_2 - V_1)(V_2 + V_1)} - \frac{h_1}{V_0 - V_1} \sqrt{(V_2 - V_0)(V_2 + V_0)} \right\}. \tag{27}$$

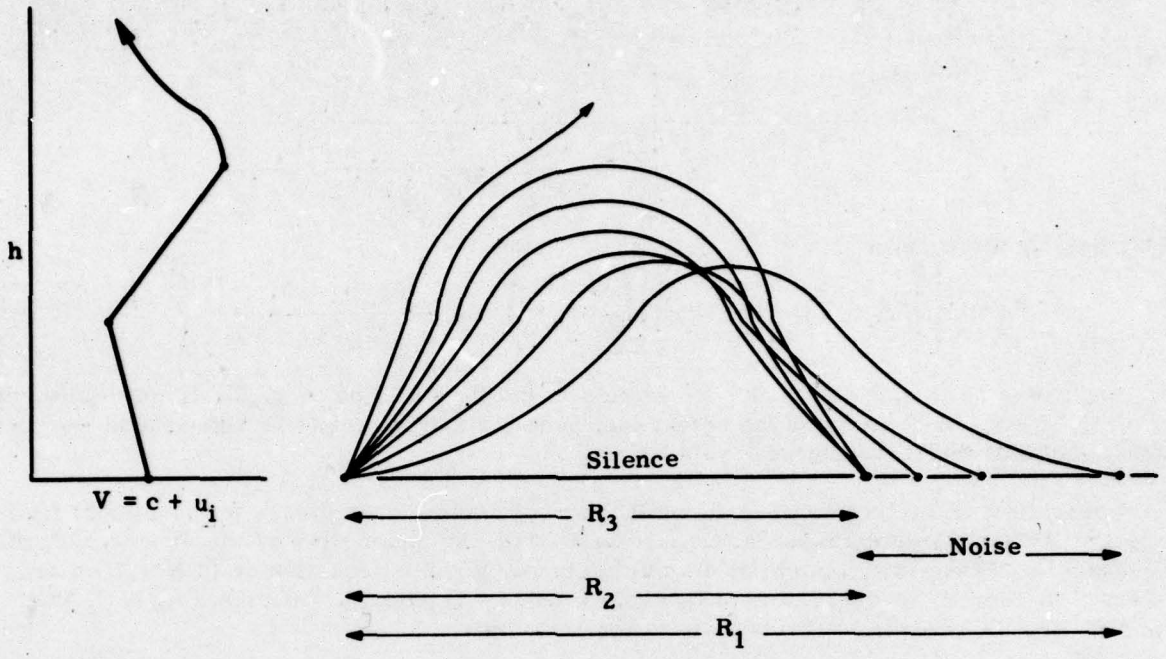


Fig. 7a

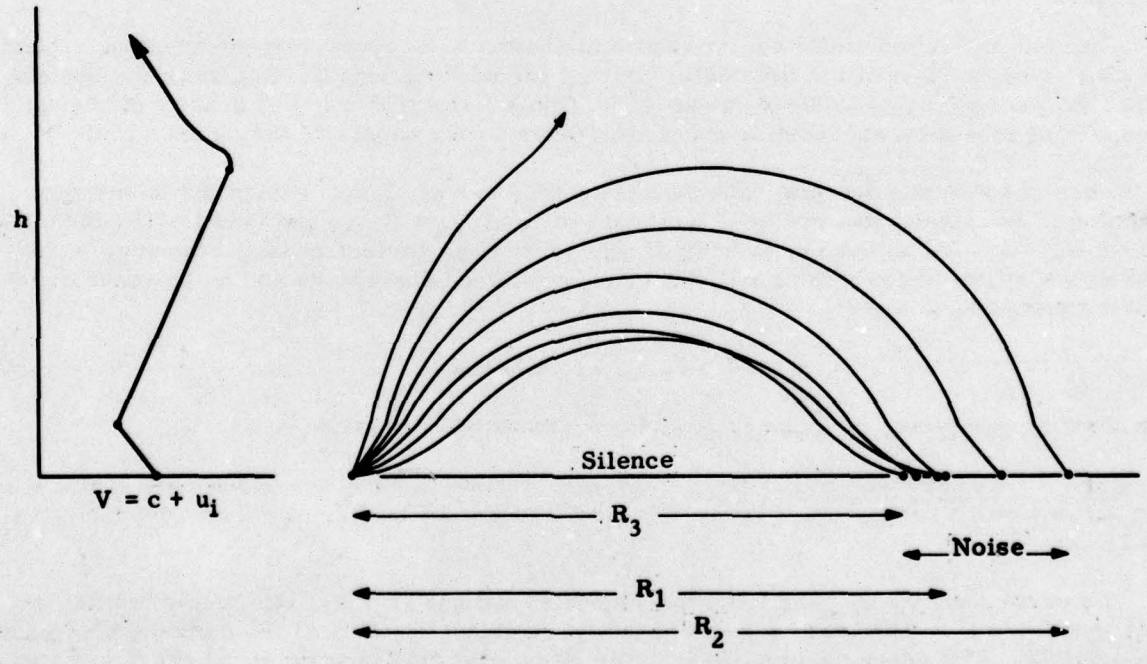


Fig. 7b

Interest in a third ray originates from the fact that equation 25 has a minimum value which can be determined by setting the derivative, $dR/d\Theta_0$, equal to zero. The initial inclination of this ray is

$$(\Theta_0)_{min} = \tan^{-1} \frac{h_1}{V_0 (V_0 - V_1)} \left[\frac{(V_0 + V_1)(V_0 - V_1)}{\left(\frac{h_2 - h_1}{V_2 - V_1}\right)^2 + \frac{2h_1 (h_2 - h_1)}{(V_0 - V_1)(V_2 - V_1)}} \right]^{1/2}, \quad (28)$$

and its landing distance is

$$R_3 = 2 \left\{ \left[(V_0 + V_1)(V_0 - V_1) \right] \left[\left(\frac{h_2 - h_1}{V_2 - V_1}\right)^2 + \frac{2h_1 (h_2 - h_1)}{(V_0 - V_1)(V_2 - V_1)} \right] \right\}^{1/2}. \quad (29)$$

Depending on the gradients and the extents of the V vs h lines (Fig. 6), R_1 or R_2 may be maximum, and R_2 or R_3 may be the actual minimum. Figures 7a and 7b show sound ray plots of both cases and their associated V vs h graphs.

Uncertainty in stating whether R_2 or R_3 is a minimum, even though the functional form of equation 25 has a minimum value, is associated with the upper limit of the second integral in equation 25. If the initial angle of the minimum ray given by equation 28 is less than arc cos (V_0/V_2), then R_3 is the minimum landing distance. If $(\Theta_0)_{min} >$ arc cos (V_0/V_2), then R_1 and R_2 are the bounding rays, and R_1 is the maximum.

A listener standing in the zone of silence hears nothing. In the first zone of noise, however, the shock may be very intense and damaging. All of the blast starting from the source within the angle between 0^o and arc cos (V_0/V_2) swats between R_{min} and R_{max}. If this distance $(R_{max} - R_{min})$ is small, the focus is sharp and the punch may be severe.

After one reflection sound rays repeat their paths. The radial dimension of the second noise zone is double that of the first, etc. Except for wind squeezing, tangential dimensions of zones expand cylindrically about the source. Consequently the surface density of energy at corresponding locations within noise zones decreases as the square of the number of the zone.

Zones of noise can overlap, thus canceling all zones of silence except the innermost. A situation of the type shown in Fig. 7 can exist with $2R_{min} \leq R_{max}$ and thus destroy the second region of silence. In the band of overlap of noise zones the surface density of energy is the sum of contributions from both zones. The zone of silence disappears and noise zones overlap for all distances D where

$$D \geq n R_{max} \geq (n + 1) R_{min}, \quad (30)$$

and n is an integer giving the number of silent zones which will exist.

Case 4 - Explosion on the Ground. -- Figure 8 shows a condition which combines a long sound pattern with a focus. Rays trapped beneath altitude h_1 behave exactly as described in Case 2.

The particular ray starting from the source at arc cos (V_1/V_0) effectively 'splits' on reaching altitude h_1. The lower section of this ray returns to earth at the distance prescribed by equation 20. The upper section has its apex at the elevation of point P, where $V = V_1$.

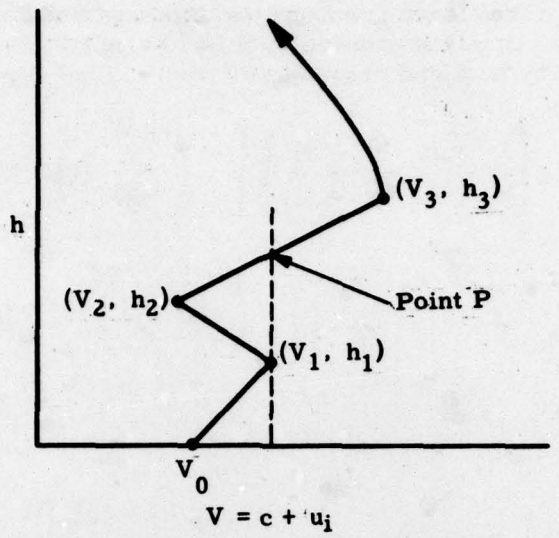


Fig. 8

Focused energy returns to earth from the layer between h_p and h_3 and as in the solution to Case 3, three distances need be computed* to determine boundaries of the focus. The ray whose apex is at altitude h_p lands at a distance

$$R_1 = 2\left\{ h_1\sqrt{\frac{V_1 + V_0}{V_1 - V_0}} + \left[\frac{h_2 - h_1}{V_1 - V_2} + \frac{h_3 - h_2}{V_3 - V_2}\right] \sqrt{(V_1 - V_2)(V_1 + V_2)} \right\} \tag{31}$$

The ray having its apex at altitude h_3 lands at

$$R_2 = 2\left\{ \frac{h_1}{V_1 - V_0}\left[\sqrt{(V_3 - V_0)(V_3 + V_0)} - \sqrt{(V_3 - V_1)(V_3 + V_1)}\right] + \right.$$
$$\frac{h_2 - h_1}{V_1 - V_2}\left[\sqrt{(V_3 - V_2)(V_3 + V_2)} - \sqrt{(V_3 - V_1)(V_3 + V_1)}\right] +$$
$$\left. \frac{h_3 - h_2}{V_3 - V_2}\sqrt{(V_3 - V_2)(V_3 + V_2)} \right\} . \tag{32}$$

---

*The reader may have noticed that many terms in the equations used for computing ray landing distances are of identical form,

$$(V_\alpha \cdot V_\beta)^{1/2} \cdot V_\gamma^{-1} \cdot H \cdot 2$$

where H is a difference in heights, V_α and V_γ are differences in velocities, and V_β is a sum of velocities. In Case 2, equation 20 has only one such term, and in that instance V_α and V_γ are equal. In Case 3, equation 26 has two such terms, and equation 27 has three. Since only multiplication, division, and square roots are involved in the term form, the A, B, C, and D scales of a simple slide rule easily give term values which are then added algebraically as indicated in the equations.

UNCLASSIFIED
RESTRICTED

Unfortunately the ground incidence angle establishing minimum landing distance of the focused energy can not be simply expressed as it was by equation 28 for Case 3. It can, however, be established by trial and error substitution in the following equation:

$$\frac{h_1}{V_1 - V_0} - \left[\frac{h_1}{V_1 - V_0} + \frac{h_2 - h_1}{V_1 - V_2}\right]\left[1 - \left(\frac{V_1^2}{V_0^2} - 1\right)\cot^2 (\Theta_0)_{min}\right]^{-1/2} +$$

$$\left[\frac{h_2 - h_1}{V_1 - V_2} + \frac{h_3 - h_2}{V_3 - V_2}\right]\left[1 - \left(\frac{V_2^2}{V_0^2} - 1\right)\cot^2 (\Theta_0)_{min}\right]^{-1/2} = 0. \qquad (33)$$

If this value of $(\Theta_0)_{min} >$ arc cos (V_0/ V_3), equations 31 and 32 give landing distances of the boundary rays of focused energy. If $(\Theta_0)_{min} <$ arc cos (V_0/ V_3), the focused energy is bounded between R_1 as determined from equation 31, and

$$R_3 = 2 V_0 \left\{\frac{h_1}{V_1 - V_0} \tan (\Theta_0)_{min} - \left[\frac{h_1}{V_1 - V_0} + \frac{h_2 - h_1}{V_1 - V_2}\right]\left[\sec^2 (\Theta_0)_{min} - \frac{V_1^2}{V_0^2}\right]^{1/2} +\right.$$

$$\left.\left[\frac{h_2 - h_1}{V_1 - V_2} + \frac{h_3 - h_2}{V_3 - V_2}\right]\left[\sec^2 (\Theta_0)_{min} - \frac{V_2^2}{V_0^2}\right]^{1/2}\right\}. \qquad (34)$$

Focused energy is contained within the initial angle

$$\text{arc cos } (V_0/ V_3) - \text{arc cos } (V_0/ V_1).$$

Since the lowest level positive gradient sends energy bouncing on from the source to infinity, there is no zone of silence. Focused energy intensifies certain zones of the general noise field.

Case 5 - Explosion in the Air. -- This case (Fig. 9) treats a uniform negative gradient extending from ground up to or higher than the height of burst, h_B, where V equals V_B in the direction of interest. At no altitude does sound velocity in the direction of interest have as high a value as at ground level. Sound rays starting out in the upper quadrant from the burst point are refracted upward initially if $h_B < h_1$. Even if h_B equals h_1, these rays do not reach the ground.

Some rays from the source starting in the lower quadrant do strike the ground, others do not. The limiting ray is the one which just grazes the surface and according to equation 13 leaves the source at minus arc cos (V_B/ V_0). Its striking distance, measured from the point immediately below the burst commonly known as ' ground zero' , is

$$R_{max} = h_B \sqrt{\frac{V_0 + V_B}{V_0 - V_B}} \qquad (35)$$

Rays strike the ground at all points between ground zero and R_{max} and are of course reflected. However, after one reflection the rays curve upward and completely unlike Case 2 do not return to the earth.

UNCLASSIFIED
RESTRICTED

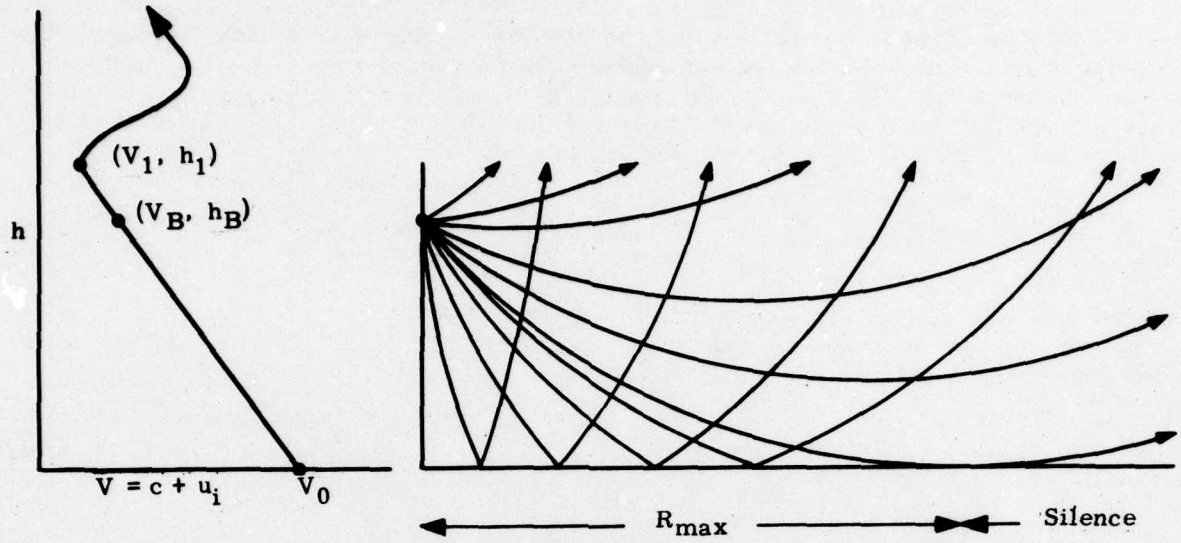


Fig. 9

Energy striking the ground in this direction of interest is that contained within the initial angle

$$\pi/2 - \arccos (V_B/V_0).$$

Behavior of true shock waves striking a horizontal reflector is far more complex[6] than this simple acoustical treatment indicates. However, for receiving stations located at great distances compared with h_B the simple acoustical theory can be expected to hold.

Case 6 - Explosion in the Air. -- A very interesting set of sound rays originates when a uniform positive gradient extends from the ground up to or beyond the burst height h_B (Fig. 10). All rays emitted in the lower quadrant strike ground once, but only some of them are reflected repeatedly. Some of the rays emitted into the upper quadrant escape upward and others are curved downward enough to strike the ground. Energy striking the ground once is that included in the angle

$$\pi/2 + \arccos (V_B/V_1);$$

but after the first strike only that included between + arc cos (V_B/V_1) and - arc cos (V_B/V_1) is repeatedly reflected.

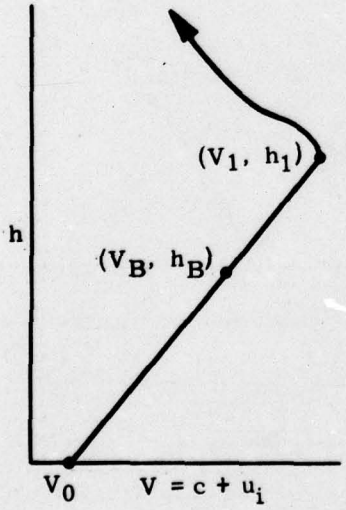


Fig. 10

The ray which makes its initial strike at the greatest distance from ground zero is that which leaves the source in the upper quadrant and becomes horizontal at altitude h_1. Its initial striking distance is

$$R_{max} = \frac{h_1}{V_1 - V_0}\left[\sqrt{V_1^2 - V_0^2} + \sqrt{V_1^2 - V_B^2}\right] \quad (36)$$

The ray leaving the source horizontally is repeatedly reflected and has its apex at the lowest altitude, which is h_B. Although this ray has the shortest span of reflection, it is not the ray which after one reflection strikes ground nearest to ground zero.

The intial striking distance of any ray which undergoes repeated reflections, ie, those included between -arc cos (V_B/V_1) and +arc cos (V_B/V_1), is

$$R_{\text{first strike}} = \frac{h_1 V_0}{V_1 - V_0}\left[\tan\Theta_0 \pm \sqrt{\sec^2\Theta_0 - \frac{V_B^2}{V_0^2}}\right], \tag{37}$$

where the plus sign applies to rays starting in the upper quadrant and the minus sign applies to rays starting from the source in the lower quadrant. After n reflections a ray starting in the lower quadrant lands at

$$R_n = \frac{h_1 V_0}{V_1 - V_0}\left[(2n+1)\tan\Theta_0 - \sqrt{\sec^2\Theta_0 - \frac{V_B^2}{V_0^2}}\right]. \tag{38}$$

This expression has a minimum value which occurs at

$$(\tan\Theta_0)_{\min R_n} = \frac{\sqrt{V_B^2 - V_0^2}}{2V_0} \cdot \frac{2n+1}{\sqrt{n(n+1)}}. \tag{39}$$

Since equation 39 includes a term containing the number of reflections, the particular ray which lands nearest to ground zero after one reflection is not the ray which lands nearest to ground zero after two or more reflections. The general expression for the minimum landing distance after n reflections is

$$(R_n)_{\min} = \frac{2h_1\sqrt{n(n+1)(V_B^2 - V_0^2)}}{V_1 - V_0}. \tag{40}$$

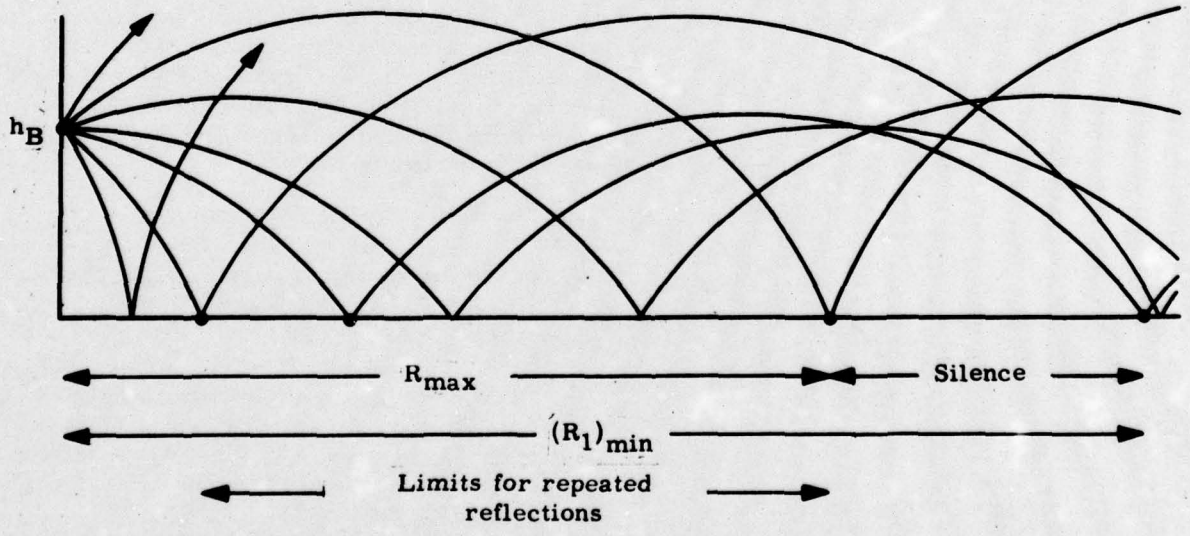


Fig. 11

[redacted]

The minimum landing distance of once-reflected rays can exceed the R_{max} given by equation 36, and a zone of silence will therefore exist between R_{max} and $(R_1)_{min}$. In general n zones of silence will exist, where n is the lowest integer satisfying the inequality

$$2\sqrt{V_B^2 - V_0^2}\ \sqrt{n(n+1)} \geq (2n-1)\sqrt{V_1^2 - V_0^2} + \sqrt{V_1^2 - V_B^2}\ . \qquad (41)$$

Ray paths for Case 6 are shown in Fig. 11. It is especially important to note that when there is a simple positive gradient extending upward from the earth a surface burst can lead to no zones of silence, whereas zones of silence can exist for air bursts.

Case 7 - Explosion in the Air. -- For an airburst which occurs in the lower negative gradient section of an atmosphere such as that shown in Fig. 12 the ray path situation can not be regarded as simple. Some of the rays starting downward strike ground, others do not. Some of the rays starting upward are bent back to ground, others are not. In these two respects the situation is quite like a direct combination of Cases 5 and 6, but some of the rays which would normally escape after striking ground once, as in Case 5, are not permitted to escape in Case 7.

Rays which start from the source at angles between +arc cos (V_B/V_0) and -arc cos (V_B/V_0) are 'channeled' and therefore never strike ground and never travel higher than h_p.

Downward starting energy which strikes ground initially is contained within the angle

$$\pi/2 - \text{arc cos}\,(V_B/V_0).$$

Only that energy contained originally between -arc cos (V_B/V_0) and -arc cos (V_B/V_2) undergoes repetitive reflection following the initial strike.

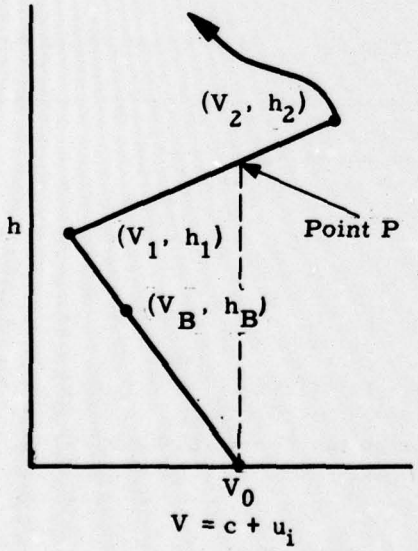


Fig. 12

Of the energy initially starting upward only that part contained between +arc cos (V_B/V_0) and +arc cos (V_B/V_2) strikes ground and is repetitively reflected.

Both bundles of rays which strike ground repetitively are 'focused' and thus create a bifocal situation. The foci may be separate or may overlap.

Minimum-landing-distance rays similar to those treated in Cases 3, 4, and 6 could be computed for both the upper and lower starting bundles, but the mathematics would be too complex to improve the general picture. Landing distances have been computed for only four rays:

That starting downward at -arc cos (V_B/V_0) lands after n reflections at

$$R_1 = n\,(R_1)_{\text{Eq 26}} + h_B\sqrt{\frac{V_0 + V_B}{V_0 - V_B}}\ ; \qquad (42)$$

That starting downward at -arc cos (V_B/V_2) lands after n reflections at

$$R_2 = n\,(R_2)_{\text{Eq 27}} + \frac{h_1}{V_0 - V_1}\left[\sqrt{V_2^2 - V_B^2} - \sqrt{V_2^2 - V_0^2}\right] \tag{43}$$

That starting upward at +arc cos (V_B/V_0) lands after n reflections at

$$R_3 = (n+1)\,(R_1)_{\text{Eq 26}} - \frac{h_1}{V_0 - V_1}\sqrt{V_0^2 - V_B^2}\,; \tag{44}$$

That starting upward at +arc cos (V_B/V_2) lands after n reflections at

$$R_4 = (n+1)\,(R_2)_{\text{Eq 27}} - \frac{h_1}{V_0 - V_1}\sqrt{V_2^2 - V_B^2}. \tag{45}$$

Figure 13 shows some ray paths for this situation.

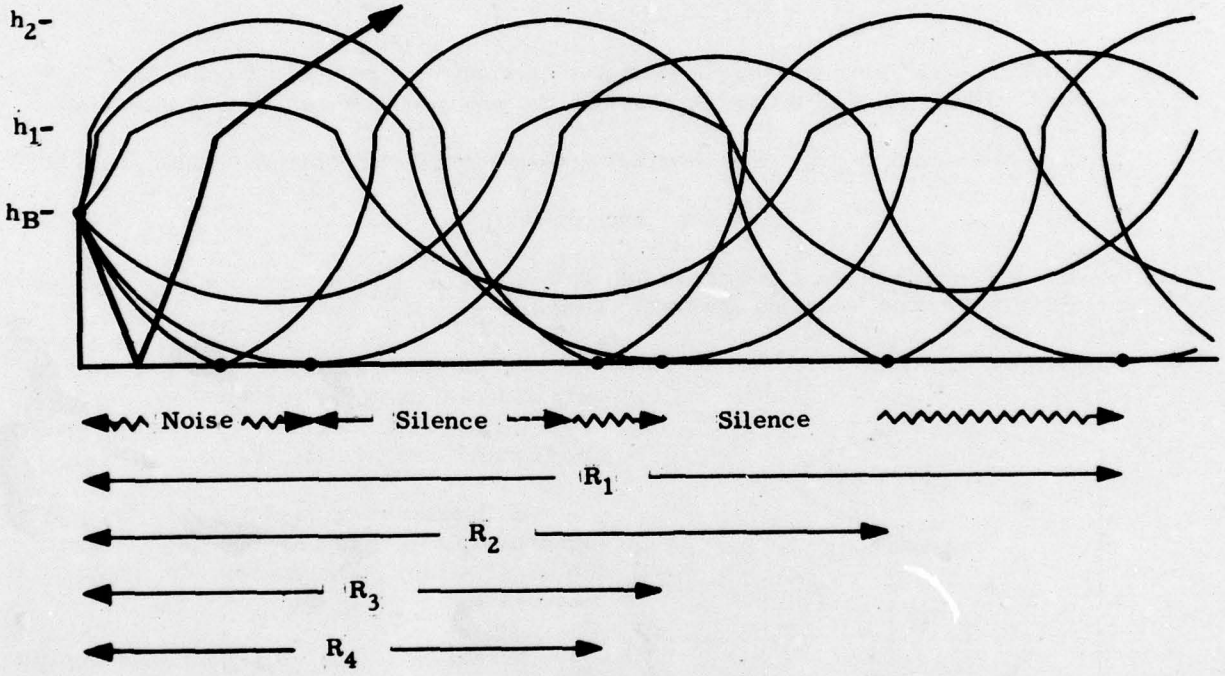


Fig. 13

Case 8 - Explosion in the Air. -- For an explosion occurring at an altitude h_B^* which lies between h_1 and h_p of Fig. 14, ray paths are similar to those in Case 7 and are not illustrated. Four landing distances have again been computed. These are similar to those of equations 42-45. The ray which starts downward at -arc cos (V_B/V_0) strikes the ground at glancing incidence and after n reflections lands at

$$R_1 = (n + 1/2)\,(R_1)_{\text{Eq 26}} - \frac{h_2 - h_1}{V_2 - V_1}\sqrt{V_0^2 - V_B^2}\,. \tag{46}$$

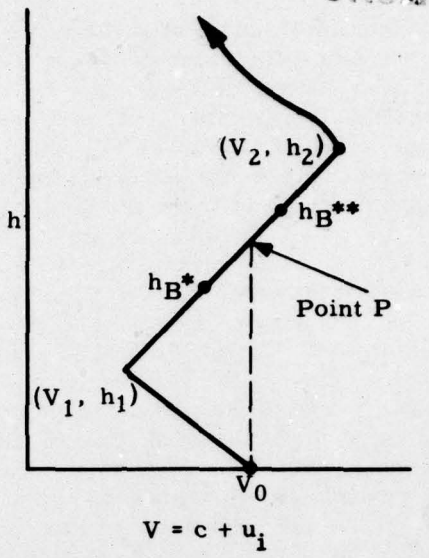


Fig. 14

The ray which starts downward at -arc cos (V_B/V_2) is one of the rays which after reflection has its apex at altitude h_2. Its landing distance after n reflections is

$$R_2 = (n + 1/2)\,(R_2)_{Eq\ 27} - \frac{h_2 - h_1}{V_2 - V_1}\sqrt{V_2^2 - V_B^2}\,. \tag{47}$$

The ray which starts upward at +arc cos (V_B/V_0) is bent to become horizontal at altitude h_p. Its landing distance after n reflections is

$$R_3 = (n + 1/2)\,(R_1)_{Eq\ 26} + \frac{h_2 - h_1}{V_2 - V_1}\sqrt{V_0^2 - V_B^2}\,. \tag{48}$$

The ray which starts upward at +arc cos (V_B/V_2) is the other ray having its apex at altitude h_2 and its landing distance is

$$R_4 = (n + 1/2)\,(R_2)_{Eq\ 27} + \frac{h_2 - h_1}{V_2 - V_1}\sqrt{V_2^2 - V_B^2}\,. \tag{49}$$

For a burst which occurs at altitude h_B^{**} and lies between h_p and h_2 equations 47 and 49 are still valid. Equations 46 and 48 would have imaginary parts and need to be replaced by a single equation, that of the ray starting horizontally from the burst point. Its landing distance is

$$R_5 = (n + 1/2)\left\{\left[\frac{h_1}{V_0 - V_1} + \frac{h_2 - h_1}{V_2 - V_1}\right]\sqrt{V_B^2 - V_1^2} - \frac{h_1}{V_0 - V_1}\sqrt{V_B^2 - V_0^2}\right\}. \tag{50}$$

RAOB measurements seldom depict ideal situations like those treated in Cases 1-8, but these cases are excellent for treating meteorological forecasts. Ray paths through actual atmospheres as determined by RAOB can be plotted by using the method developed and explained by the British scientist, Rothwell[7]. All the sound ray plots which appear in Figs. 32-44 result from Rothwell's method applied as if all bursts had occurred on the ground. In these plots no account of ground irregularities has been taken; it has been assumed that the burst point on the ground and all receiving stations were at the same elevation.

In the discussion of Case 2 it was shown that transit times of sound signals were not independent of path when winds were present. This statement can be generalized to include all other simple and complex cases. If sound rays can travel by more than one path from an explosion to an observer, the observer will usually hear more than one 'bang'. In Case 7 it was shown that two foci result and that these foci could overlap. An observer standing in the region of overlap would be likely to hear two distinct 'booms' having a time separation depending on the wind structure. An explosion occurring between altitude h_1 and altitude h_3 of Fig. 8 might normally be expected to produce not more than two booms at an observation point in the overlap of the two foci. However, ground zero for an atomic bomb burst is struck by a tremendous amount of energy which should not be expected to undergo specular reflection. Energy emitted from ground zero at low angles of incidence would then be trapped beneath altitude h_1 and the observer would hear a third boom. Actual atmospheres could lead to even more 'booms'. The time required for a shock to travel from source to observers via each and every possible route may be calculated by Rothwell's method[7]; hence the time separation between booms may be predicted.

Blast Energy Concentration on the Ground

In the neighborhood of a moderate-sized TNT explosion on the ground one may assume practically even distribution of blast energy over an imaginary hemispherical dome covering the explosion at a small distance (approximately 500 feet). Let W represent the total blast energy in the hemisphere. Since only a very small fraction of the energy is absorbed by the ground, W may be taken as the entire energy released in the explosion and is proportional to the weight of explosive detonated. The energy passing through an elemental area of angular depth, $d\Theta_0$, on the sphere at latitude angle Θ_0 and longitude angle ϕ_0 will be

$$dW = W \cos \Theta_0 \cdot d\phi_0 \cdot d\Theta_0 / 2\pi . \tag{51}$$

If in the direction of azimuth ϕ_0, the sound velocity at altitude exceeds that at ground, sound rays will strike the earth at various distances R. The blast energy striking directly at R, divided by the area on which it lands, tells the direct concentration of energy, ie, the surface density of direct energy, ξ; hence

$$\xi = \frac{W}{2\pi} \cdot \frac{\cos \Theta_0}{R} \cdot \frac{d\Theta_0}{dR} \approx \frac{W}{2\pi} \cdot \frac{1}{R} \cdot \frac{d\Theta_0}{dR} . \tag{52}$$

For the simple inversion of Case 2 the derivative term comes directly from equation 18 and

$$\xi = \frac{W}{4\pi} \frac{V_1 - V_0}{h_1 V_0} \frac{\cos^3 \Theta_0}{R} \approx \frac{W}{4\pi} \frac{V_1 - V_0}{h_1 V_0} \frac{1}{R} . \tag{53}$$

The total surface energy density available to do damage at any fixed distance R_f in Case 2 is the energy received directly (ξ_{R_f}), plus that received after one reflection from an area one-fourth as large at one-half the distance, plus that received after two reflections from an area one-ninth as large at one-third the distance, etc. Some energy, usually a very small amount, is absorbed by the ground on each impact so that the energy reflected is reduced slightly from the incident amount by a reflection coefficient r. Within the zone of direct incidence at some point like P_1 of Fig. 5 the total surface energy density is therefore

$$\xi_{\text{total}} = \frac{W}{4\pi} \cdot \frac{V_1 - V_0}{h_1 V_0} \cdot \frac{1}{R_f} \left(1 + \frac{r}{2} + \frac{r^2}{3} + \cdots + \frac{r^{n-1}}{n} + \cdots\right)$$

$$= \frac{W}{4\pi} \cdot \frac{V_1 - V_0}{h_1 V_0} \cdot \frac{1}{R_f} \sum_{n=1}^{n=\infty} \frac{r^{n-1}}{n}$$

$$= -\frac{W}{4\pi} \cdot \frac{V_1 - V_0}{h_1 V_0} \cdot \frac{1}{R_f} \frac{\log_e (1-r)}{r} . \tag{54}$$

Numerically, if the reflection coefficient

$$r = 90\%, \quad \xi_{\text{total}} = 2.56 \frac{W}{4\pi} \cdot \frac{V_1 - V_0}{h_1 V_0} \cdot \frac{1}{R_f}$$

$$r = 99\%, \quad \xi_{total} = 4.65 \frac{W}{4\pi} \cdot \frac{V_1 - V_0}{h_1 V_0} \cdot \frac{1}{R_f}$$

$$r = 99.9\%, \xi_{total} = 6.91 \frac{W}{4\pi} \cdot \frac{V_1 - V_0}{h_1 V_0} \cdot \frac{1}{R_f}$$

$$r = 99.99\%, \xi_{total} = 9.21 \frac{W}{4\pi} \cdot \frac{V_1 - V_0}{h_1 V_0} \cdot \frac{1}{R_f}$$

Immediately beyond R_{max} given by equation 20 at a point like P_2 of Fig. 5 only those rays reflected one or more times are incident; hence the summation begins with r/2. The generalized expression for surface energy density for the simple inversion of Case 2 thus becomes

$$\xi_{total} = \frac{W}{4\pi} \cdot \frac{V_1 - V_0}{h_1 V_0} \cdot \frac{1}{R_f} \sum_{n=N+1}^{n=\infty} \frac{r^{n-1}}{n}, \tag{55}$$

where N is the integral portion obtained on dividing R_f by R_{max}. For ease in calculation a better expression is

$$\xi_{total} = -\frac{W}{4\pi} \cdot \frac{V_1 - V_0}{h_1 V_0} \cdot \frac{1}{R_f} \left[\frac{\log_e (1-r)}{r} + \sum_{n=1}^{n=N} \frac{r^{n-1}}{n} \right]. \tag{56}$$

It is noted that within any particular zone (N = 0, 1, 2, 3, etc) the surface density of energy decreases inversely as the distance from the source. Abruptness of transition from one zone to the next depends solely on the reflection coefficient.

For an airburst occurring in an atmosphere of the type treated in Case 5 (Fig. 9) blast energy distribution on the ground is also easily determined. The increment of energy escaping through a small segment of an imaginary sphere surrounding the blast point is

$$dW = \frac{W}{4\pi} \cos \Theta_B \cdot d\phi_B \cdot d\Theta_B . \tag{57}$$

The denominator of equation 57 is twice as large as that of equation 52 since for an airburst half the energy escapes into the upper hemisphere. Some of the energy starting downward hits ground at a distance

$$R = \frac{h_1 V_0}{V_1 - V_0} \left[\frac{V_B}{V_0} \tan \Theta_B - \sqrt{\frac{V_B^2}{V_0^2} \sec^2 \Theta_B - 1} \right], \tag{58}$$

where it spreads over an area $R \cdot dR \cdot d\phi_B$. At this distance the blast energy density will therefore be

$$\xi = \frac{W}{4\pi} \frac{\cos \Theta_B}{R} \cdot \frac{d\Theta_B}{dR} . \tag{59}$$

By differentiation of equation 58, substitution in equation 59, and transformation of variables by use of equation 13 one determines that

$$\xi = \frac{W \sin \Theta_0 \cdot \cos^2 \Theta_0}{4\pi R^2} \left(\frac{V_B}{V_0} \right)^2 . \tag{60}$$

Near ground zero, $\sin \Theta_0 \approx 1$ and $\cos \Theta_0 \approx R/h_B$. Thus the maximum surface energy density is

$$\mathcal{E}_{max} = \frac{W}{4\pi} \left(\frac{V_B}{V_0}\right)^2 \frac{1}{h_B{}^2} . \tag{61}$$

Near the outer limit of ground striking rays given by R_{max} of equation 35, $\sin \Theta_0 \approx \Theta_0$ and $\cos \Theta_0 \approx 1$; therefore

$$\mathcal{E}_{limit} = \frac{W}{4\pi} \left(\frac{V_B}{V_0}\right)^2 \frac{\Theta_0}{R_{max}{}^2} . \tag{62}$$

Mathematical expressions for surface densities of energies found in the other simple cases (3, 4, 6, 7, and 8) are so complex that they give little aid to understanding. The complications come about primarily from discontinuities, zones of silence, in the energy distributions. Graphical solutions show much more clearly the regions of high and low energy concentrations or foci of energy. Equation 52 is of course applicable to all surface bursts, and equation 59 is applicable to all airbursts. If in constructing the plot of sound rays, equal and small angular increments are selected for the emanating rays, the values of $d\Theta_0$ or $d\Theta_B$ are kept constant and the span of the associated dR values gives a picture of the spread of energy. Figures 7a and 7b (associated with Case 3) have been drawn in this manner. At their starting point, the explosion, starting rays separate equal angular increments so that the amount of energy between any two starting rays is equal according to equation 51. As they land the energy is much more concentrated near the inner boundary of the noise zone than it is toward the outer boundary.

By construction of ray patterns similar to Figs. 7a and 7b it can be demonstrated that for all simple meteorological patterns leading to foci of energy, such as Cases 3, 4, 6, 7, and 8, energy concentration is much higher toward the inner boundary of the focus than it is toward the outer boundary. This is not necessarily true for real atmospheres, in which the meteorological gradients are changing continuously, and sound ray plots by Rothwell's method[7] are needed to show energy concentrations.

Blast Damage and Pressure

Energy in an acoustic wave or a blast wave (its capacity for doing work) is associated with the pressure undulations constituting the wave. Pressure by definition is force per unit area, and when force is applied to a surface such as a plate-glass window and the force exceeds that which the mountings or object can resist, failure results.

Chapter 5 of The Effects of Atomic Weapons[8] deals at considerable length with blast damage to structures. In general it may be said that when the duration of an applied force is small compared with the natural elastic period of vibration of the object to which the force is applied, the impulse associated with the force establishes the damage it will do. Alternatively if the force is applied suddenly and its duration is long compared with the natural oscillation period of the object, the peak value of applied force appears to govern damage.

The far-distant damage done by atomic bombs which burst on February 2 and 6 and November 1, 1951, consisted primarily of broken windows, cracked plaster, and broken dishes. The largest and longest-period object broken was a plate-glass window in the Sears and Roebuck store in Las Vegas on November 1, 1951. The window measured 100 by 149 inches,

and its natural period of oscillation is computed[9] to be approximately 1/3 second. Boxes of dishes stacked on shelves attached to a wall of the Desert Inn warehouse were knocked down and the dishes were shattered. Ten additional plate-glass show windows in the business district of Las Vegas were broken at the same time. The smallest measured 58 x 84 inches. None of the eleven broken plate-glass windows caved in. All were sucked out from their mountings and were found shattered on the concrete walks in front of the stores. Plate-glass window mountings are strong to inward forces but very weak against forces pushing outward. Resisting inward forces are stiff steel L- or T-beams, but on the outer side only a narrow overlap of thin phosphor bronze holds the glass in place. The writers of this report are of the opinion that essentially all damage to plate-glass windows could have been prevented on past shots and could be prevented on future shots if the stores were opened to allow pressure equalization when the pressure undulations arrive. Stronger mountings, especially on the outer side of windows, would greatly improve the situation.

Our microbarograph records show that the fundamental periods of pressure perturbations (those carrying the greatest amounts of energy) at large distances from atomic explosions are of the order of 2 to 6 seconds. From explosions of 0.6 to 2.4 tons of TNT fundamental periods are 1/4 to 3/4 second. Larger bombs appear to produce longer waves. Since the fundamental periods of atomic bomb perturbation waves are long compared with natural periods of buildings and components of buildings (the fundamental period of the Empire State building is only 8 seconds), the peak pressure criterion is probably the one which governs damage at great distances.

Microbarographs, if they are properly designed and have a sufficiently wide amplitude range, are obviously the proper instruments for determining perturbation pressure versus time. Let us see whether theory will allow us to predict the magnitudes of pressures which may be produced by explosions at great distances.

Sound intensity, the sound-energy flux density in a specified direction at a point, is the average rate of sound energy transmitted in the specified direction through a unit area normal to this direction at the point considered. In the case of a free plane or spherical wave having an effective perturbation pressure p and velocity of propagation V in a medium of density ρ, the intensity in the direction of propagation is $p^2/\rho V$. Thus at any specific location

$$\xi_{total} = \int \frac{p^2\, dt}{\rho V}\ , \tag{63}$$

where the integration extends over the complete duration of the signal.

If perturbation pressure p were sinusoidal and of constant amplitude for a finite fixed duration τ, then

$$\xi_{total} = (p_{rms})^2\ \tau/\rho V \tag{64}$$

$$= (p_{peak})^2\ \tau/2\rho V; \tag{65}$$

hence

$$p_{peak\text{-}to\text{-}peak} = 2(2\xi\rho V/\tau)^{1/2} \tag{66}$$

This is 'free' air perturbation pressure or 'side-on' overpressure. If the acoustic wave is normally incident on a rigid reflecting surface, the pressure on the surface is doubled by reflection.

On exceedingly rare occasions nature does provide freak examples which appear susceptible to calculation, ie, when ξ can be computed by equations 52, 59, or one of their applicable forms and when a microbarograph record of pressure versus time appears nearly sinusoidal with essentially constant amplitude for a definite period of time. Figure 15 shows such an exceptional record, and if the derived theory were any good, the overpressure double amplitude predicted by equation 66 should approximate that recorded by the microbarograph.

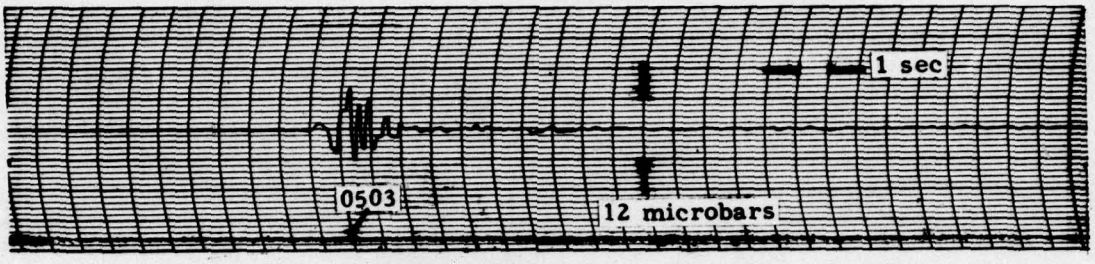


Fig. 15. -- Indian Springs, Nevada, microbarograph record of 1.2-ton TNT explosion 37.3 miles northwest. Shot time 0500:00 PST, October 6, 1951

The text paragraph which includes equation 24 shows that travel times of signals are dependent on path when winds are present. Thus whenever sound signals can travel from source to receiver by more than one path the duration of the signal received depends in some manner on the wind structure as a function of altitude. Further, the signal duration at any receiver is undoubtedly associated with the phenomenon of degeneration of shock waves into sound waves, a process to which very little theoretical or experimental study has been devoted to date. Consequently there are no equations, theoretical or empirical, by which the duration of a signal may be determined. To make any test of the theory it is necessary to conduct the experiment, measure the duration of the signal, then see what value of peak pressure equation 66 would have predicted had the duration of the signal been known in advance of the experiment.

We must therefore confess that the present theory is very weak. It is not possible to predict in advance of a shot what the peak pressure will be. After some experience a reasonable guess as to the duration of a signal may be made and entered into equation 66 to obtain an estimate of the associated peak pressure. Estimates so obtained may deviate widely from measured values.

Checks of the theory, rather than predictions from the theory, can be made after records of microbarometric pressures have been obtained. Let us apply the theory to two cases, one simple and one complex, using in each instance the recorded values of signal durations. This will at least show whether the theory so far derived is meaningful or ridiculous.

Figure 16 shows, for the direction southeast from the blast site, the data points of h versus V observed using a RAOB at blast time. If a constant positive gradient is assumed from ground (4,130 feet above mean sea level) to 7 kilofeet above mean sea level, the miss of one data point is not large and equations in Case 2 are applicable. Useful data are $V_0 = 1,110$ ft/sec, $V_1 = 1,116$ ft/sec, and $h_1 = 2,870$ feet.

Equation 20 shows the maximum striking distance of direct rays to be 1.1×10^5 feet. Since the microbarophone at Indian Springs was located 37.3 miles (1.97×10^5 feet) from the shot point, only that energy reflected one or more times reached the phone.

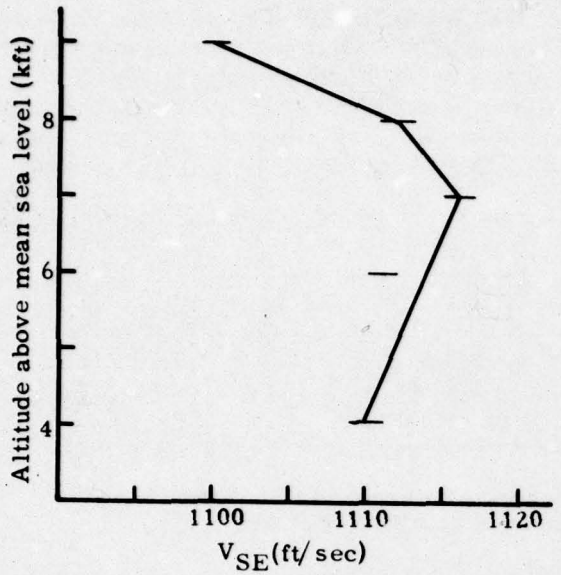


Fig. 16. -- Meteorological data computed from RAOB, 0500 PST, Oct. 6, 1951

To determine surface energy density, equation 56 is applicable when N = 1. The energy equivalent of 1.2 tons of TNT may be taken[8] as 1.2×10^9 calories = 5.0×10^{16} ergs. Let us assume a reflection coefficent r = 90%. These values introduced into equation 56 give ξ_{total} = 64 ergs/cm^2 at the Indian Springs microbarophone.

Using this value of ξ_{total}, air density as 1.1×10^{-3} gm/cm^3, and the signal duration observed from Fig. 15 as about three seconds, equation 66 shows that peak-to-peak pressure should be about 80 microbars. Figure 15 shows a recorded value of 15. When the approximations and assumptions used in arriving at the computed value of 80 are considered, it is surprising to find it wrong by only a factor of five!

* * * * *

As a second check the 1.2-ton shot of TNT at 0800 PST on November 13, 1951, was investigated. It was a most interesting case from the meteorological view point in that there was a wind 'jet stream' having velocities up to 120 knots directly over the test area at altitudes between 20 and 25 kilofeet.

Figure 17 shows sound ray plots constructed by the Rothwell method from some RAOB data taken at the AEC test site. Because the balloon escaped from the range of observation when it reached 12 kilofeet above mean sea level, above this altitude RAOB data from the Las Vegas weather bureau station were used. Figures 42a-k show meteorological data and additional sound ray plots for this day.

Beneath the sound ray plots are shown distances associated with rays which should be reflected to reach the four observation stations in the direction southeast from the shot point. Indian Springs would receive direct energy plus energy reflected one, two, and three times. No direct rays, but those reflected as many as 1 to 8 times, would reach the Henderson station.

Because each ray is identified by its angle of starting from the source, values of $d\Theta_0$ are obtainable by taking differences between starting angles. Values of dR can be found by taking differences between ray landing points. If a reflection coefficient r is assumed, and values of $d\Theta_0/dR$ are computed, these may be entered into equation 52, and the summation of these expressions will give the total surface energy density impinging on the receiving station.

As an example of the computations involved let us look at the Henderson situation. Table II shows the approximate starting angles of the ten rays which should strike Henderson according to the sound ray plot. The second column lists the number of cycles required to reach Henderson. Using an assumed reflection coefficient of 99.0% the third column lists the energy coefficient, r^{n-1}/n. The fourth column gives the value of $d\Theta_0/dR$ computed from only those rays shown in Fig. 17.

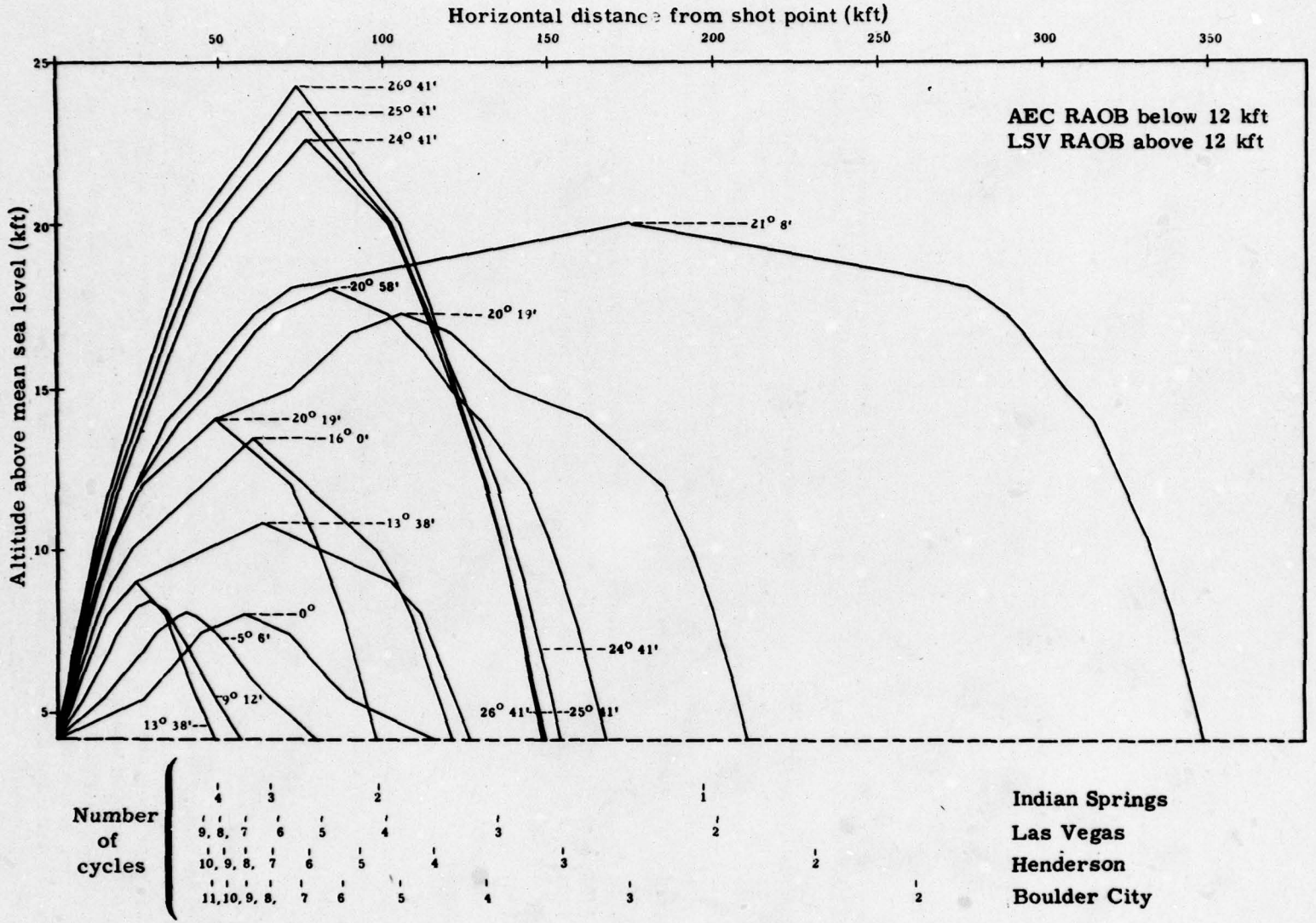


Fig. 17. -- Sound ray plots for direction SE from shot point, November 13, 1951, at 0800 PST

DECLASSIFIED

TABLE II

Approximate ray angle	No. of cycles	Reflection coefficient (r^{n-1}/n)	$d\Theta_0/dR$ (cm^{-1})
21° 03'	2	0.495	5.2×10^{-10}
22° 15'	2	0.495	1.04×10^{-8}
24° 30'	3	0.327	1.43×10^{-7}
17° 00'	4	0.242	1.07×10^{-7}
0° 00'	4	0.242	8.09×10^{-8}
3° 00'	5	0.192	8.09×10^{-8}
5° 20'	6	0.159	1.02×10^{-7}
7° 00'	7	0.135	1.02×10^{-7}
9° 00'	8	0.116	3.17×10^{-7}
11° 30'	9	0.103	3.17×10^{-7}

To compute the total surface energy density at Henderson the summation of the products of columns 3 and 4 is substituted for $d\Theta_0/dR$ in the approximate expression of equation 52.

Microbarograph records from the four receiving stations southeast of the blast point are shown in Fig. 18. These four excellent records are far more typical than Fig. 15. They show that overpressure is not generally sinusoidal, not of constant amplitude, and that the signal dies out gradually. It is nearly impossible to state its duration. Only an approximate time can be selected during which the signal remained relatively large, and this value for the signal duration may be used to compute peak pressure by use of equation 66.

Table III lists stations, computed values of surface energy density, values of large signal durations selected from Fig. 18, and computed and measured values of peak-to-peak overpressures. Again, agreements between computed and measured values are not good, but they are better than we had any right to expect.

TABLE III

Station	Distance (km)	Computed $\mathcal{E}_{total}$ ($ergs/cm^2$)	Large signal duration (sec)	Computed $p_{peak\text{-}to\text{-}peak}$ (microbars)	Measured $p_{peak\text{-}to\text{-}peak}$ (microbars)
Indian Springs	60	296	5	132	187
Las Vegas	123	92	7	62	41
Henderson	142	120	4	94	110
Boulder City	160	63	10	40	86

The fact that the computed values have compared fairly well with measured values is remarkable when phenomena between shot point and receiving stations are considered. Pressure versus time measurements near a blast point have a shape somewhat as shown in Fig. 19. (For the real shapes of shock waves from atomic weapon bursts, see WT-304 by B. F. Murphey, 1952.) A Fourier analysis of this graph would show the presence of an infinity of frequencies; the sharp rise time leads to a large number of high-frequency components. In the medium between the shot point and distant microbarometric stations absorption [10] would take out most, if not all, the high frequencies.

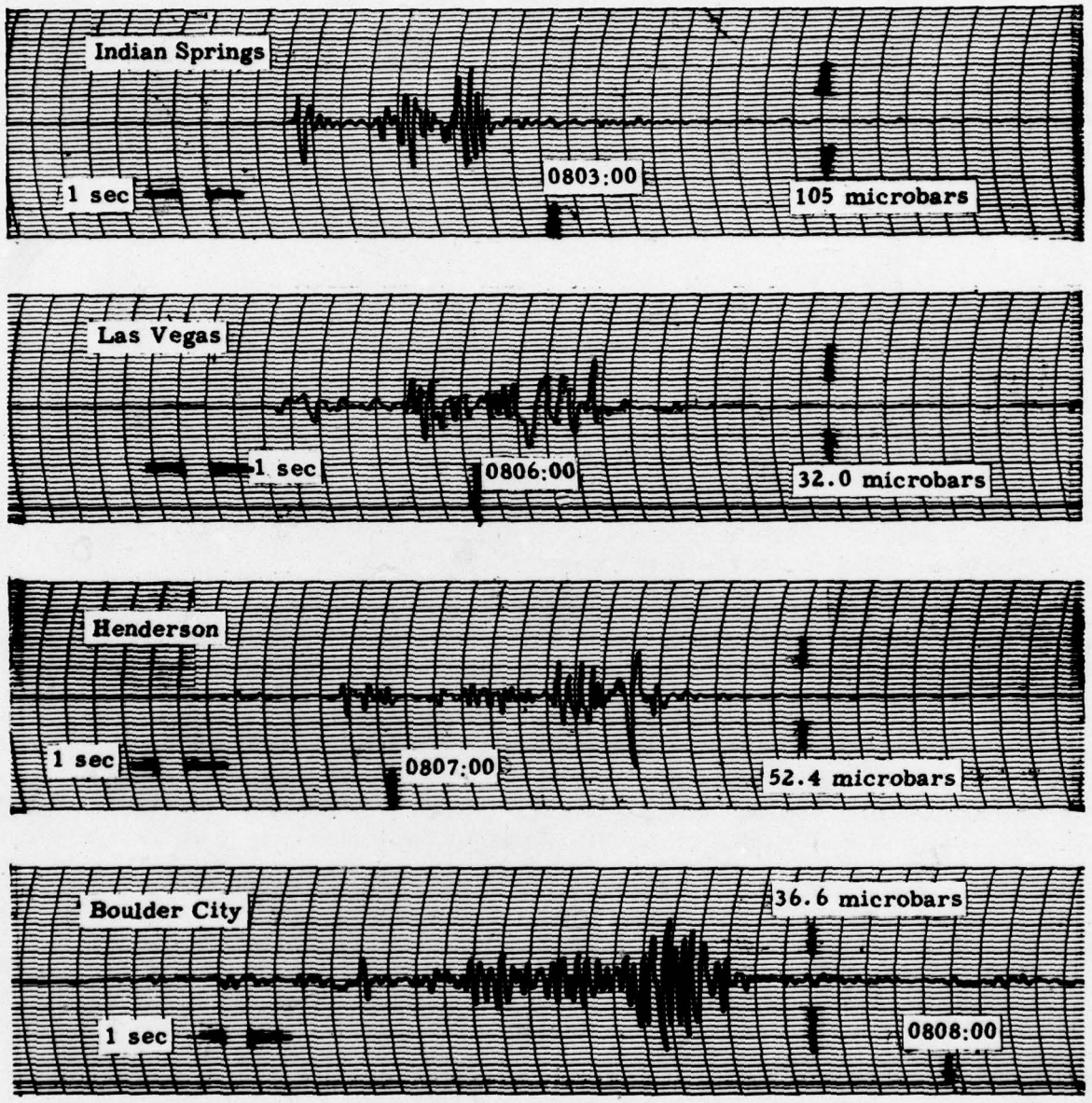


Fig. 18. -- Microbarograph records of troposphere signals recorded southeast from 1.2-ton TNT shot, 0800 PST, November 13, 1951

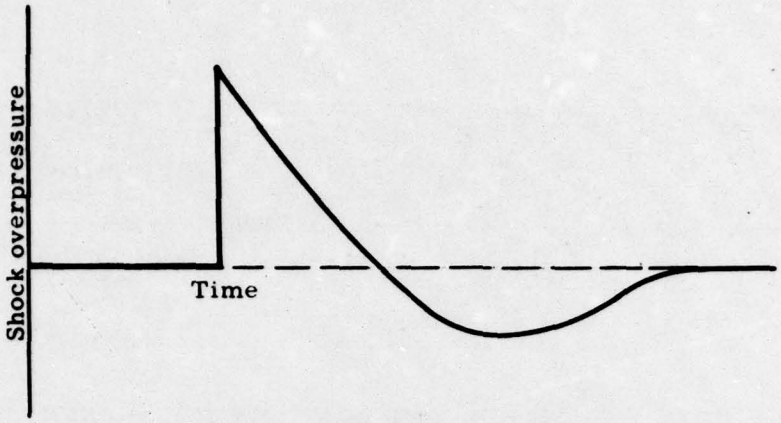


Fig. 19

Because of dispersion[11] frequency components not absorbed en route will reach various microbarometric stations in different phases. The shape and peak-to-peak amplitude of a sum of various frequency components are most sensitive to the phases of the components. Any simple mathematical treatment which pretends that peak-to-peak amplitudes of complex waves have remained constant for a finite duration τ might well give predictions of an order of magnitude inconsistent with measured values.

Since the theory which ignores absorption and dispersion has given reasonable results, we are encouraged to carry it still further. If more were known about time durations of signals, it might be possible to use equation 66 in a comparative manner rather than in an absolute manner by rewriting it in the form

$$P_{\text{peak-to-peak}} = W^{1/2} \tau^{-1/2} [f(R)] . \qquad (67)$$

If the signal duration τ did not depend on the size of explosion, then during a period of constant meteorological conditions peak pressure would vary as the square root of the charge weight.*

*Two series of experiments were performed in an effort to learn the dependence of peak-to-peak pressures on charge weights. At 10-minute intervals 0.6, 1.2, and 2.4 tons of TNT were fired on the ground at points separated by less than 100 yards. Good signals which had traveled through the troposphere were recorded at Caliente and Goldfield. Table IV shows recorded values of peak-to-peak pressures for the three different charge weights. To a very rough approximation three of the four cases seem to show that peak pressures increase as the square root of the charge weight.

TABLE IV

Troposphere signals, peak-to-peak pressures (microbars)

Date	Station	Pressure per given weight of TNT		
		0.6 ton	1.2 tons	2.4 tons
Oct 8, 1951	Caliente	4.1	6.4	2.4
Oct 9, 1951	Caliente	8.3	13.3	23.8
Oct 8, 1951	Goldfield	2.0	4.2	4.5
Oct 9, 1951	Goldfield	0.6	2.3	2.9

By bursting a relatively small charge a short time before an intended shot of an atomic weapon and measuring the microbarometric pressures associated with the small blast, overpressures might be scaled from the predicted yield of the atomic weapon by the square root of the ratio of yields.

However, signal durations do appear to depend on the size of explosion, and to date it has not been possible to determine a satisfactory relation. From 1.2-ton TNT explosions excellent signals were observed having durations as short as 3.2 seconds and as long as 1.5 minutes. Some of the signals from atomic weapon blasts have lasted at least 6.2 minutes! Echoes arising from terrain irregularities near the shot point effectively increase durations of measured signals and may also increase the amount of acoustic energy sent in some specific direction.

A statistical distribution of measured signal durations related to 1.2-ton TNT explosions might be presented here, but since basic interest is in peak-to-peak pressures, it appears more profitable to show these pressures statistically. This plot can then be employed comparatively for any weather situation. A short time before an intended atomic weapon burst a 1.2-ton charge may be exploded and pressures recorded by a suitable array of microbarographs. If measured pressure appear high compared with the means of those shown in Fig. 20, a damaging situation may well exist.* If measured values are well below average, a relatively safe condition exists for moderate atomic weapons.

The reader's attention is called to the tremendous span of peak-to-peak pressures shown in Fig. 20, and even here the plotted points do not show the full range of signals. When the microbarographs are set for maximum sensitivity, a signal having a strength of 0.06 microbar is discernible. On at least one occasion, a shot at 0500 PST on September 28, 1951, the Indian Springs microbarograph did not register a signal even this large (Fig. 36). From the same size explosion at 0700 PST on November 1, 1951, this same microbarograph station recorded 194 microbars (Fig. 40). This means that peak-to-peak pressure ratios equal to or greater than 3,200 to 1 have been observed for the same size explosions.

The upper recording limit of our microbarographs was about one millibar. Peak-to-peak pressures received at many of our microbarometric stations on the occasions of atomic weapon bursts exceeded recording limits of the instruments. Thus peak-to-peak pressures on these occasions were greater than one millibar, but it is not really known how large the pressures were. No damage was reported except in Las Vegas following the Buster Dog shot. The microbarograph in Las Vegas showed a peak-to-peak pressure greater than 1.12 millibars. The recording barograph at the U.S. Weather Bureau Station at McCarran Field, Las Vegas, showed a peak-to-peak pressure of 2.4 millibars, which is five pounds per square foot. Nothing is known concerning the response of the McCarran Field barograph to rapid changes in pressure, but a value of about 5 lbs/ ft^2 sounds reasonable when the damage is considered. We believe that a small increase in pressure over that which struck Las Vegas on November 1, 1951, would bring about a rapid increase in the amount of damage produced by the shock. We know now that when weather conditions are similar to those on November 1 it is certainly not safe to fire large atomic weapons.

---

*A graph similar to Fig. 20, but for 0.6-ton charges, is presented as Fig. 31.

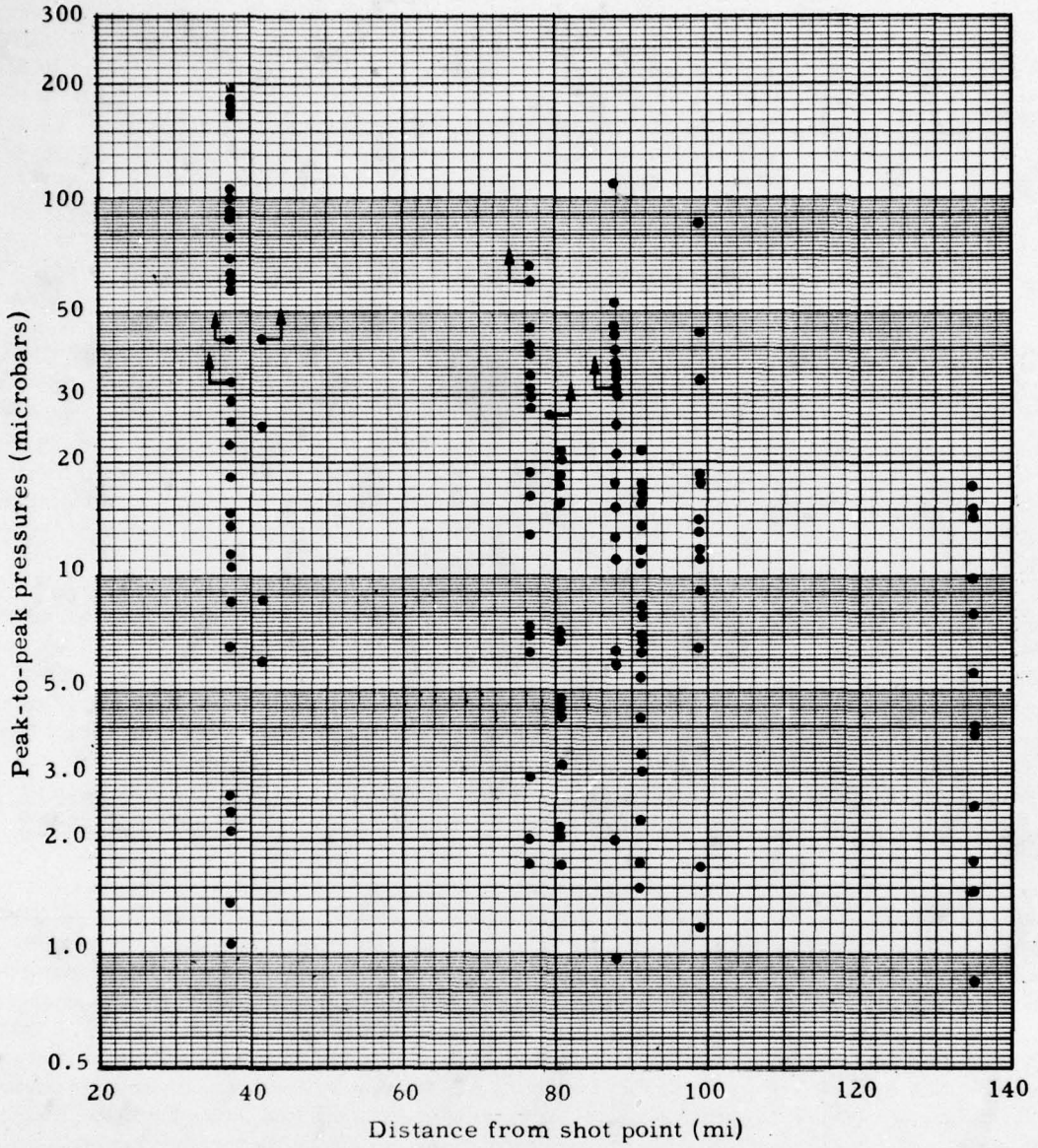


Fig. 20. -- Peak-to-peak microbarometric pressures of troposphere signals from 1.2-ton TNT shots. Arrows show microbarograph went off scale. For ozonosphere and ionosphere signal strengths see Fig. 27. For 0.6-ton TNT shot results see Fig. 31.

Figures 37 through 44 show weather conditions and plots of some sound rays for the occasions of each Buster and Jangle test. Peak-to-peak pressures recorded on each of these shots are plotted (Figs. 21a-g). Measured values have not been corrected for the frequency response of the microbarographs, but full response is assumed (Fig. 30). For those occasions when the microbarograph went off scale an arrow is attached to the plotted point to show that the real pressure exceeded that plotted. Also shown (Figs. 21a-g) are the peak-to-peak pressures from the 1.2-ton test shots set off in advance of the fission weapons. These advance test shots were fired between one-half and two hours before the fission weapon shots, the majority of them at minus one hour. Good correlation between the strengths of signals obtained from the test shots and those from the fission weapon shots was anticipated. Unfortunately weapon shots were ordinarily planned for early morning when temperatures and winds were changing rapidly. Correlations were therefore only fair.

If durations of signals were independent of explosion yields, it would be possible to predict, by comparison, the peak-to-peak pressures at various distances from weapon explosions, using the scaling law (equation 67). Records show in general that signal durations increase as the weight of explosives increases when meteorological conditions remain constant. For this reason, when microbarometric pressures expected from explosion of a fission weapon are predicted by application of the scaling law and the increasing signal duration is neglected, the peak-to-peak pressure values predicted are usually greater than those measured. Application of equation 67, ignoring the signal duration change, thus gives conservative (high) values of pressures to be expected. Application of these statements to a condition when weather functions are rapidly changing can lead to very erroneous conclusions.

The state of the science of predicting troposphere signal strengths which will be received at stations at various distances from an explosion is:

If simple calculations or sound ray plots are used, it is possible to tell *reasonably well from good weather predictions* (better from RAOB measurements) when a good, bad, or medium situation exists.

When the pressure points of Fig. 20 are compared with those obtained by microbarographs operated during a 1.2-ton TNT explosion fired one hour or less before an intended A-weapon blast, the acoustic situation prior to the A-weapon explosion can be confirmed.

When conditions are average or worse, ie, when the pre-atom-bomb 1.2-ton explosion produces pressures greater than the average of Fig. 20, it is not possible to predict with any degree of certainty how much damage an atomic weapon will cause even though its yield has been accurately predicted. When equation 67 is used to predict peak pressures by the scaling law and the increase in signal duration is neglected, the predicted peak pressures from the atomic weapon are usually too high. Therefore damage is predicted whenever a marginal situation, perhaps even a safe one, exists. We can say where the damage, if any, will occur.

[redacted] UNCLASSIFIED

A pressure-signal ratio exceeding 3200:1 has been observed to result solely from weather changes. Since peak-to-peak pressure increases as the square root of charge size, this means that to observe this same ratio under constant weather conditions, we could fire charges ranging from one ton to ten million tons. Having been successful in predicting signal strengths for the changed weather conditions, we have enough confidence in the present prediction system to state that, under certain weather conditions, really big bombs could be fired at the Nevada Proving Grounds withough causing significant damage to any inhabited area of Nevada or Utah.



UNCLASSIFIED [redacted]

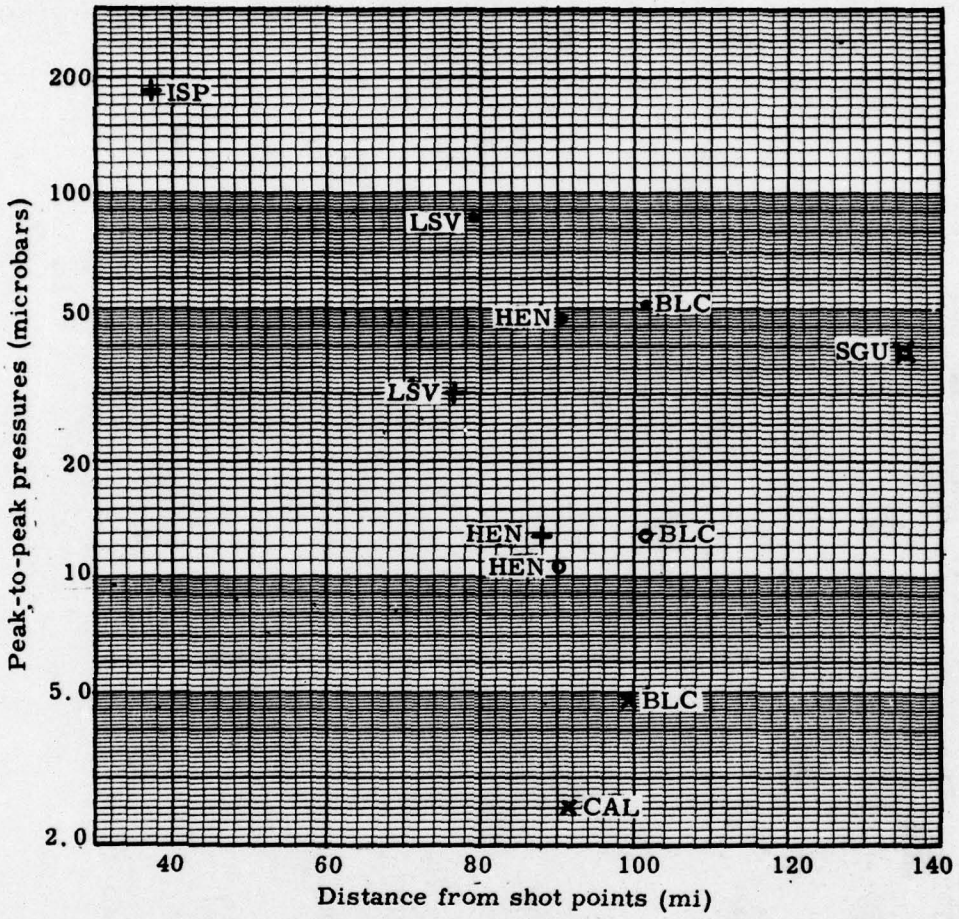


Fig. 21a. -- Peak-to-peak pressures from Buster Able Shot fired at 0600 PST on October 22, 1951, and from the advance 1.2-ton TNT shot fired at 0500 PST. Solid dots are Able troposphere signals, open circles are Able ozonosphere signals, upright crosses are advance shot troposphere signals, and X's are advance shot ozonosphere signals. Oscillation periods (sec) prominent in Able Shot signals were: LSV 0.5; HEN 0.6 and 0.8; BLC 0.7; CAL 0.7; SGU 0.5 and 0.9.

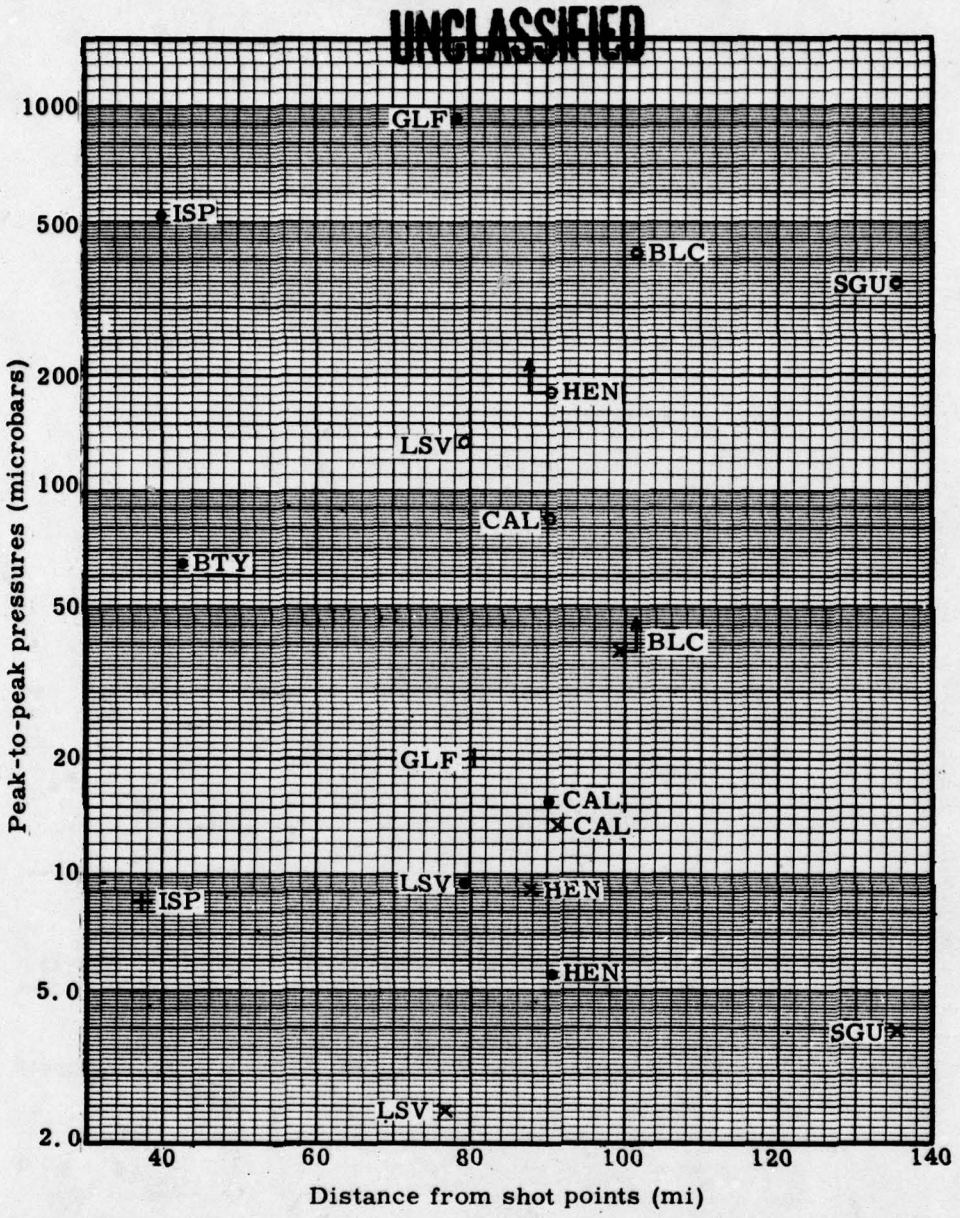


Fig. 21b. -- Peak-to-peak pressures from Buster Baker Shot fired at 0720 PST on October 28, 1951, and from the advance 1.2-ton TNT shot fired at 0600 PST. Solid dots are Baker troposphere signals, open circles are Baker ozonosphere signals, upright crosses are advance shot troposphere signals, and X's are advance shot ozonosphere signals. Arrows show microbarographs went off scale. Oscillation periods (sec) prominent in Baker Shot signals were: ISP 0.4 and 1.4; BTY 1.2; LSV 2.4 and 3.7; HEN 0.9, 2.4, and 3.2; BLC 1.4 and 3.4; CAL 0.5, 1.2, and 3.1; GLF 1.4; SGU 1.2 and 2.9.

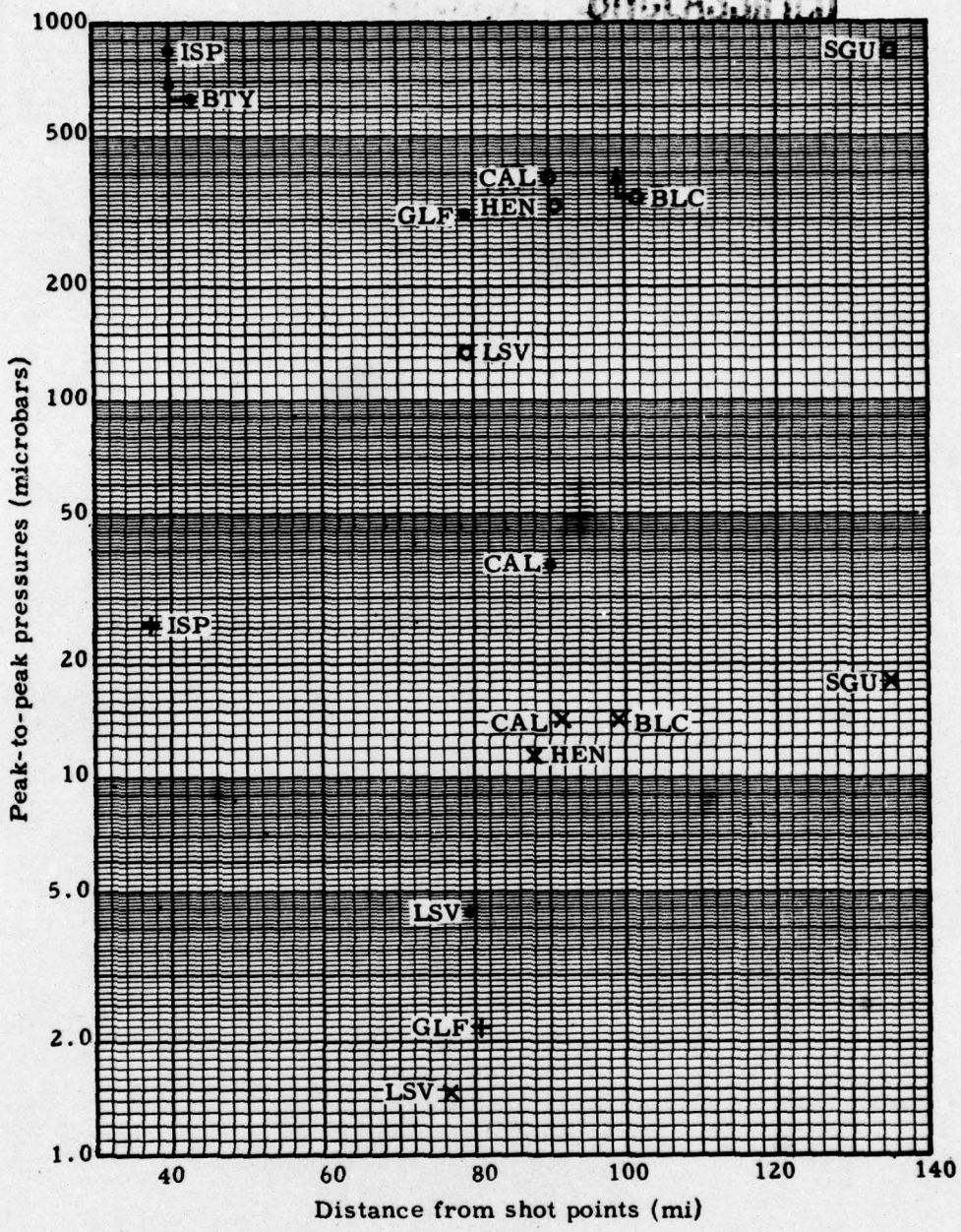


Fig. 21c. -- Peak-to-peak pressures from Buster Charlie shot fired at 0700 PST, October 30, 1951, and from advance 1.2-ton TNT shot fired at 0600 PST. Solid dots are Charlie troposphere signals, open circles are Charlie ozonosphere signals, upright crosses are advance shot troposphere signals, and X's are advance shot ozonosphere signals. Arrows show microbarographs went off scale. Oscillation periods (sec) prominent in Charlie Shot signals were: ISP 4.2; BTY 1.0 and 4.7; LSV 0.4 and 1.9; HEN 0.5 and 1.3; BLC 1.0; CAL 1.9 and 2.4; GLF 2.3 and 4.0; SGU 1.0 and 2.0.

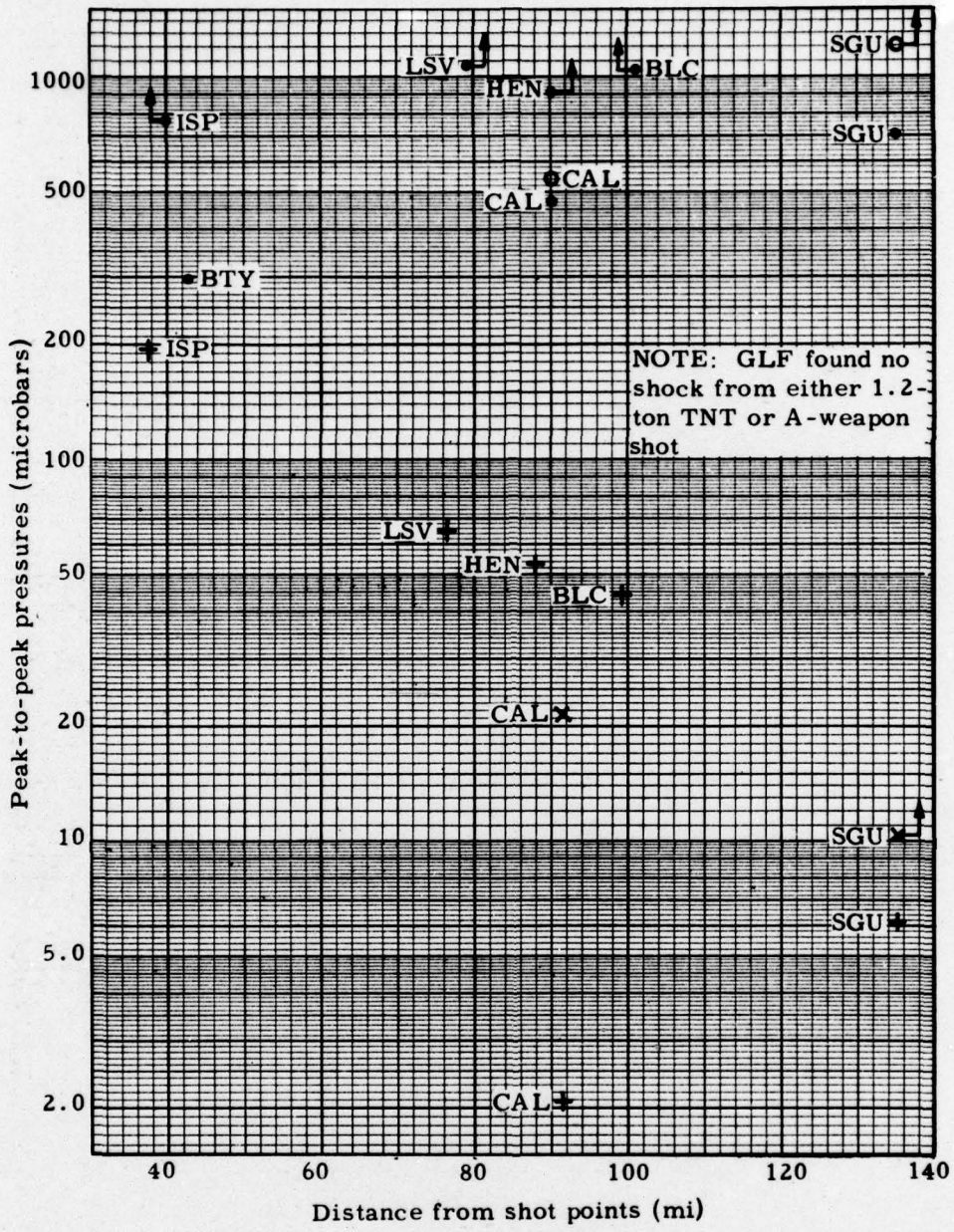


Fig. 21d. -- Peak-to-peak pressures from Buster Dog Shot fired at 0700 PST, November 1, 1951, and from advance 1.2-ton TNT shot fired at 0700 PST. Solid dots are Dog troposphere signals, open circles are Dog ozonosphere signals, upright crosses are advance shot troposphere signals, and X's are advance shot ozonosphere signals. Dog troposphere signals broke eleven plate-glass windows in Las Vegas (LSV). Arrows show microbarographs went off scale. Oscillation periods (sec) prominent in Dog Shot signals were: ISP 0.3, 1.1, and 4.5; BTY 4.5; LSV 0.7, 1.1, and 5.0; HEN 1.3 and 3.5; BLC 1.3; CAL 1.4 and 6.0; SGU 0.3 and 1.6.

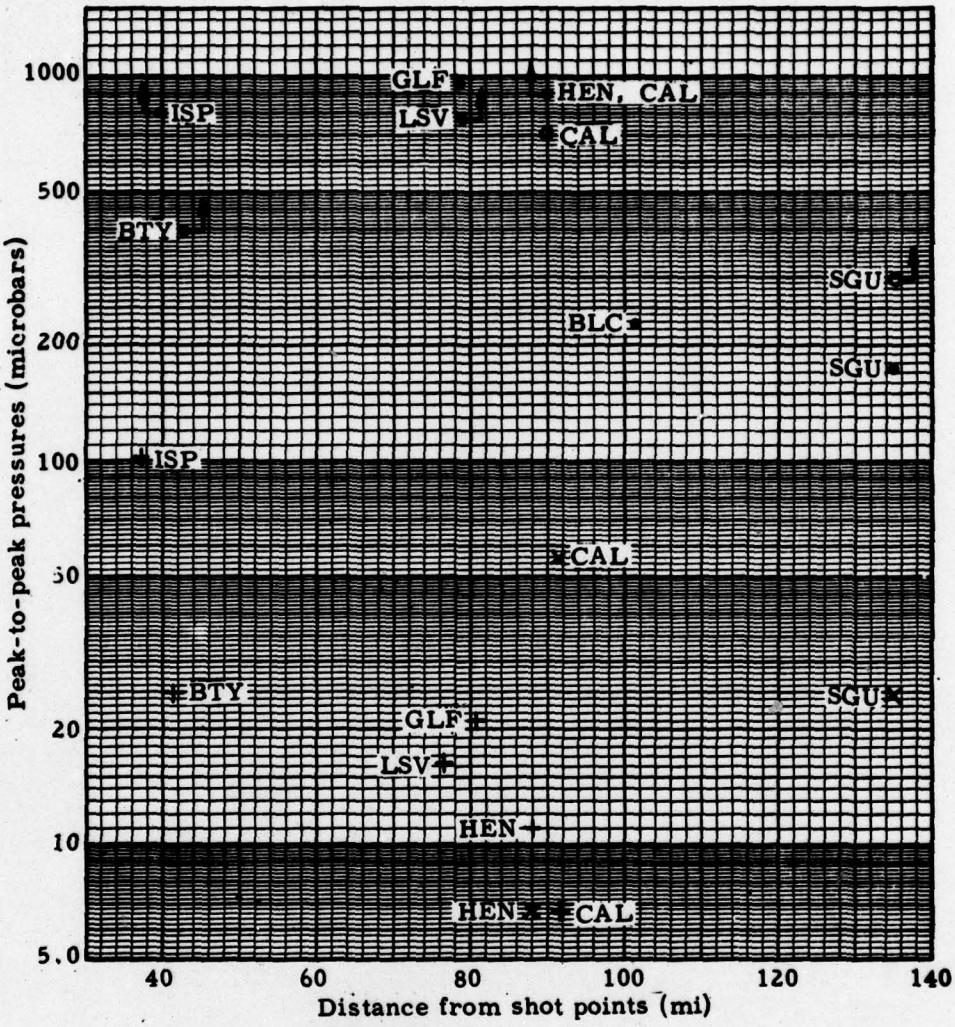


Fig. 21e. -- Peak-to-peak pressures from Buster Easy Shot fired at 0830 PST, November 5, 1951, and from advance 1.2-ton TNT shot fired at 0730 PST. Solid dots are Easy troposphere signals, open circles are Easy ozonosphere signals, upright crosses are advance shot troposphere signals, and X's are advance shot ozonosphere signals. Arrows show microbarographs went off scale. Oscillation periods (sec) prominent in Easy Shot signals were: ISP 1.8 and 2.4; BTY 1.2; LSV 1.0 and 2.4; HEN 1.2; BLC 1.2 and 1.9; CAL 0.5, 2.6, and 6.0; GLF 1.0 and 1.9; SGU 1.0, 4.0, and 6.2.

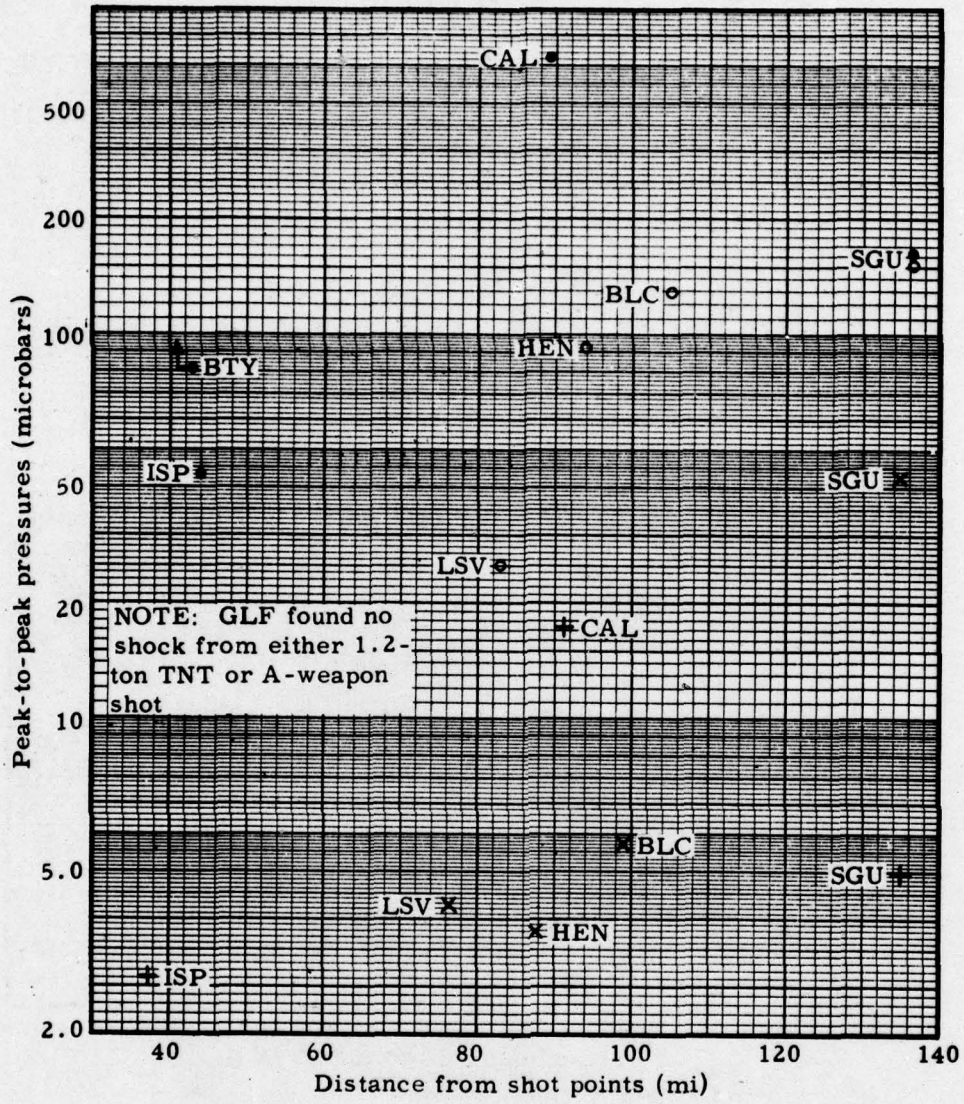


Fig. 21f. -- Peak-to-peak pressures from the first Jangle shot, fired at 0900 PST, November 19, 1951, and from the advance 1.2-ton TNT shot fired at 0800 PST. Solid dots are the troposphere signals from the first shot, open circles are the ozonosphere signals from the first shot, upright crosses are advance shot troposphere signals, and X's are advance shot ozonosphere signals. Arrow shows microbarograph went off scale. Oscillation periods (sec) prominent in nuclear shot signals were: ISP 1.7 and 2.1; BTY 1.9 and 2.9; LSV 2.0 and 3.0; HEN 1.7 and 2.7; BLC 0.6 and 2.8; CAL 2.1; SGU 1.7 and 3.1.

UNCLASSIFIED

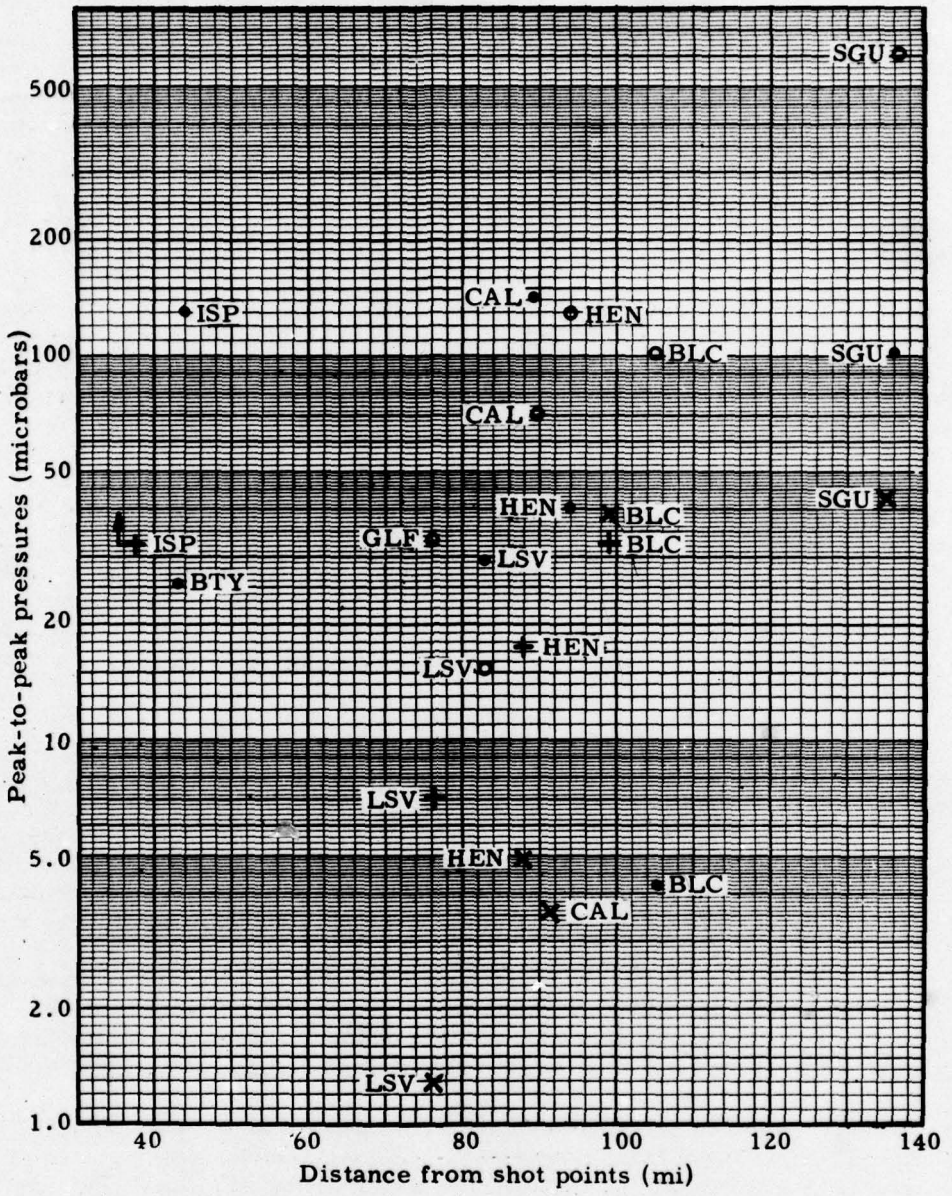


Fig. 21g. -- Peak-to-peak pressures from the second Jangle shot, fired at 1200 PST, November 29, 1951, and from advance 1.2-ton TNT shot fired at 1000 PST. Solid dots are troposphere signals from the second shot, open circles are ozonosphere signals from the second shot, upright crosses are advance shot troposphere signals, and X's are advance shot ozonosphere signals. Arrow shows microbarograph went off scale. Oscillation periods (sec) prominent in the nuclear shot signals were: ISP 2.0; BTY 1.4 and 3.0; LSV 1.9 and 2.0; HEN 1.3; BLC 1.6; CAL 2.0 and 2.4; GLF 2.7; SGU 1.3 and 2.4.

UNCLASSIFIED

Ozonosphere Signals

During the funeral of Queen Victoria in 1901 guns were fired at minute intervals in London as part of her funeral rites. Since the noise was rhythmic, the source could be easily identified. Booms were heard distinctly in London and again far to the north, but between the two areas of audibility there was a skip zone of silence. A zone of audibility beyond a zone of silence was observed to encircle completely an explosion in Moscow on May 9, 1920. Minimum distance from the source to this zone of audibility was 90 miles.

Following World War I some scientific experiments were performed in connection with destruction of European ammunition dumps. Determinations of apparent sound velocities between shot points and receivers located in audibility zones about one hundred miles from the sources gave values far less than those which would result from application of Laplace's equation 6. The bass noises received in audibility zones separated from the source by one or more zones of silence consequently became known as 'abnormal' sounds.

Astrophysicists Lindemann and Dobson, who were working in a scientific field completely divorced from acoustics, concluded in 1923 that to explain the behavior of meteorites it was necessary to assume that some regions of the earth's upper atmosphere have temperatures considerably higher than those ordinarily found at the earth's surface. After reading the publication of Lindemann and Dobson, F. J. W. Whipple saw an immediate possible explanation for the abnormal sound phenomenon and carried out a few sample calculations[12] to show that his proposition was reasonable.

As a result of the need for tables of properties of the atmosphere at high altitudes the U.S. National Advisory Committee for Aeronautics in January 1946 appointed a panel on the upper atmosphere. This panel assembled all available knowledge and theories of the upper atmosphere and published[13] a set of tables of atmospheric properties for altitudes of 20 to 120 kilometers (65 to 394 kilofeet). Among the data the panel considered were results of all abnormal sound measurements published prior to 1947. Figure 22 is a graph of the speed of sound versus altitude adapted by the NACA panel for their 'standard atmosphere'.

Figure 22 shows nothing at all concerning winds. From sea level up to an altitude of 256 kilofeet air composition is assumed to remain constant; hence sound velocity is a function of temperature only. At altitudes greater than 256 kilofeet oxygen molecules dissociate; hence above 256 kilofeet γ and M as well as K are allowed to vary in Laplace's equation 6.

Considerable scientific evidence shows that concentration of atmospheric ozone is higher in the region above 60 kilofeet than it is near the ground. Ozone is a very strong absorber of certain wave lengths of ultraviolet light profusely emitted by the sun. Between 250 and 100 kilofeet the ozone in the atmosphere is assumed to extract essentially all this ultraviolet energy and convert it into heat, which is assumed to raise the temperature of the ozonosphere to a level exceeding that of the atmosphere next to the ground.

If winds were absent, all sound rays from an explosion below the tropopause would be bent upward initially. On reaching the tropopause, rays would maintain constant inclinations

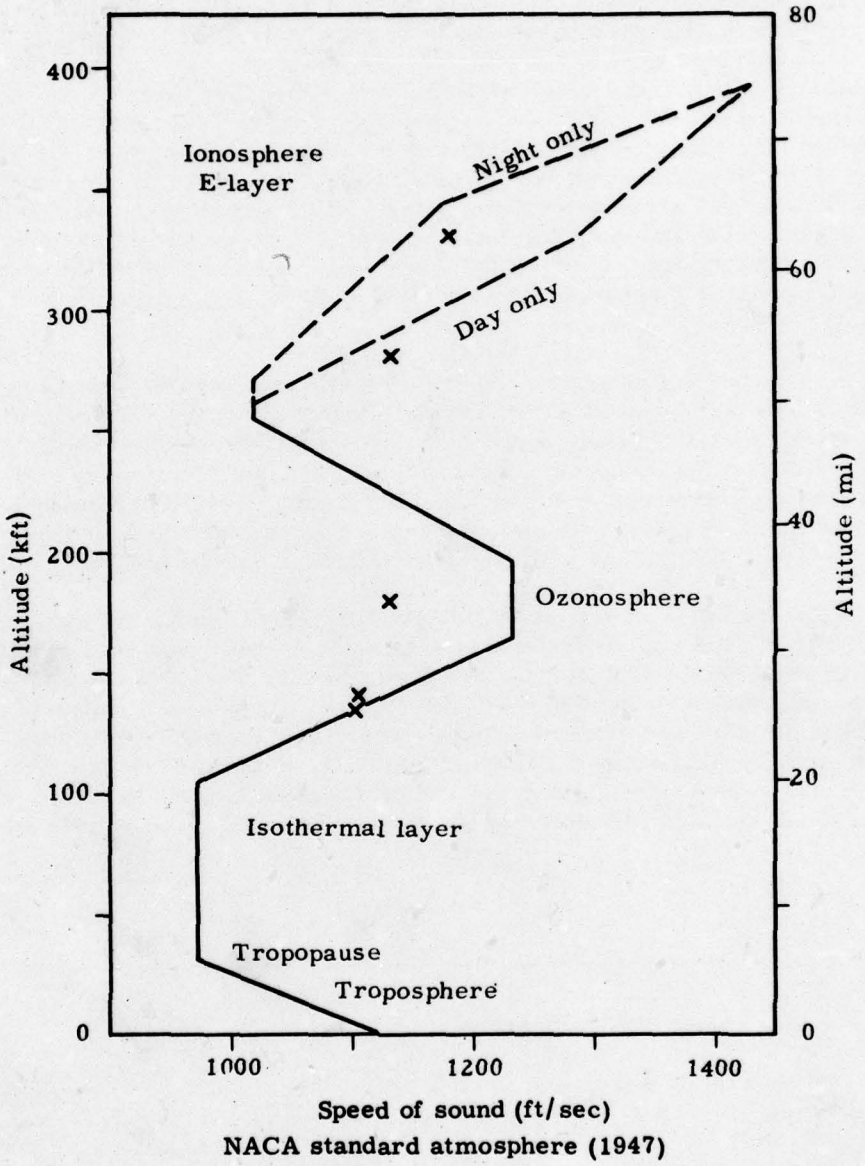

Ionosphere
E-layer
Night only
Day only
Ozonosphere
Isothermal layer
Tropopause
Troposphere
Altitude (kft)
Altitude (mi)
400
300
200
100
0
80
60
40
20
0
1000
1200
1400
Speed of sound (ft/sec)
NACA standard atmosphere (1947)

Fig. 22

to an altitude of 105 kilofeet. Between 105 and 165 kilofeet all rays would be bent toward the horizontal, and some would be bent downward on symmetrical paths to the earth. The situation is similar to that treated in Cases 3 and 7 of this report. If the speed of sound, ie, the temperature, in the ozonosphere is higher than the speed of sound at earth level, then a skip zone and a zone of abnormal sound will exist. The distance between the source and the nearest landing ray and the concentration of sound energy in the zone of abnormal sound depend entirely on the functional relation between speed of sound and altitude.

Five data points obtained from abnormal sound measurements at the time of the Helgoland 'Big Bang' on April 18, 1947, and reported by Cox[14, 15] are plotted (Fig. 22). These experimental points, which were confirmed by V-2 flight measurements at White Sands, New Mexico (Fig. 8, reference 14), show significantly lower values of sound velocity in the ozonosphere than does the standard atmosphere graph. If the velocity of sound in the ozonosphere were much greater than that near the earth, large amounts of acoustic energy would be dumped into abnormal audibility zones. If, on the other hand, sound velocities in the ozonosphere were only slightly larger than those at earth level, the acoustic energy in zones of abnormal audibility could not be large.

As in all the troposphere cases treated so far in this report, sound rays refracted back to earth are reflected and repeat their paths at regular intervals. When or if winds were absent, abnormal audibility zones would form concentric circles around the explosion point. A zone of silence would exist between the shot point and the first zone of abnormal audibility. Additional zones of silence separating consecutive zones of audibility might or might not exist, depending on whether the minimum distance to the second audibility zone was greater or less than the maximum landing distance of rays in the first abnormal audibility zone.

High concentration of energy is found near the inner boundary of abnormal audibility zones[16]. Except for the high altitudes and greater horizontal distances involved, sound ray paths shown in Fig. 23 are similar to those shown in Fig. 7b, which also led to high energy concentration near the inner edge of the focus region. The fact that acoustic energy traveling to distant areas via an ozonosphere route can cause blast damage and leave all areas between the shot point and the first zone of abnormal audibility untouched is proved by the experience of the U.S. Pacific Fleet during gun practices off Catalina Island. Windows were broken in Bakersfield, California, 150 miles from the guns, although only weak sounds were heard in Los Angeles.[17]

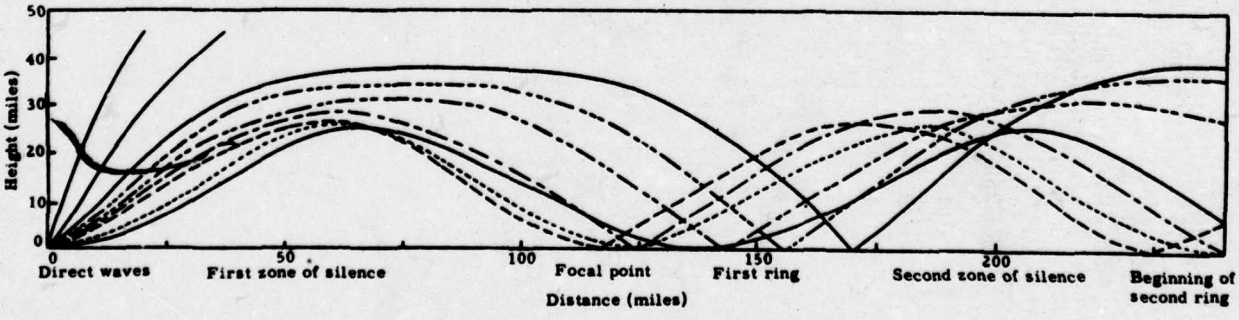


Fig. 23. -- Paths of abnormal sound waves (from Gutenberg)

The inner boundary of the first abnormal audibility zone immediately beyond which the highest concentration of blast energy is most likely to occur seems to be a regular function of the season or month of the year.[18] As shown in Fig. 24 the inner boundary is farthest from the source in July and August (about 120 miles), and nearest to the source in January and February (about 65 miles).* Outer boundaries of abnormal audibility zones are much less easily determined; in fact Cox[19] shows that the acoustic energy in abnormal audibility zones may simply decrease with distance from the source; the real outer boundary for each abnormal zone occurs at infinity.

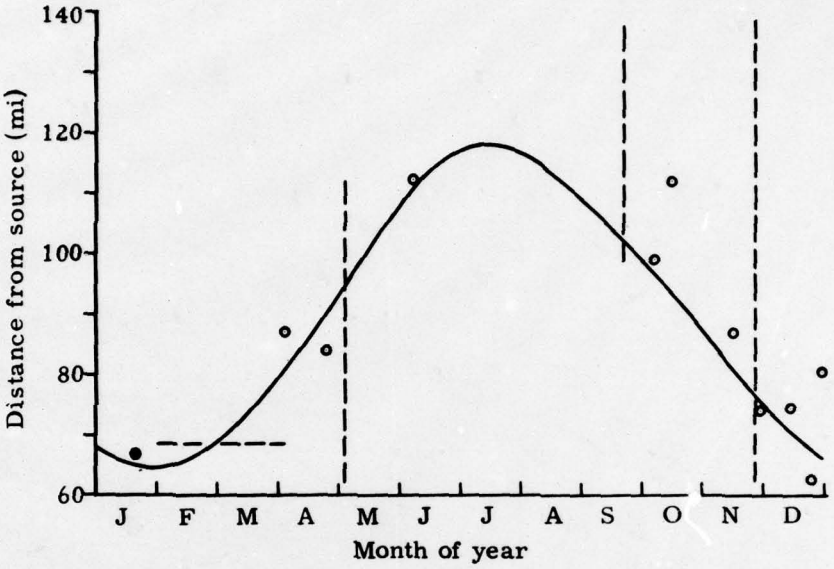


Fig. 24. -- Distance from explosion to inner boundary of first abnormal audibility zone (after A. Wegener, 1925)

Much remains to be learned about abnormal sounds. In the treatment of troposphere signals the profound effects of meteorology on propagation of sound waves has been shown. In matters concerning upper atmosphere meteorology the scientific world is at present very ignorant. Meteorological balloons have not returned data from altitudes exceeding 125 kilofeet so that knowledge of winds, temperatures, and atmospheric composition at higher altitudes is based for the most part on indirect data such as abnormal sound measurements. There is good evidence that stronger and more frequent signals via the ozonosphere route are received east of the source during winter months and west of the source during summer months[20] although some published material supports an exactly opposite point of view. Winds at high elevations, if known, would possibly explain these phenomena, and prevailing winds are very probably a function of latitude; hence latitude variations of abnormal sound propagation might be expected. Since the ozonosphere receives its heat from sunlight, diurnal as well as latitude changes in abnormal sound zones might also be expected. Several of these effects are being investigated by the USAF Geophysical Research Directorate, Cambridge Field Station, Cambridge, Mass. Their publications[21] to date shed some light on the problems but do not in any sense contain answers to all the quandaries.

---

*Some of the damage in Las Vegas during Operation Ranger on Feb. 2 and 6, 1951, may have been caused by ozonosphere signals. No accurate transit-time observations were made, so there is now no way to decide whether ozonosphere signals made any contribution to the damaging blast energy supply which struck Las Vegas.

Molecules composing air are relatively sparse at altitudes above 20 miles, and higher absorption would be expected to result from large mean free molecular paths. Schrödinger treated this problem[22] and concluded that the dependence of sound absorption on wave length and altitude would be as shown in Fig. 25. Significantly less high-frequency content should be expected in abnormal sound signals than in normal ones, ie, those which have traveled entirely within the troposphere. The present experiments confirm this theory. Predominance of low-frequency content is evident in the several sample ozonosphere signals pictured in Fig. 26.

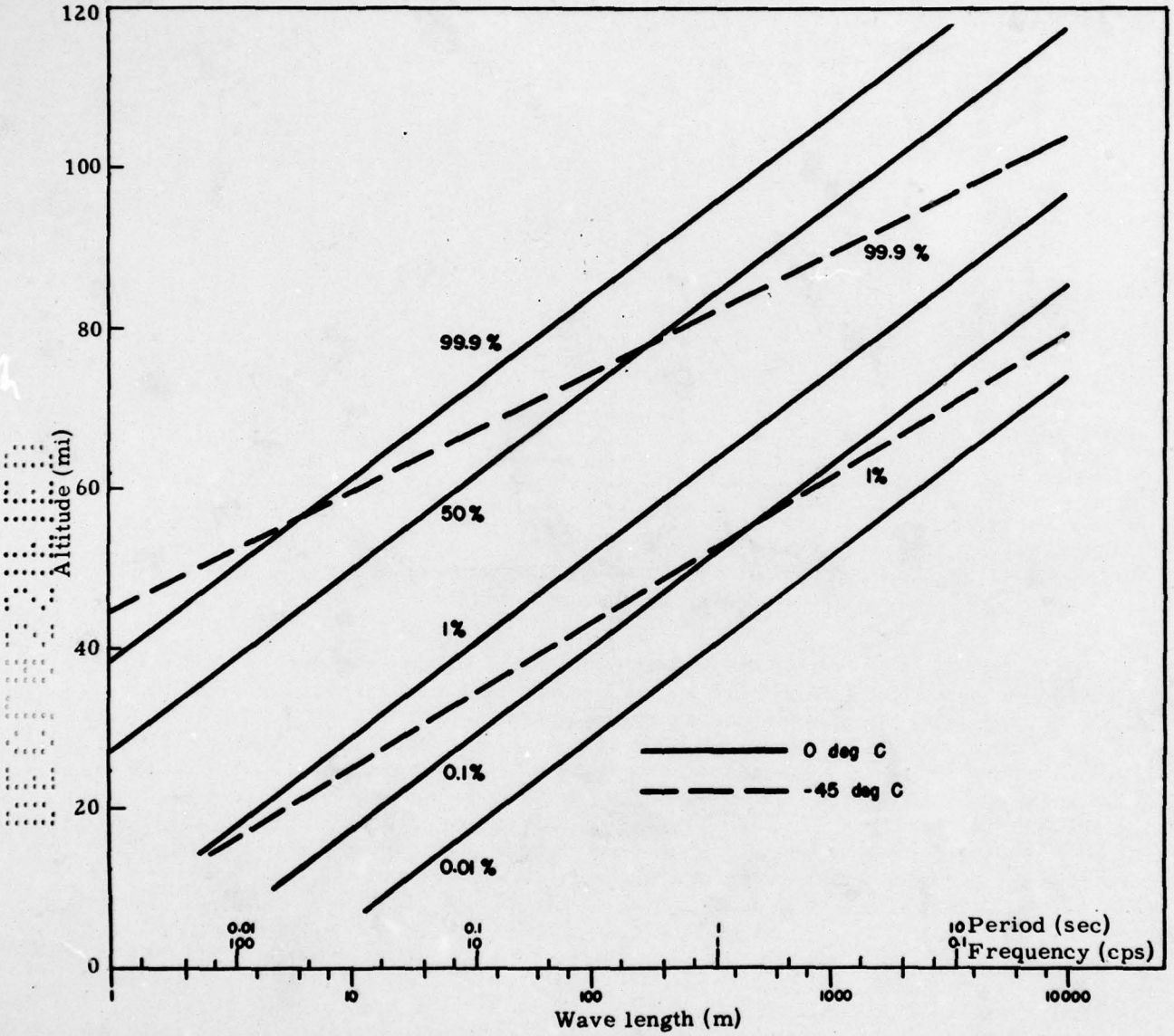


Fig. 25. -- Sound energy absorption per km of path in an isothermal atmosphere (Schrödinger).

Identification of signals which are bent back to earth from the ozonosphere is relatively easy when an accurate measure of travel times of the sound waves from shot point to receivers can be made. From the plot of signal travel times to 135 miles shown in Fig. 2, it is seen that a group of signals arrives at a mean value of 645 seconds. These are normal troposphere signals. Next, a batch of signals which required between 705 and 755 seconds to travel this same distance can be observed. If the apparent velocity of any of these signals which arrived late was computed by dividing horizontal distance from the source by the observed travel time,

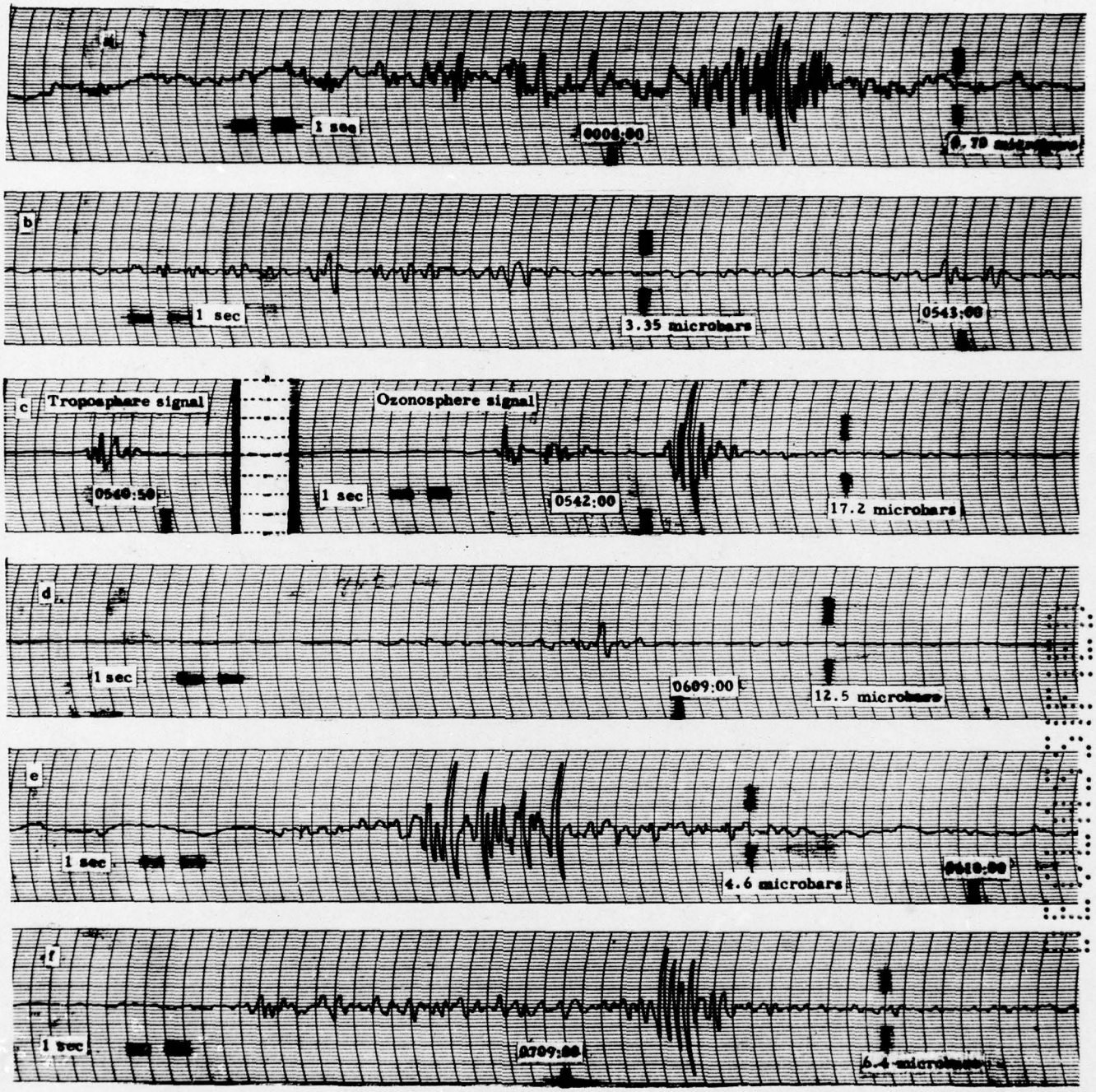


Fig. 26. -- Sample microbarograph records of ozonosphere signals from TNT shots, 1951

(a) Goldfield record of 0.60-ton shot 80.4 miles southwest; shot time 0000:00 PST, September 9. (b) Las Vegas record of 2.4-ton shot 76.6 miles northwest; shot time 0535:00 PST, October 8. (c) St. George record of 1.2-ton shot 135.1 miles east; shot time 0530:00 PST, October 17. (d and e) Henderson and Boulder City records of 1.2-ton shot 87.9 and 99.1 miles, respectively, northwest; shot time 0600:00 PST, October 30. (f) Caliente record of 1.2-ton shot 91.3 miles southwest; shot time 0700:00 PST, November 1.

an abnormally low value of acoustic velocity would result. Signals which arrive late are also shown in Fig. 2 to have been recorded at stations between 75 and 105 miles from the several sources. These signals also are believed to have traveled parts of their paths through the ozonosphere.

If the additional path length required for a signal to reach a selected horizontal distance via an ozonosphere path is considered, it might be surmised that ozonosphere signals would always be weak and incapable of doing damage, but the Bakersfield experience reported by Gutenberg and Richter shows this assumption to be false. Measured peak-to-peak pressures of ozonosphere signals originated by 1.2-ton TNT shots are shown in Fig. 27. At distances beyond 70 miles from the shot point as many ozonosphere signals having peak-to-peak values greater than 50 microbars were observed as troposphere signals having these strengths. Comparison of Figs. 27 and 20 clearly shows this fact. At St. George, 135 miles from the shot points, large signals were always the ones which had traveled via the ozonosphere route. Figure 21, which shows signal strengths of atomic-weapon shots of Operations Buster and Jangle, records many large ozonosphere signals; the largest is greater than 1.2 millibars at St. George following the Buster Dog Shot on November 1, 1951.

Although there were no microbarographs in other than the first abnormal audibility zone, reliable reports of audio observations from the second abnormal zone were received. Rumbling noises were heard in Prescott, Arizona, on the occasion of the Dog and Easy Shots of Operation Buster, and the U.S. Weather Bureau barograph there recorded a pip on each occasion.

Nevada and Utah, both primarily desert, have large diurnal variations of temperature at the earth's surface. If the highest temperature in the ozonosphere were equal to the mean daily temperature at the earth's surface and stayed constant throughout a 24-hour day, one might then expect to find abnormal signals growing weaker during morning daylight hours and increasing in strength during twilight and early night. Abnormal signals would be absent during that part of the day when the temperature at the earth's surface was higher than that of the ozonosphere. Several series of shots were run in a hurried attempt to observe some regular diurnal variation in ozonosphere signal strength, but these initial trials were most inconclusive. Upper atmosphere winds, which we are unable to measure using a simple array of only eight microbarographs, would vitiate any conclusions drawn from these hurried experiments.

In the experiments to determine the dependence of troposphere signal strengths on charge weight (Table IV) several microbarographs recorded ozonosphere signals. Table V shows peak-to-peak values of these abnormal signals. The fact that the peak pressures apparently increased as the first power, not the square root, of the explosive weight caused alarm. If this evident trend had continued, abnormal signals from atomic-weapon shots would have been tremendous and would undoubtedly have caused great damage in St. George and Caliente. The fact that strengths of abnormal signals did not continue to increase proportionally with weapon yield is shown by the recorded values in Fig. 21. We have no explanation for this apparent discrepancy. Further, we can think of no reason why abnormal signal strengths should increase as the first power of charge weight since the theory for these signals should be quite similar to that for troposphere signals, which increase in strength roughly as the square root of charge weight.

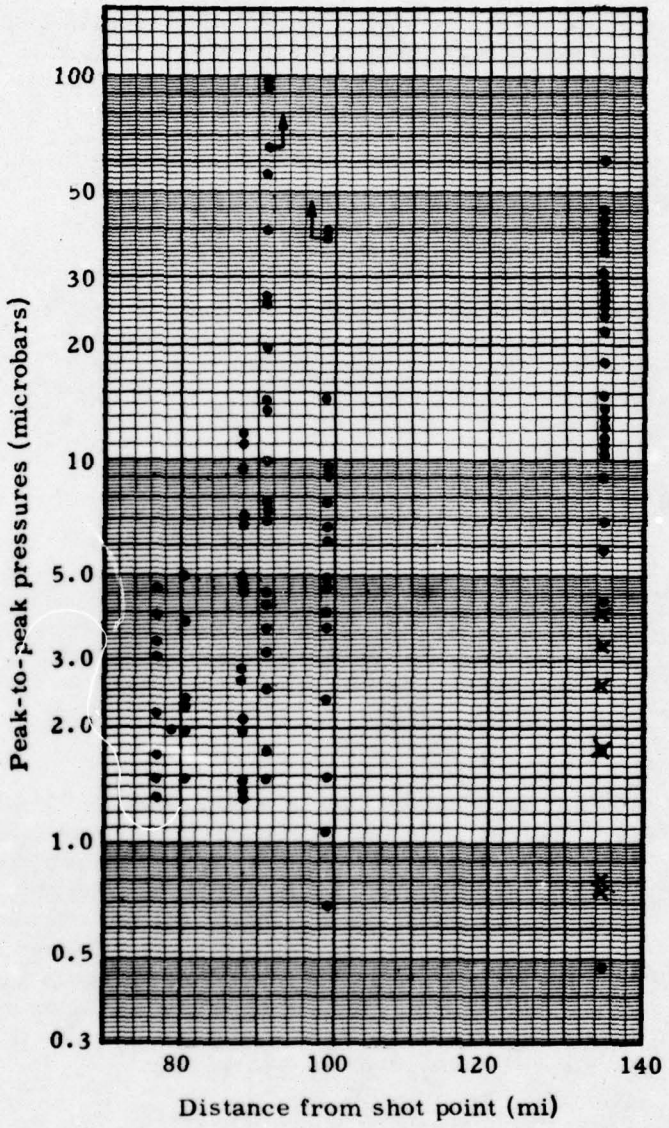


Fig. 27. -- Peak-to-peak pressures of ozonosphere (•) and ionosphere (x) signals from 1.2-ton TNT shots, Nevada, September - November. Arrows show microbarograph went off scale.

UNCLASSIFIED

TABLE V

Ozonosphere and ionosphere signals, peak-to-peak pressures (microbars)

Date	Station	Pressure per given weight of TNT 0.6 ton	1.2 tons	2.4 tons
Oct. 8, 1951	Las Vegas	0.71	1.7	3.5
	Henderson	1.0	2.1	x
	Boulder City	x	5.8	x
	Caliente	2.7	4.5	6.4
	Goldfield	0.8	1.5	1.6
	St. George (ozonosphere)	5.9	12.1	25
	St. George (ionosphere)	0.48	0.74	1.6
Oct. 9, 1951	Las Vegas	1.9	1.5	2.7
	Henderson	2.0	2.6	5.1
	Boulder City	bb	1.5	3.2
	Caliente	2.8	4.2	5.2
	Goldfield	0.63	2.3	2.9
	St. George (ozonosphere)	21	21	28
	St. George (ionosphere)	0.82	3.3	2.1

x - station not operating
bb - bad background noise
Shot schedule Oct. 8: 1.2 tons, 0515 PST; 0.6 tons, 0525 PST; 2.4 tons, 0535 PST.
Oct. 9: 1.2 tons, 0100 PST; 0.6 tons, 0110 PST; 2.4 tons, 0120 PST.

Except for determining by advance TNT shots where abnormal blast waves will concentrate and how strong they will be, the behavior of abnormal sounds can not be predicted. It is believed that there is a statistical trend in minimum landing distances as shown in Fig. 24. In predicting signal strengths to be expected from an atomic weapon shot planned for a specific hour on a certain day, however, one should not be content with statistics containing large variance. The Santa Fe Operations Office of the Atomic Energy Commission has consequently asked the Sandia Laboratory to continue microbarometric experiments throughout a calendar year in an effort to improve predictability, especially of abnormal signals. If improved equipment can be obtained in the near future in sufficient quantities to make the experiments meaningful, these experiments will be reported at a later date.

Ionosphere E-Layer Signals

Dissociation of oxygen and increasing temperature [23] give rise to increased sound velocity in the NACA standard atmosphere at altitudes above 260 kilofeet (Fig. 22). If the velocity of the sound in this atmospheric band (the ionosphere E-layer) is truly higher than it is in both the ozonosphere and troposphere, then sound signals, also abnormal in character, should be returned to earth from the ionosphere.

UNCLASSIFIED

[redacted]
UNCLASSIFIED

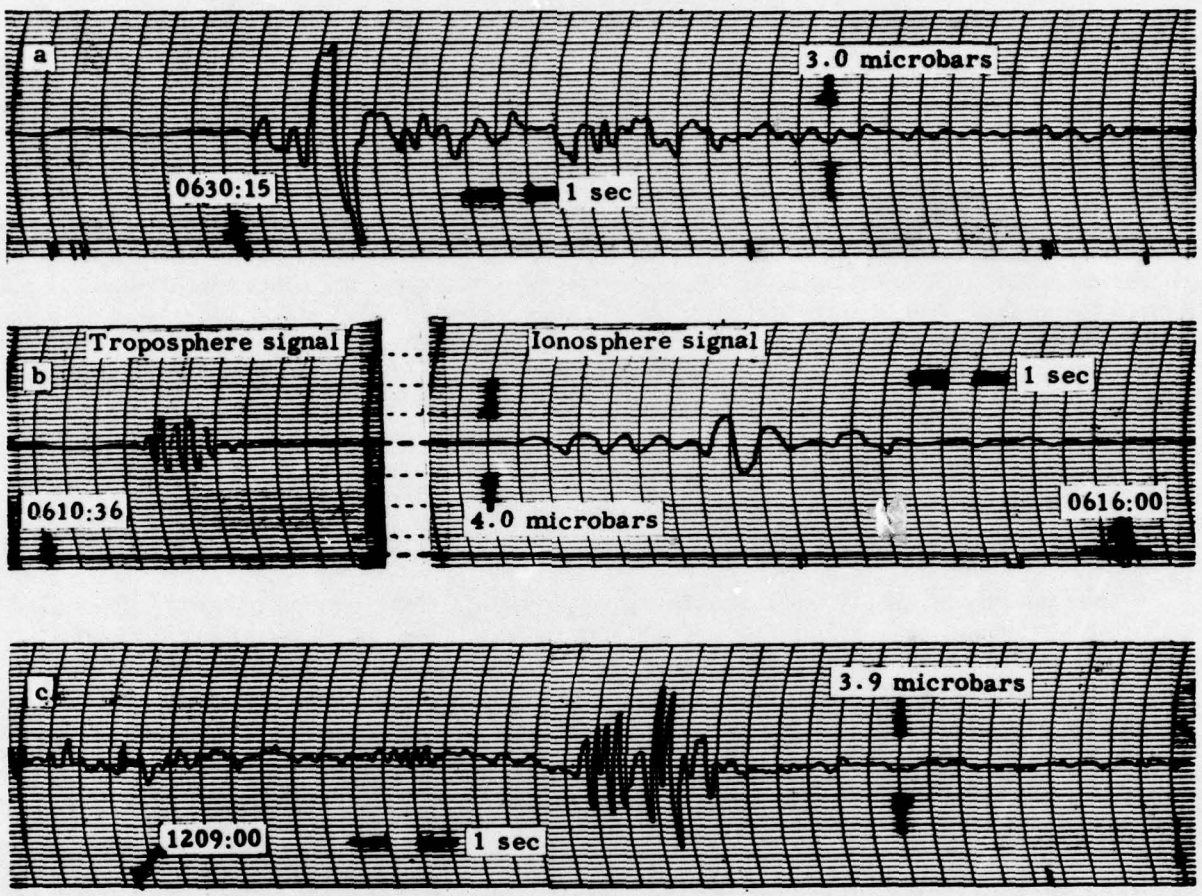


Fig. 28. -- Microbarograph records of ionosphere signals

a Section of St. George, Utah, record from 0.60-ton TNT explosion 133.6 miles west. Shot time 0615:00 PST, September 11, 1951.

b Sections of St. George, Utah, record from 1.2-ton TNT explosion 135.1 miles west. Shot time 0600:00 PST, September 22, 1951.

c Probable ionosphere signal recorded at Goldfield, Nevada, from 0.60-ton TNT shot 80.4 miles southeast. Shot time 1200:00 PST, September 7, 1951.

[redacted]
UNCLASSIFIED

Figure 2 shows some ten signals having exceptionally long travel times to a horizontal distance of 135 miles. In their travel to St. George these signals have required more than four minutes longer than troposphere signals and almost three minutes longer than ozonosphere signals. Because of these extreme delays and the character of the signals we are quite convinced they have been refracted to earth from the ionosphere. Similar signals, although of poorer quality, were observed from the Helgoland 'Big Bang' and have been reported by Cox et al.[15] Schrödinger's absorption graph (Fig. 25) shows that only very long wave lengths could be present in ionosphere signals recorded on earth, and the samples of these signals shown in Fig. 28 are unquestionably devoid of high frequencies.

To date, signals returned from the ionosphere E-layer from 0.6- and 1.2-ton TNT shots have all been less than eleven microbars peak-to-peak amplitude. Strengths of these signals are shown in Figs. 27 and 31 with ozonosphere signals. Natural microbarometric background is often found to be this high or higher. There is no present evidence then that we need fear blast damage resulting from ionosphere signals. The recordings in Fig. 28 are regarded only as excellent proof that scientific investigation of the atmosphere above 250 kilofeet might well be feasible using carefully planned microbarometric experiments.

The Microbarograph

When audible sounds are discerned at great distances from explosions, they are heard as very-low-frequency bass rumbles. There is, in fact, some doubt whether the audible sounds originate in the explosion or whether they come from windows, doors, and the like which have been shaken by infrasonic, inaudible pressure perturbations. It is known that between the explosive source and a distant observer essentially all high-frequency components have been lost by absorption in the air and that the main energy-carrying frequency components received at distant stations are infrasonic. Consequently any equipment employed to measure blast pressures at distant stations must be capable of responding to infrasonic perturbations and need not be responsive to audio frequencies.

The microbarograph (infrasonic microphone) used in the present operations was designed and constructed by the Rieber Research Laboratory, New York.* Figure 29 is a schematic diagram of the system. The diaphragm of the microphone controls the tension in a vibrating wire which is driven in its first mode by an electromagnet. A pickup coil, which samples the oscillation amplitude of the vibrating wire, controls the frequency and power of the driving coil through a feedback circuit. A matched electromechanical system, except for the diaphragm, forms the other half of the system, and leads from both pickup coils terminate in a frequency difference discriminator. When both oscillating strings are vibrating at the same frequency, the output from the frequency difference discriminator to the recorder is zero. When the diaphragm of the microphone is depressed by application of pressure on its outer face, the tension in the microphone string is lessened and its oscillation frequency reduced. The discriminator now sees two strings vibrating at different frequencies, and the output to the recorder is an indication of the excess pressure on the face of the diaphragm.

---

*Mr. Frank Rieber, founder and owner of Rieber Research Laboratory, died in 1948; therefore the laboratory is no longer operating.

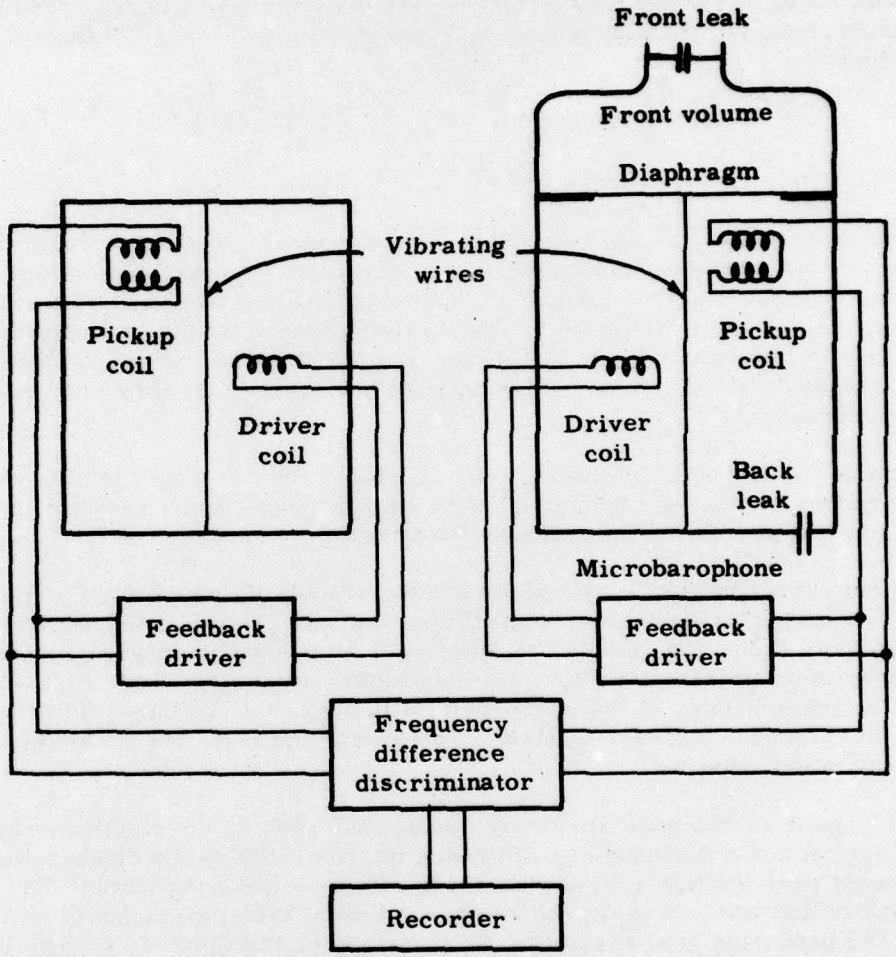


Fig. 29. -- Schematic of microbarograph

The first mode oscillation frequency of a vibrating string is given by the formula

$$\nu = \frac{1}{2L}\sqrt{\frac{T}{m}} \tag{68}$$

where ν is the frequency, L is the string length, T is the tension, and m is the mass per unit length of string. If one end of the string is fixed and the other end is attached to the center of a diaphragm which may deflect, any movement of the diaphragm will cause a change in both length and tension of the string. The change in tension, dT, and change in length, dL, causes a change in frequency

$$d\nu = \left[dT/2LT^{1/2} - T^{1/2}\, dL/L^2\right] / 2m^{1/2}$$

$$\approx dT/4L\,(mT)^{1/2}. \tag{69}$$

For the microbarophone the first term in the brackets is much larger than the negative term, and we may ignore the second term with respect to the first. For any plate diaphragm, deflection of its center is proportional to applied overpressure. Since one end of the vibrating string is fastened to the center of the diaphragm, the change in tension in the string is, according to Hook's law, proportional to the diaphragm deflection, which in turn is proportional to the applied overpressure. Therefore the change in frequency of the vibrating string is proportional to applied overpressure.

Thus the microbarograph recorder, which literally records only the difference in frequencies between two oscillating strings, makes a record proportional to the overpressure, or under-pressure, applied to the microphone diaphragm.

If the volume of air back of the diaphragm were sealed off completely from outside air, any change in barometric pressure, no matter how slow, would deflect the diaphragm. To free the system from recording diurnal and other very slow changes in pressure, including those produced by thermal effects on the microbarophone, a slow air leak, called the back leak, connects the back volume of the microphone with outside air. This leak becomes a high-pass filter for the electromechanical system. The slower the leak, the lower the frequencies to which the system will respond.

Since the signals in which we are interested are infrasonic, the electromechanical system is designed to cut out audio frequencies. To reach the front face of the diaphragm pressure perturbations must pass through a front leak which acts as a low-pass filter. The double-leak system, one before and one behind the diaphragm, forms a band-pass filter to select frequencies of interest. The band pass can, of course, be varied by changing either or both leaks. Figure 30 typifies the response versus frequency curve of the microbarographs as they were used.

When a microbarophone as illustrated in Fig. 29 is exposed outdoors, wind turbulences in the vicinity of the instrument create local changes in pressure which are entirely insignificant in our study of pressure from explosions. This background noise is a great nuisance, for it frequently masks signals which are desirable to observe and measure. As a partial remedy to the problem of background noise four 25-ft lengths of garden hose were laid on level ground in the design of a + sign. At 5-ft intervals along each hose length a small metal plug was inserted through the hose wall, and the outer end of each hose was blocked. Each metal plug had an orifice 0.055 inch in diameter and was 1/2 inch long. Adjacent ends of the four hose lengths terminated in a small volume which capped the diaphragm. When these arrays are used, small turbulences do not affect the microphone, but pressure perturbations having wave lengths exceeding 50 feet are faithfully registered.

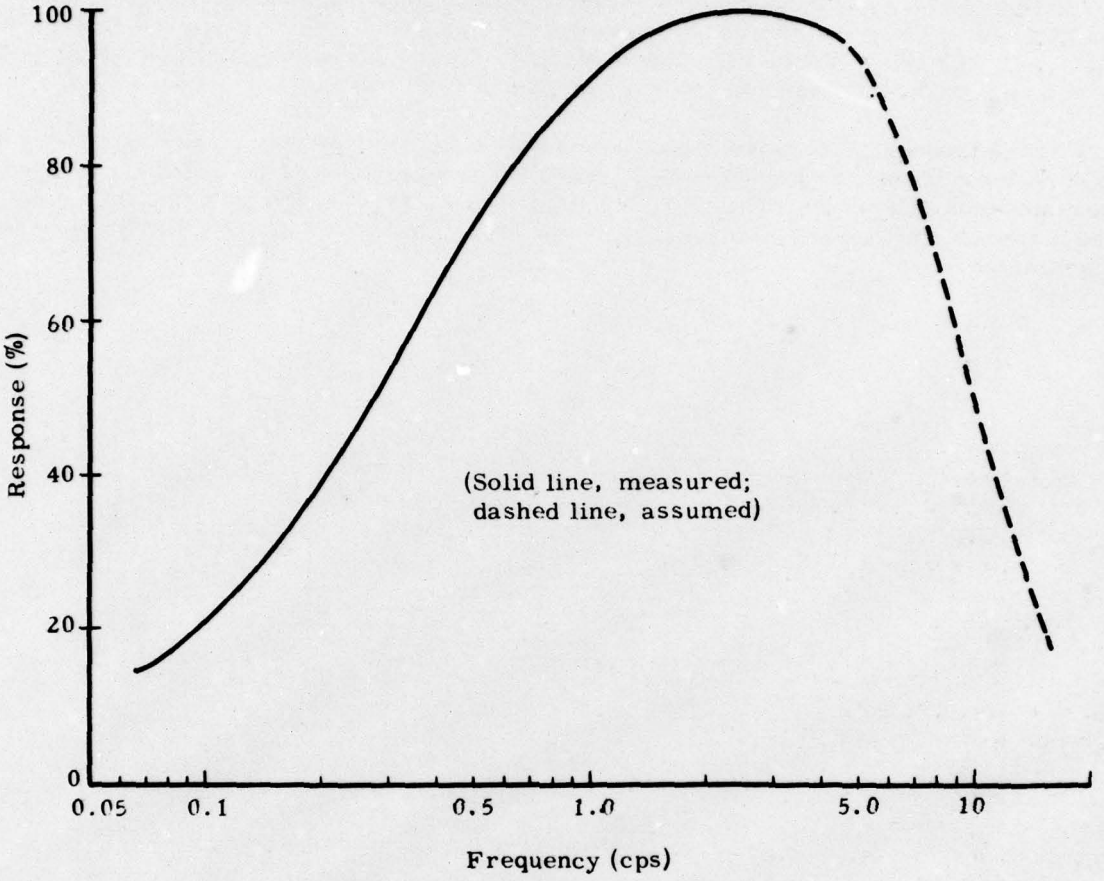


Fig. 30

Amplitude calibration of the system was performed using an electrically driven piston pump which acted into a five-gallon carboy. A small battery-powered motor rotated an eccentric cam, which in turn drove the piston at the rate of 2 cps. The piston motion gave adiabatic compression to the air in the carboy. During calibration the hose array was disconnected from the front volume, and the carboy and piston system was connected to the volume capping the diaphragm. The calibration pressure customarily employed was 13.8 microbars peak-to-peak.

The dynamic range of the microbarographs used is very great; yet from the experience already reported on atomic weapon tests the maximum pressure these particular instruments could record was not enough for the job. Control of the dynamic range is supplied by the amplifiers associated with the frequency difference discriminator. The amplifiers contain a continuous variable resistor which can be changed using a screwdriver, and step-resistance attenuators were arranged to give amplifications of 1 to 256 units in steps of two. The most sensitive (highest gain) setting produced a full-scale deflection of 40 millimeters on the Brush recorder when incident pressure on the microbarophone was 2.5 microbars peak-to-peak. The least sensitive operation of the equipment, in which all available attenuation was inserted into the electrical system, gave full-scale operation of the Brush recorder for approximately one millibar peak-to-peak pressure on the diaphragm.

Each microbarograph station was supplied with a radio set capable of receiving WWV time signals. A side pen attached to an electrical relay was installed on each Brush recorder and the electrical relay connected to the radio set. Timing accuracies to the beginning of each recorder signal are therefore judged to be about 0.2 second.

When the experiments were begun in September, an attempt was made to conserve TNT by using 0.6-ton shots. Figure 31 shows peak-to-peak pressures of the signals recorded. In so many instances, however, natural background was so large compared with the signals recorded that we were forced to use larger charges to obtain signals which could be measured with confidence.

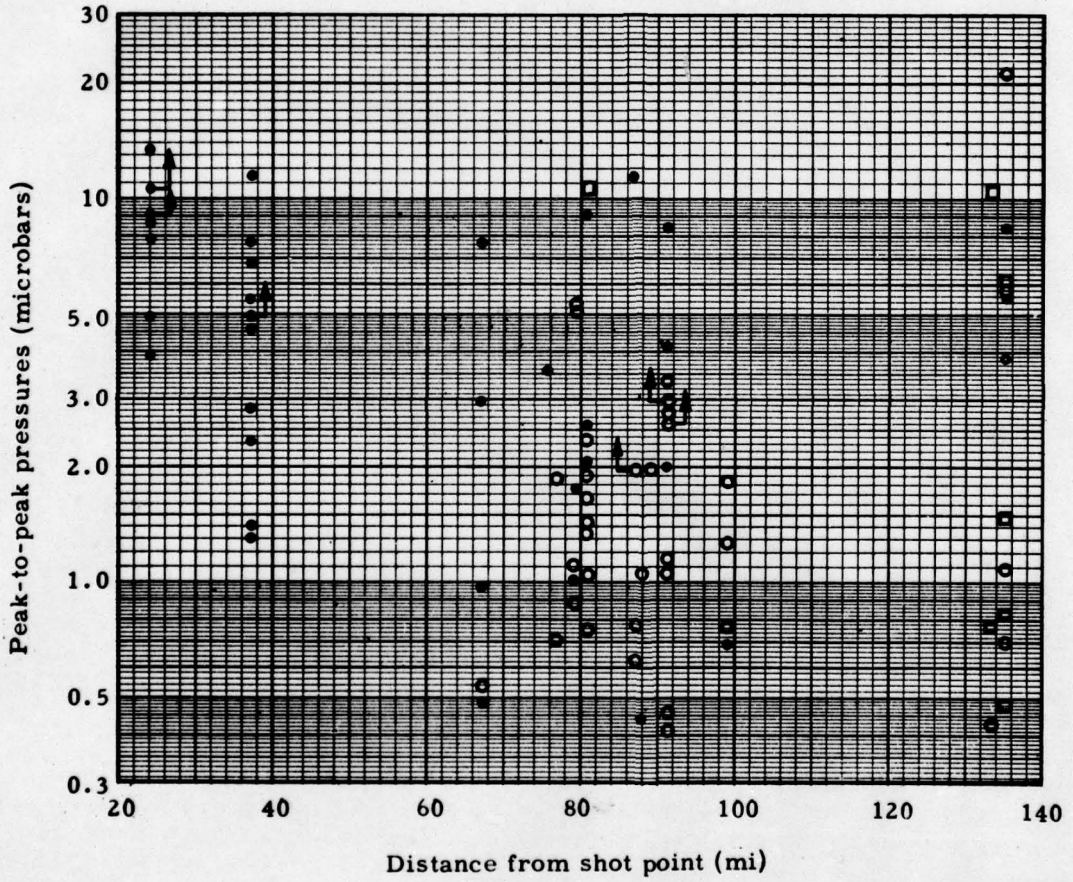


Fig. 31. -- Peak-to-peak pressures of troposphere (•), ozonosphere (o), and ionosphere (□) signals from 0.6-ton TNT shots.

LIST OF REFERENCES

1. Becker, R., Zeits. für Physik 8, 321(1923); Thomas, L. H., J. Chem. Phys. 12, 449(1944); Patterson, G. N., UTIA Report No. 1, The Institute of Aerophysics, University of Toronto, May 1948; Mott-Smith, H. N., AEC - WASH - 28, January 9, 1950

2. Stokes, E. E., Phil. Mag 34, 52(1849)

3. Lord Rayleigh, The Theory of Sound, Vol 2, Sec 270, Dover Publications, New York, 1945

4. Ibid, Sec 289

5. Fujiwhara, S., Bull. Cent. Meteor. Obs. Japan 2 (1) (1912) and 2, (4) (1916)

6. Smith, L. G., Division 2 OSRD Report No. 6270, 1945, and numerous theorectical papers by J. von Neumann, S. Chandrasekhar, R. J. Seeger, H. Polachek, K. O. Friedrichs, A. Weise

7. Rothwell, P., J. Acoust. Soc. Amer. 19, 205(1947)

8. The Effects of Atomic Weapons, Prepared under the direction of the Los Alamos Scientific Laboratory, U. S. Government Printing Office, 1950

9. Timoshenka, S., Vibration Problems in Engineering, 2nd ed., Van Nostrand, New York (1947) p 423

10. Schilling, H. K., et al, J. Acoust. Soc, Amer. 19, 222(1947) and many related papers by E. Hiedemann, W. H. Peilemeier, H. O. Kneser, etc

11. Maulard, Compt. rend. 229, 25(1949); Abbey and Barlow, Australian J. Sci. Res. 1 (A), 175 (1948)

12. Whipple, F. J. W., Nature 111, 187(1923)

13. NACA Technical Note No. 1200(1947)

14. Cox, E. F., Amer. J. Phys. 16, 465(1948)

15. Cox, E. F., Atanasoff, J. V., Snavely, B. L., Beecher, D. W., and Brown, J., J. Meteor. 6, 300(1949). The bibliography of this report contains 55 references to abnormal sound and related subjects

[redacted] UNCLASSIFIED

LIST OF REFERENCES (cont)

16. Gutenberg, B., Zeits. f. Geophysik 2, 101(1926)

17. Gutenberg, B., and Richter, C. F., Gerlands Beitrage zür Geophysik 31, 155(1931)

18. Wegener, A., Meteor. Zeit. 42, 261(1925)

19. Cox, E. F., J. Acoust. Soc. Amer. 21, 6(1949)

20. Final report on project authorization B/ 10/ A/ ONR/ NEL by C. T. Johnson, F. E. Hale, and A. B. Focke, Naval Electronics Laboratory, San Diego, September 30, 1951 (Confidential)

21. Crary, A. P., Geophysical Division Technical Report No. 40, Parts I-IV, Air Force Cambridge Research Laboratories, 1948 and 1949

22. Schrödinger, E., Phys. Zeits 18, 445(1917); see also Lindsay, R. B., Amer. J. Phys., 16, 371(1948)

23. Penndorf, R., J. Geophys. Res. 54, 7(1949); Phys. Rev. 77, 561(1950); Bull. Amer. Meteor. Soc. 31, 71 and 126(1950); J. Meteor. 7, 243(1950)

UNCLASSIFIED [redacted]

Appendix A to:
Damaging Air Shocks At Large
Distances From Explosions

A SIMPLIFIED METHOD FOR COMPUTING SOUND RAY PATHS THROUGH THE ATMOSPHERE

by Capt. J. W. Reed, USAF

Although Rothwell[7] makes a number of assumptions in deriving his system of figuring sound ray paths through the atmosphere, one additional assumption makes a very significant reduction in the amount of calculation required to plot rays. All through his work Rothwell employs the accurate statement of Snell's law given by equation 9, but since present-day RAOB measurements of meteorological functions can not be counted on to give wind velocities of greater accuracy than perhaps three feet per second, use of equation 13 in place of equation 9 is fully justified. This amounts to assuming that the wind component along the inclined ray is equal to the measured horizontal wind.

The horizontal distance increment, dx, along a sound ray path is related to the vertical increment dh by equation 14. Combination of equations 13 and 14 gives

$$dx = \left[\left(\frac{V_0}{V}\right)^2 - \cos^2 \Theta_0\right]^{-1/2} \cos \Theta_0 \cdot dh. \tag{70}$$

Meteorological data in general are supplied at fixed elevations, usually at 1000-ft intervals. With no knowledge of the behavior of the functions between these elevations, interpolation is usually linear. A plot of V vs h thus becomes a number of straight-line segments. Let subscript i represent the i^{th} level; then between the i^{th} level and the $(i + 1)^{th}$ level

$$V = V_i + k\,(h - h_i), \tag{71}$$

where k is the line slope.

Following insertion of equation 71 into equation 70 the expression can be integrated by substituting

$$q = \frac{V_0}{V} = V_0 / \left[V_i + k\,(h - h_i)\right] \tag{72}$$

and

$$dh = -V_0 \cdot dq / kq^2. \tag{73}$$

Integration gives

$$x_{i+1} - x_i = (V_0 / k \cos \Theta_0) \left[\frac{(q_{i+1}^2 - \cos^2 \Theta_0)^{1/2}}{q_{i+1}} - \frac{(q_i^2 - \cos^2 \Theta_0)^{1/2}}{q_i}\right]. \tag{74}$$

Returning now to the original coordinates

$$x_{i+1} - x_i = \left[\frac{h_{i+1} - h_i}{V_{i+1} - V_i}\right] \left\{ \left[\left(\frac{V_0}{\cos \Theta_0} \right)^2 - V_{i+1}^2 \right]^{1/2} - \left[\left(\frac{V_0}{\cos \Theta_0} \right)^2 - V_i^2 \right]^{1/2} \right\}. \quad (75)$$

At the apex of a ray path the ray is horizontal, and $\cos \Theta_p = 1$. Hence the horizontal travel distance from ground level to level p where the ray is horizontal is

$$x_p - x_0 = \sum_{i=0}^{i=p} \left[\frac{h_{i+1} - h_1}{V_{i+1} - V_i}\right] \left\{ \sqrt{V_p^2 - V_{i+1}^2} - \sqrt{V_p^2 - V_i^2} \right\}. \quad (76)$$

The total horizontal distance traveled in a complete arc returning to the ground is $2(x_p - x_0)$. This form is found to be very convenient for tabular computations. When wind velocity and air temperature (or speed of sound) are provided for every 1000-ft level, the only aid required to make all computations is a wind-resolving chart described by Rothwell (Fig. 3 of reference 7).

A minor change in procedure is required in the occasional case $V_{i+1} = V_i$. No refraction takes place at the boundary between these two layers, and $\Theta_{i+1} = \Theta_i$. But since

$$\cos \Theta_{i+1} = \frac{V_{i+1}}{V_p}, \quad (77)$$

then

$$x_{i+1} - x_i = (h_{i+1} - h_i) \cot \Theta_{i+1} = \frac{(h_{i+1} - h_i)\, V_{i+1}}{\sqrt{V_p^2 - V_{i+1}^2}}. \quad (78)$$

In practice, to facilitate refracted energy distribution analysis, it is recommended that the V vs h graph be drawn for each direction of interest. Significant levels where the slope of V changes appreciably may be noted and the initial elevation angle Θ_0 for the ray which would become horizontal at each level can be calculated from equation 13 or 9. Also the altitude at which convenient intermediate rays would become horizontal can be determined from either of these equations.

When the various rays and corresponding significant levels have been determined from preliminary analysis of the V vs h graphs, one tabulation of data common to all rays in a particular direction is made, and another tabular computation is then performed for each ray angle desired. Headings for the blank forms used are shown in Tables VI and VII.

TABLE VI

Sound ray calculations

Date_____
Time_____
Direction_____

Col No.	1	2	3	4	5	6	7	8
Level	Height (h)	c = speed of sound	u = wind component	V = (Col 2 + Col 3)	$V^2 = (\text{Col } 4)^2$	$h_{i+1} - h_i = \Delta(\text{Col } 1)$	$V_{i+1} - V_1 = \Delta(\text{Col } 4)$	$\frac{h_{i+1}-h_i}{V_{i+1}-V_i} = (\text{Col } 6/\text{Col } 7)$
0	X	X	X	X	X	X	X	X
1	X	X	X	X	X	X	X	X
2	X	X	X	X	X	X	X	X
3	X	X	X	X				

TABLE VII

Sound ray calculation

Date_____
Time_____
Direction_____
Θ_____

Col No.	I	II	III	IV
Level	$V_p^2 - V_{i+1}^2 = (\text{Col } 5)_p - (\text{Col } 5)_{i+1}$	$\sqrt{V_p^2 - V_{i+1}^2} = \sqrt{\text{Col I}}$	$\Delta(\text{Col II})$	(Col III x Col 8)
0	X	X	X	X
1	X	X	X	X
2	X	X	X	X
3	X	X		

Total horizontal travel distance = 2Σ (Col IV)

UNCLASSIFIED

[redacted]

Appendix B to:
Damaging Air Shocks at Large Distances from Explosions

The following collection of graphs, Figs. 32-44, depicts meteorological situations and sound ray paths for a number of interesting cases, including those for the Buster and Jangle Shots.

Fig. 32a

Southeast

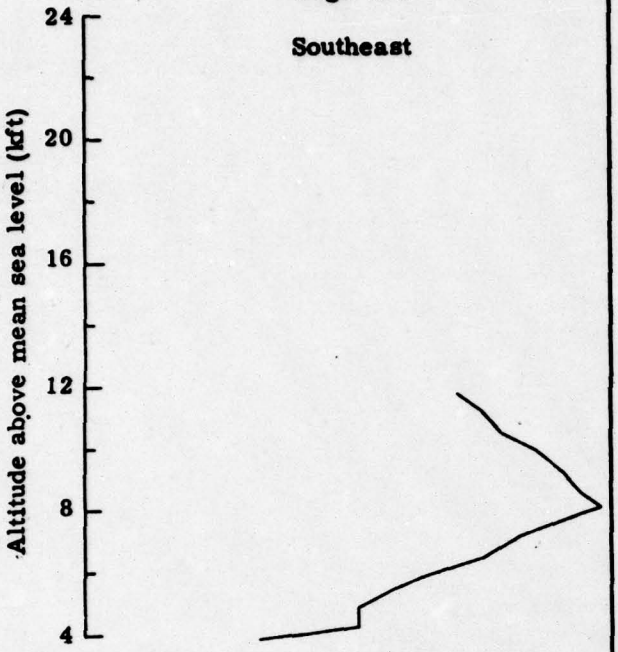


Fig. 32b

Southeast

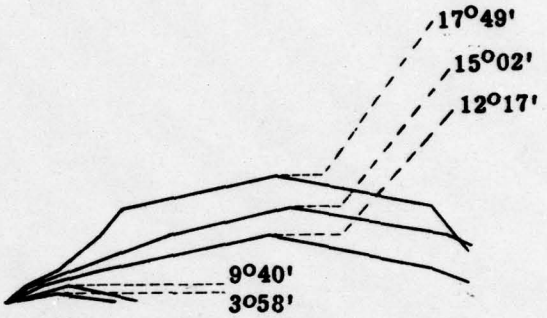


Fig. 32. -- Meteorological conditions and sound ray paths, February 6, 1951, at 0700 PST

Fig. 33a

Southeast

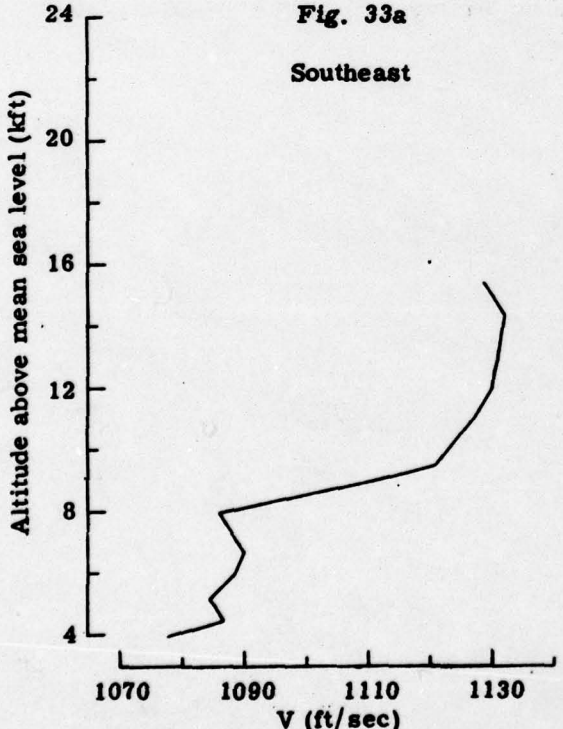


Fig. 33b

Southeast

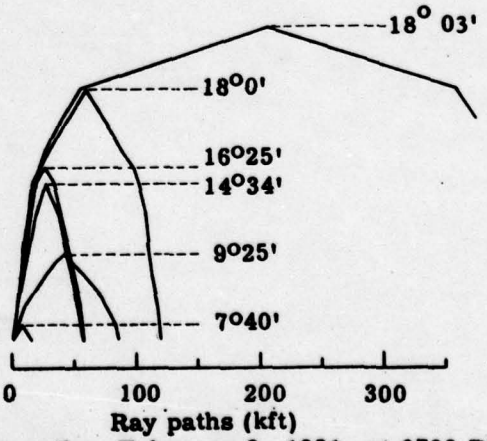


Fig. 33. -- Meteorological conditions and sound ray paths, February 2, 1951, at 0700 PST

RANGER DOG AND EASY SHOT

Figures 32 and 33 show conditions southeast of Frenchman Flat on February 6 and 2, 1951, during Operation Ranger. Wind shear on both dates sent large acoustic signals southeast from the shot point. Ground zero was 68 miles (3.6×10^5 feet) from Las Vegas and 24.2 miles (1.3×10^5 feet) from Indian Springs.

As can be seen by comparison with later graphs of this appendix the quantity of acoustic energy held within the troposphere was very great on both of these dates and amounted to essentially 18^o in each instance. Figure 32b shows that on February 6, 1951, Las Vegas must have received a small amount of direct energy and a small amount of energy reflected once, but rays reflected two or more times brought a large amount of energy to Las Vegas. On this same date Indian Springs received a heavy direct shock, and all reflected rays added significant energy to the direct load. Heavy damage was reported from Indian Springs and minor damage from Las Vegas.

Figure 33b shows conditions on February 2, 1951, an intense focus occurring at 60 kilofeet, and a band of strong energy which covers the span from 60 to 120 kilofeet. The focal point at 60 kilofeet fell slightly short of half the distance to Indian Springs but after five reflections struck Las Vegas. Las Vegas therefore received potent second, third, fourth, and fifth reflections. On the other hand, Indian Springs received a powerful first reflection and only weak reflections of higher order up to the sixth. The heavy damage in Las Vegas was probably a result of the sharp focus occurring at 60 kilofeet.

No microbarographs were operating at the time of the Ranger Shots; so no pressure data are available.

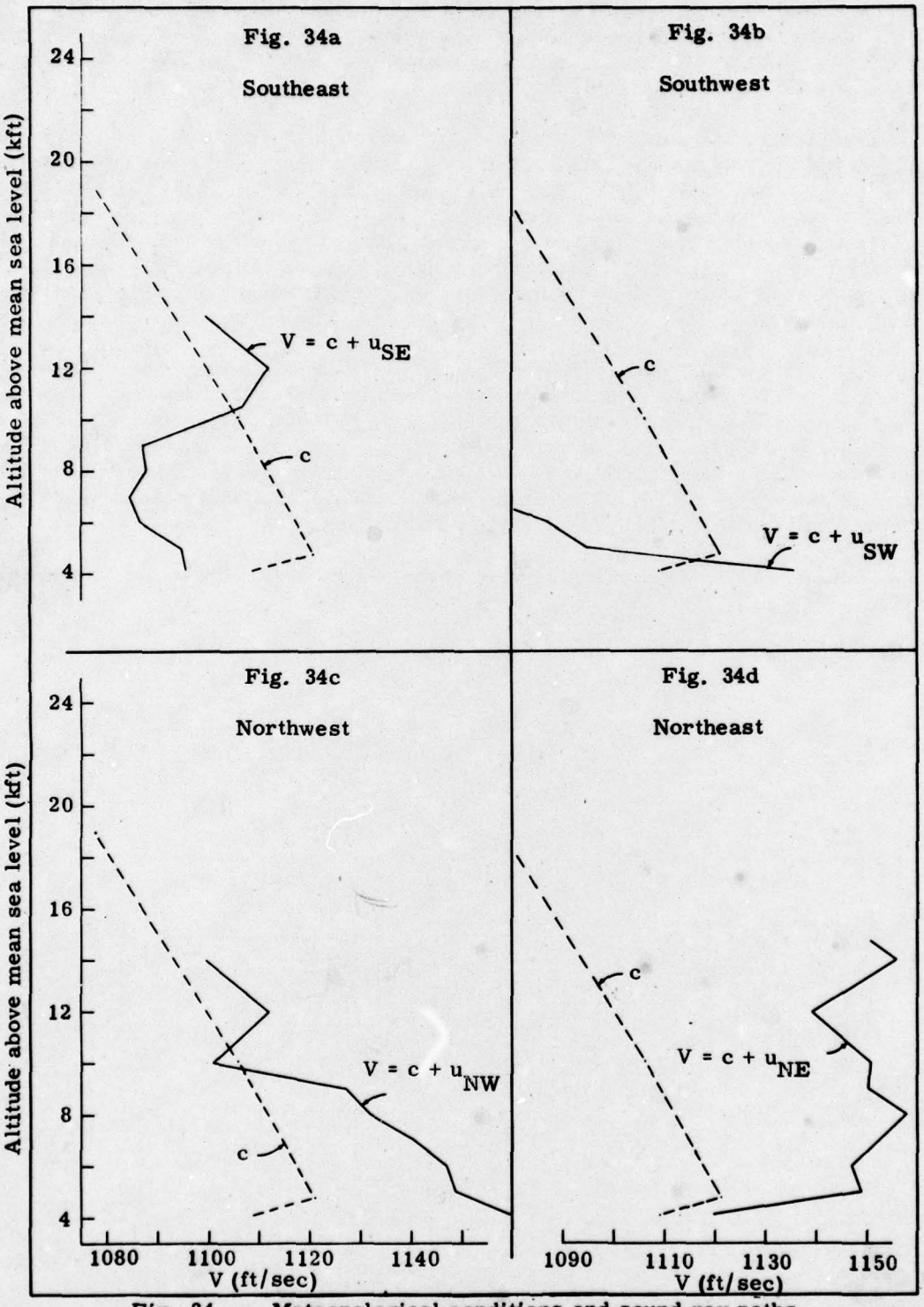


Fig. 34. -- Meteorological conditions and sound ray paths, August 29, 1951, at 0830 PST

TNT SHOTS

The series of microbarometric experiments covered by this report began on August 29, 1951, when one microbarograph was installed at Indian Springs for instruction purposes. An excellent record was obtained following a 0.6-ton TNT explosion at Site T-3. Unfortunately the amplitude calibration equipment was not ready for use, so we have no measure of the signal strength.

The case is presented in Figs. 34a-f to illustrate a very interesting and unusual meteorological condition. Dashed lines on Figures 34a-e show sound velocity c as a function of altitude, and the solid lines show the results of adding wind components to the c curve. From the surface up to 9000 ft above mean sea level there was a positive wind component toward the northeast. Above this altitude the shift in wind direction caused total sound velocity in the southeasterly direction to exceed its value at the earth's surface; consequently there was sound propagation to the southeast as shown in Fig. 34f. This case shows that one may never conclude from only surface observations that damaging shocks will not travel in a direction against the wind.

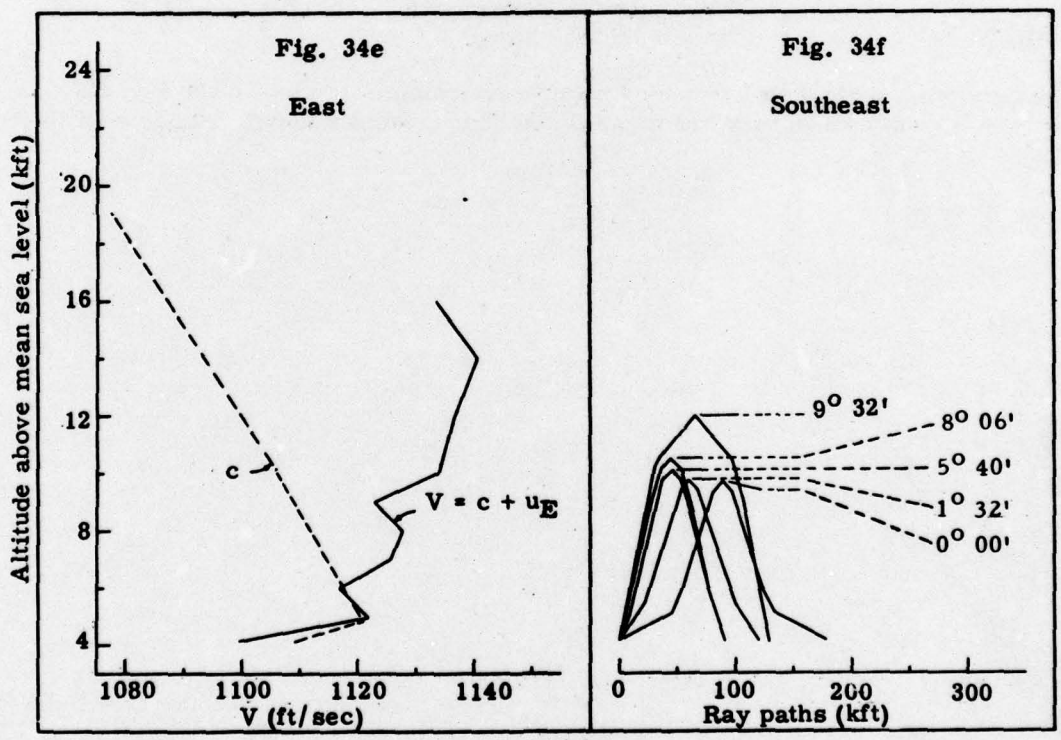


Fig. 34 (cont)

TNT SHOTS

Figures 35 and 36, which deal with 1.2-ton TNT shots at 0600 MST on September 22 and 28, 1951, are of interest largely because of their contrast.

On September 22, 1951, the following signal strengths were recorded:

TABLE VIII

Station	Travel time (sec)	Signal type	Peak-to-peak pressure (microbars)
Indian Springs	171	Troposphere	105
Las Vegas	391	Troposphere	> 27
Henderson	423	Troposphere	> 31
Boulder City	462	Troposphere	18.6
	553	Ozonosphere	0.68
Caliente	437	Troposphere	4.2
	516	Ozonosphere	1.71
Goldfield	475	Ozonosphere	3.76
St. George	639	Troposphere	3.6
	940	Ionosphere	4.0
Beatty	No identifiable signal.		

Figures 35a-35d show that the temperature inversion in the lower 500 feet of the atmosphere was strong enough to overrule all winds there, so an acoustic signal went in all directions.

TNT SHOTS

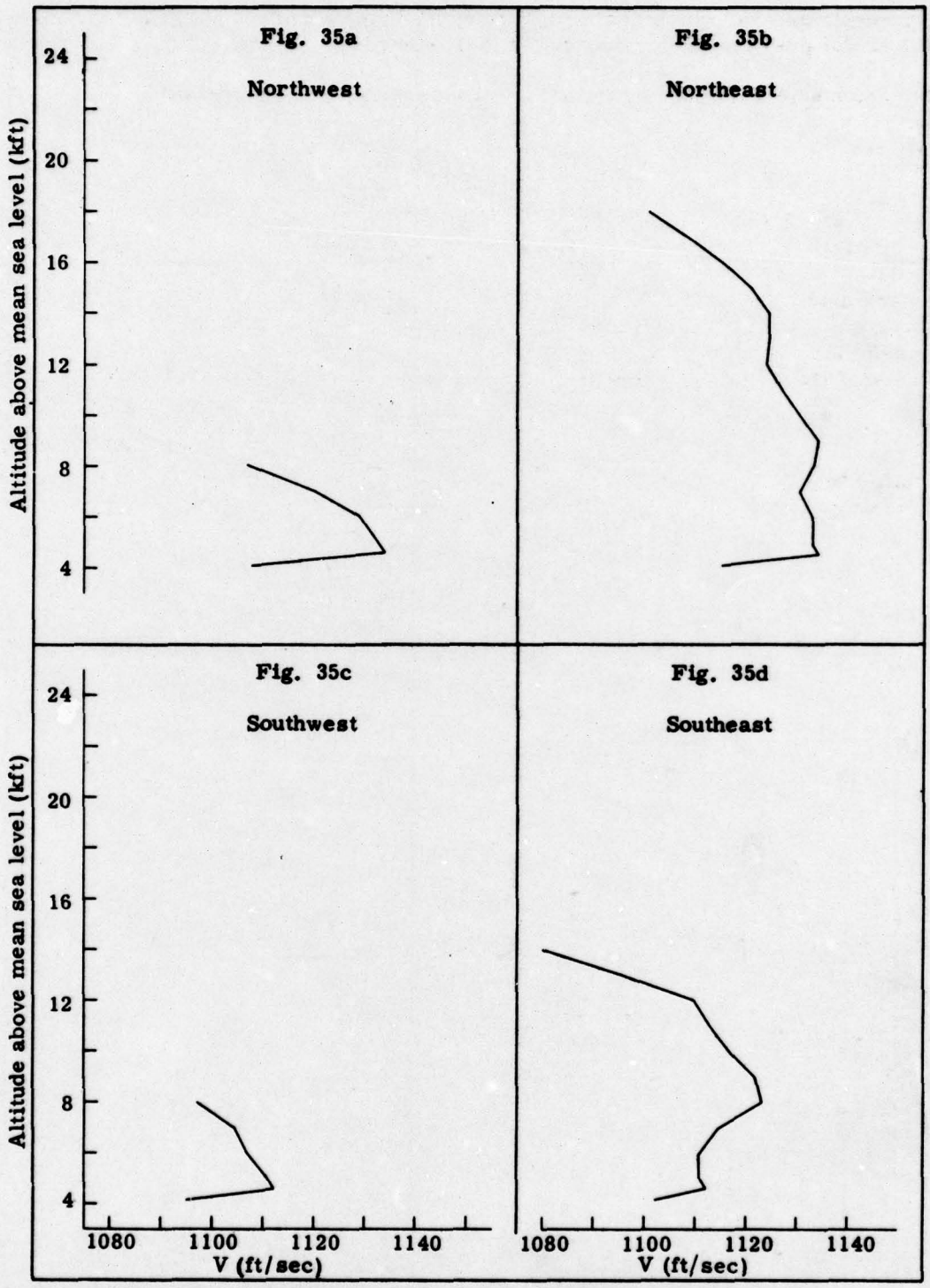


Fig. 35. -- Meteorological conditions and sound ray paths on September 22, 1951, at 0600 MST

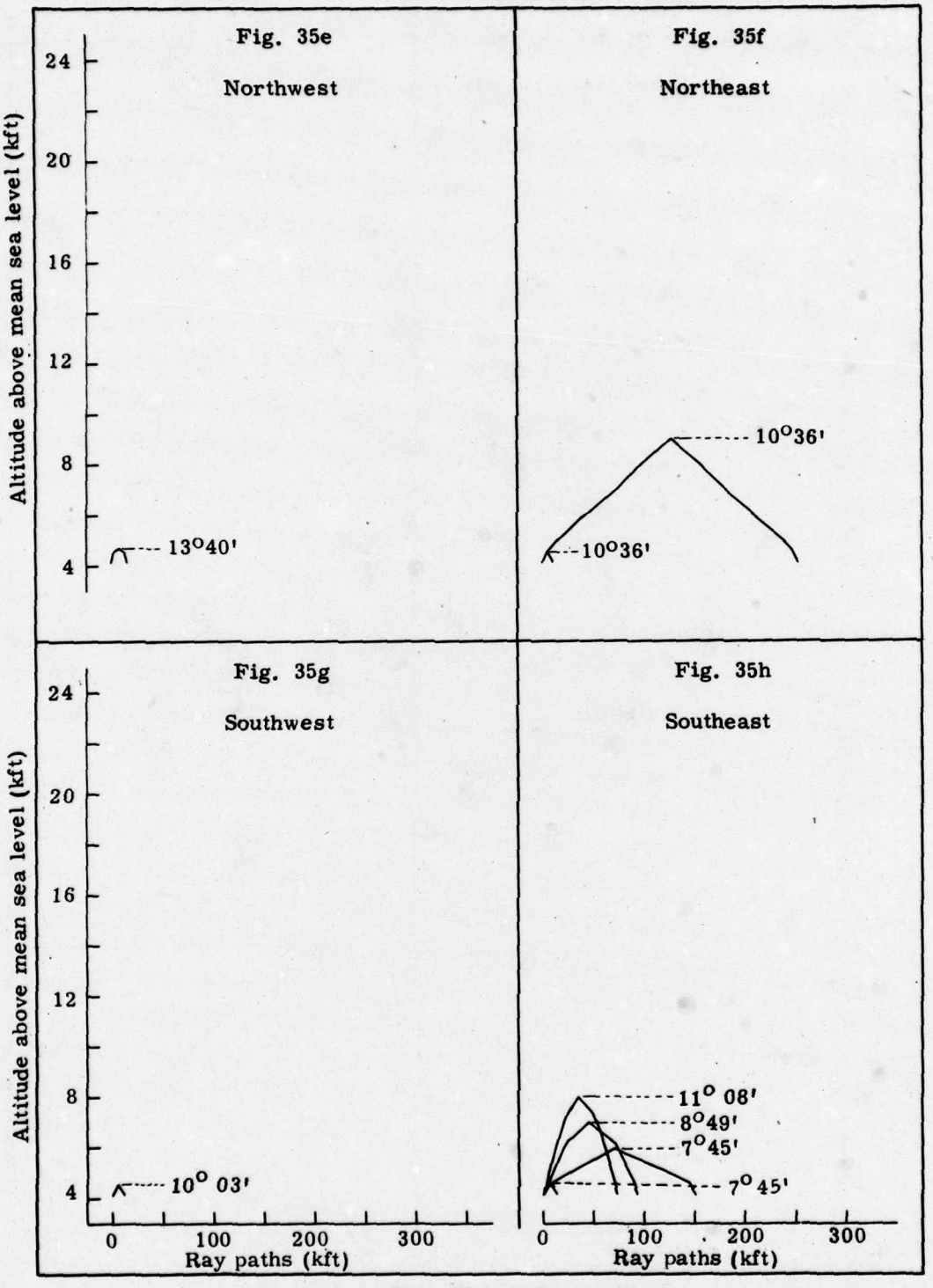

Fig. 35e
Northwest
Fig. 35f
Northeast
Fig. 35g
Southwest
Fig. 35h
Southeast
Altitude above mean sea level (kft)
24
20
16
12
8
4
13°40'
10°36'
10°36'
10° 03'
11° 08'
8°49'
7°45'
7°45'
0
100
200
300
Ray paths (kft)

Fig. 35 (cont)

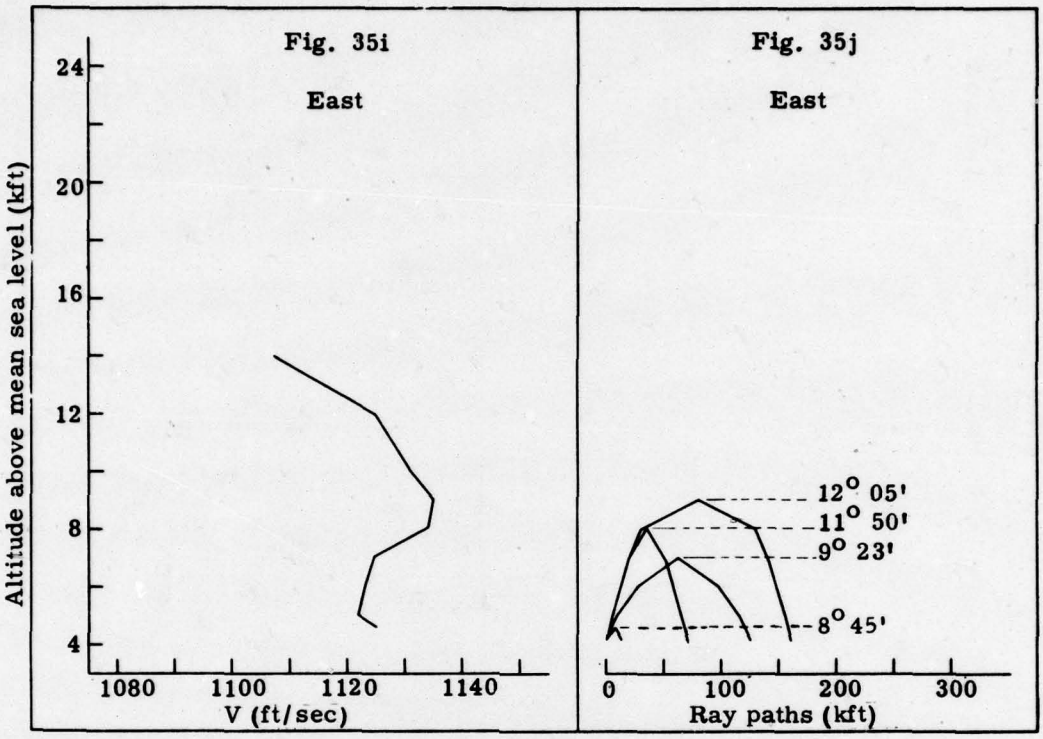

Fig. 35i
East
Altitude above mean sea level (kft)
24
20
16
12
8
4
1080
1100
1120
1140
V (ft/sec)
Fig. 35j
East
12° 05'
11° 50'
9° 23'
8° 45'
0
100
200
300
Ray paths (kft)

Fig. 35 (cont)

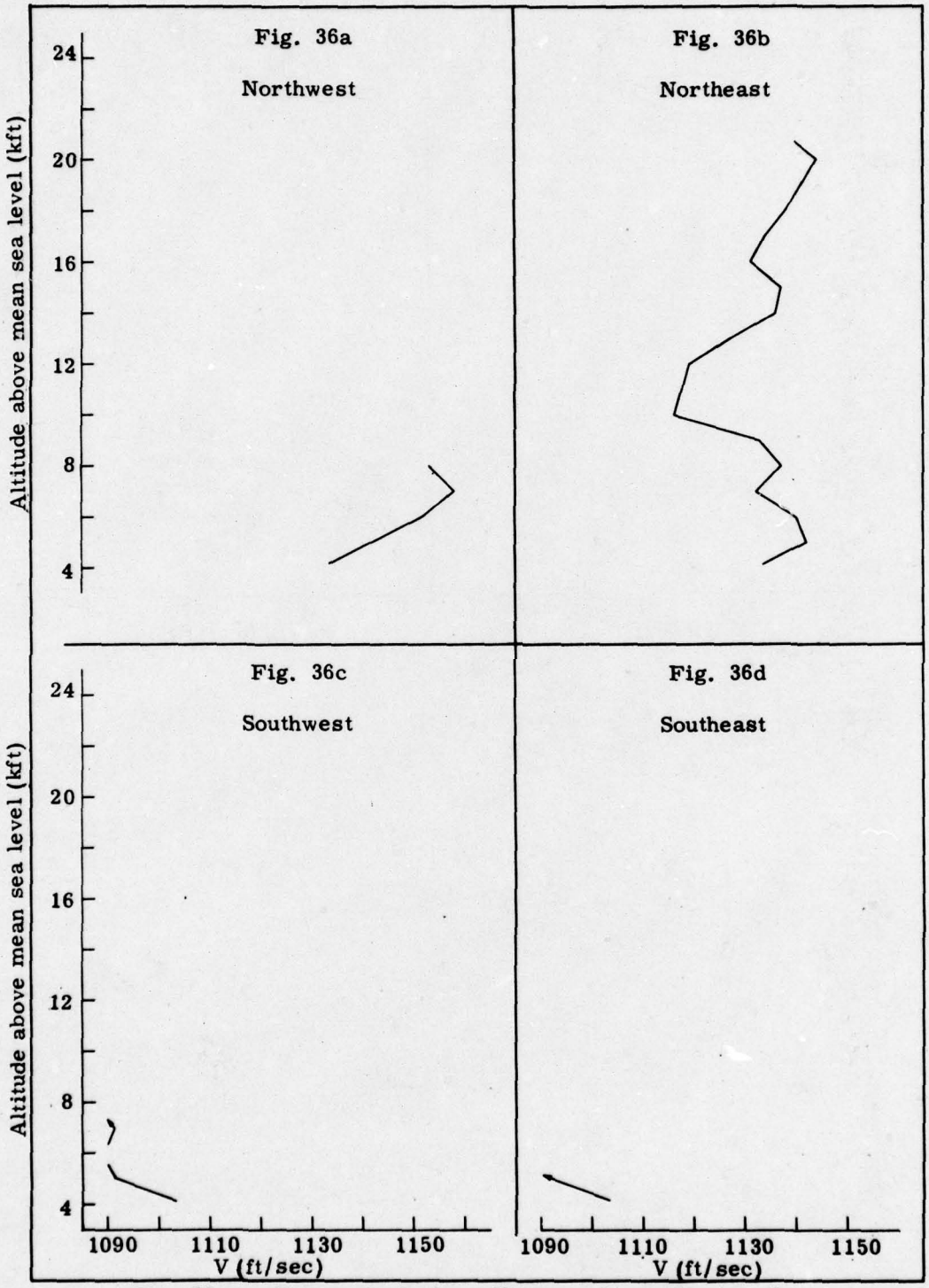


Fig. 36. -- Meteorological conditions and sound ray paths, September 28, 1951, at 0700 MST

TNT SHOTS

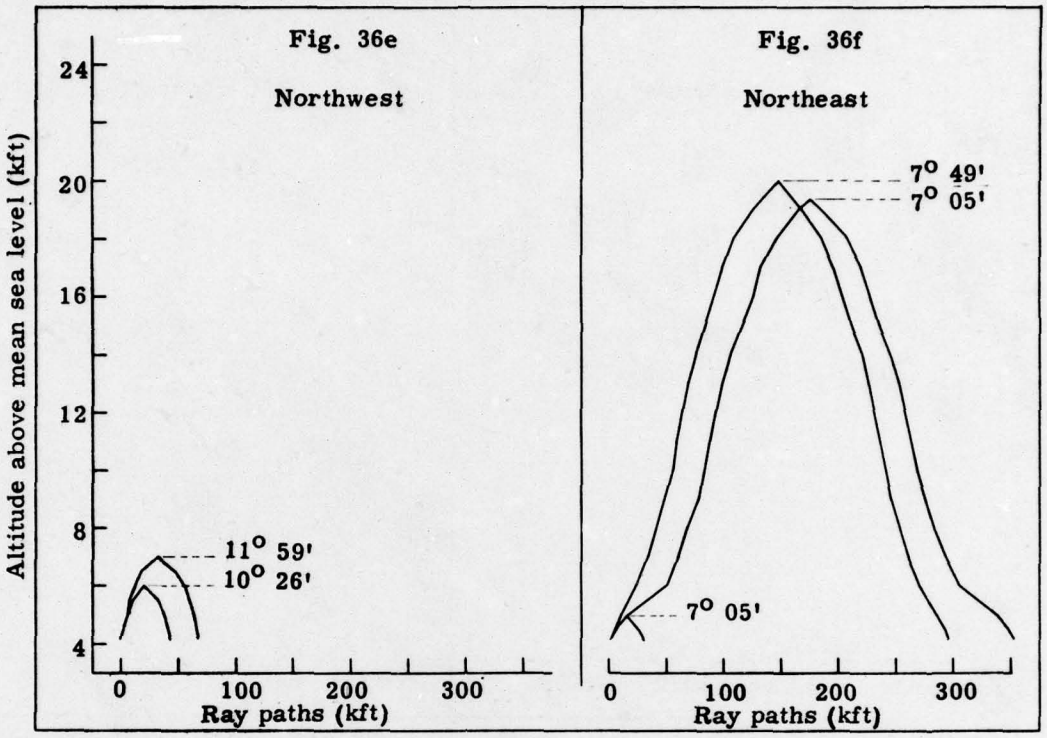


Fig. 36 (cont)

In contrast, Figs. 36a-36d show that on September 28, 1951, no acoustic signal could land in any southerly direction. The strongest troposphere signal would travel to the northwest, and a weak signal to the northeast. Microbarograph data from September 28, 1951, are as follows:

TABLE IX

Station	Travel time (sec)	Signal type	Peak-to-peak pressure (microbars)
Indian Springs	No signal		< 0.06
Las Vegas	Lost in background		
Henderson	515	Ozonosphere	1.42
Boulder City	No signal		
Caliente	432	Troposphere	0.5
	516	Ozonosphere	0.6
Goldfield	Bad background		
St. George	Bad background		
Beatty	Bad background		

BUSTER ABLE SHOT

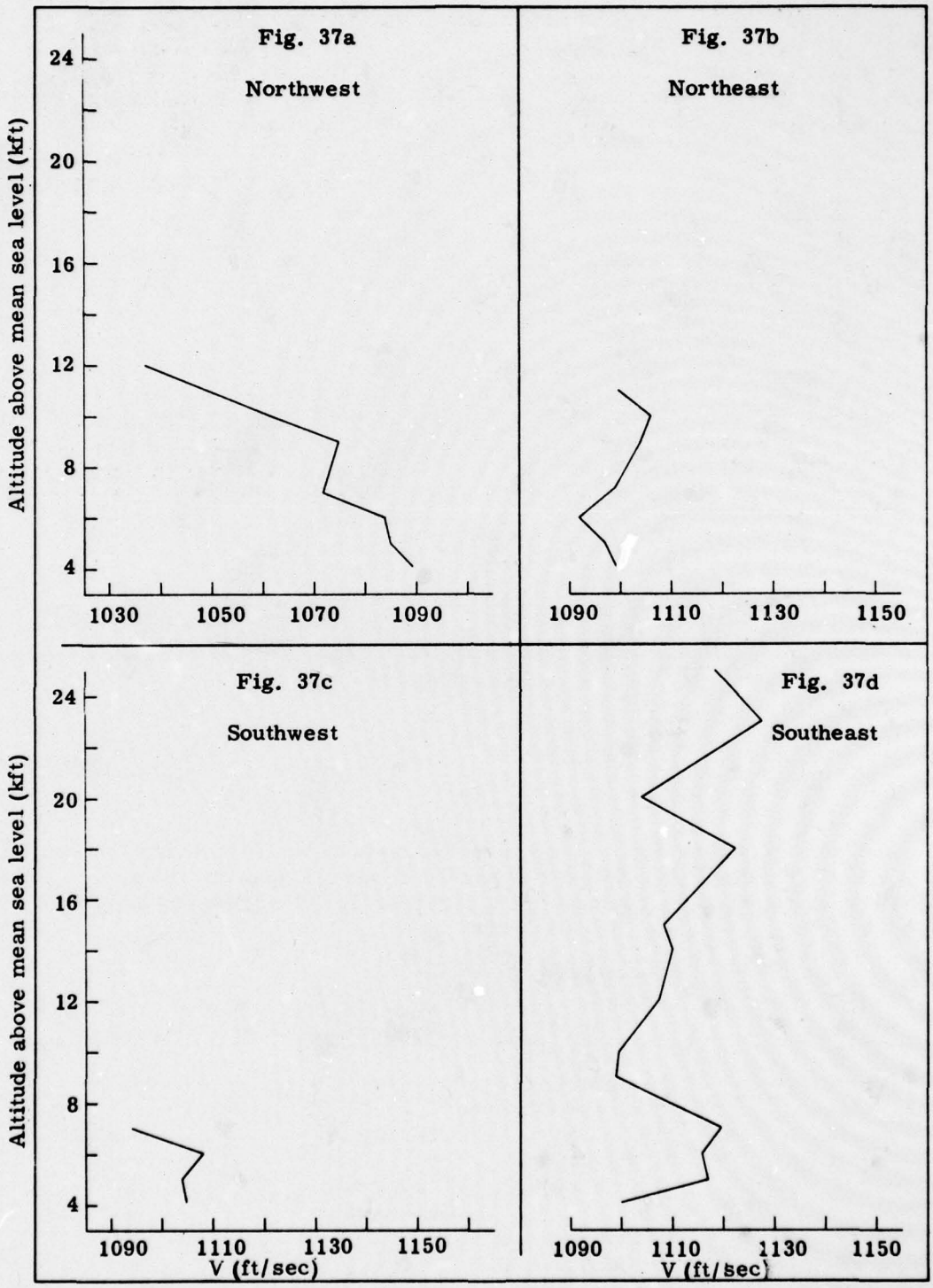


Fig. 37. -- Meteorological conditions and sound ray paths, October 22, 1951, at 0600 PST

BUSTER ABLE SHOT

When an open circuit prevented firing on October 19, 1951, the Buster Able tower shot was rescheduled for 0600 PST on October 22, 1951. To confirm meteorological predictions a 1.2-ton TNT charge was fired at 0500 PST. The microbarograph readings from the 1.2-ton advance shot gave us just cause for concern, particularly in the direction of Indian Springs, Las Vegas, Henderson, and Boulder City. Figure 37d shows sound velocity $V = c + u_{SE}$, and Fig. 37g shows some sound ray paths southeast from the shot point. The 12° of energy held in the troposphere produced very large troposphere signals as may be seen by comparing Fig. 21a with Fig. 20.

The Test Director was warned that the meteorological situation was anything but favorable for firing a fission weapon; but since the predicted yield was small and the test had been delayed several days by the misfire and by subsequent bad weather, a decision was made to go ahead with the fission weapon shot.

From the point of view of damage to the populated areas southeast from the AEC Test Site, we believe it was fortunate that the yield was trivial. Indian Springs had been warned that damage might occur, and as part of the general precautionary measures, the Air Force base power plant was shut down. With no power available at our microbarograph station, we obtained no record at Indian Springs. Excellent records were obtained at Las Vegas, Henderson, Boulder City, and St. George, however. Peak-to-peak pressures for both the advance shot and Buster Able Shot are shown In Fig. 21a.

Fig. 37e

Northeast

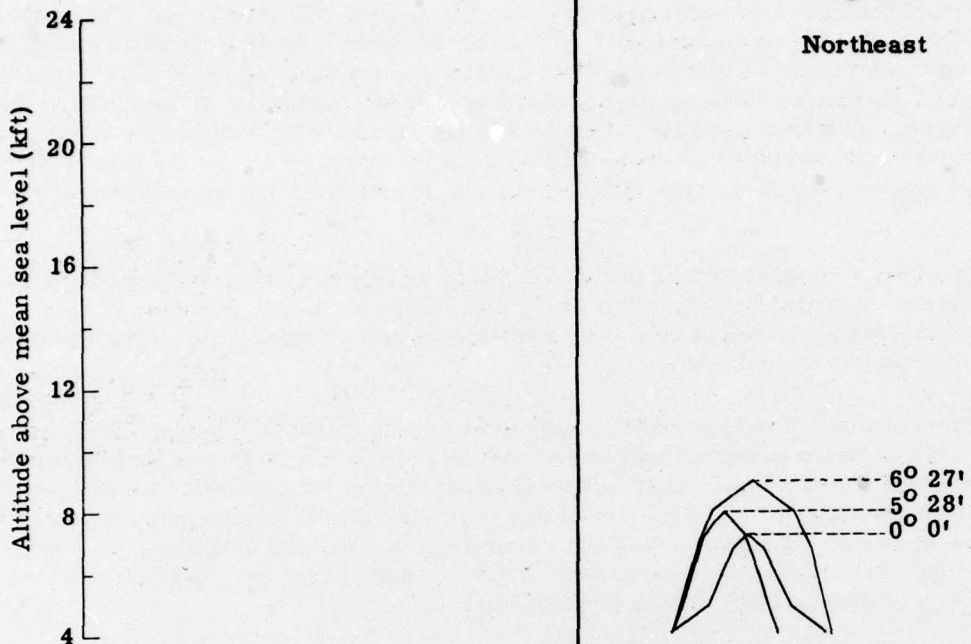


Fig. 37f

Southwest

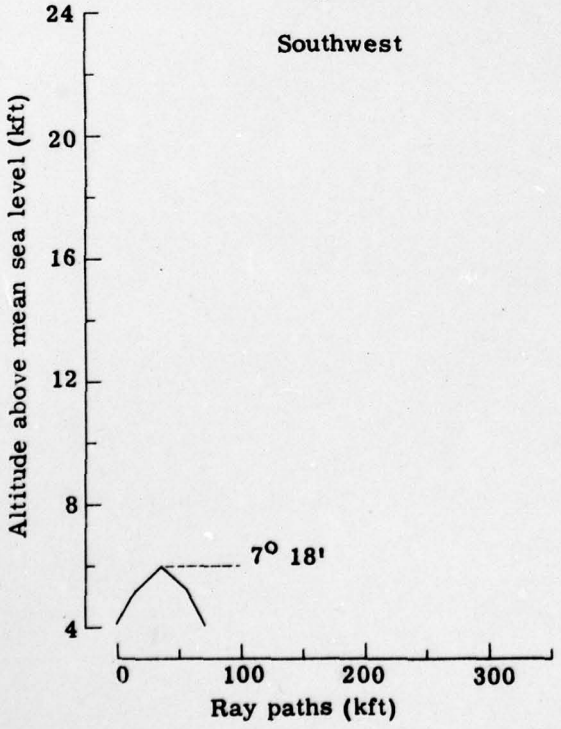


Fig. 37g

Southeast

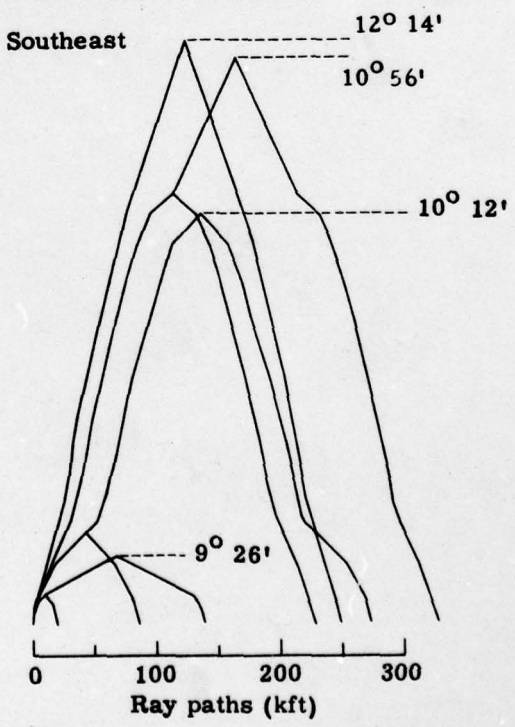


Fig. 37 (cont)

Las Vegas Morning Sun, October 29, 1951

Military, Washington Brass Here for A-Blasts

Observers View Huge Atom Test

In the vanguard of congressional and other high defense department officials expected momentarily for the atomic tests, nearly 1200 military officials from posts throughout the country poured into Las Vegas yesterday as AEC scientists prepared for its biggest experiment, which presumably will come tomorrow.

With activity stirring at a fast clip in the desolate Yucca Pass proving grounds after unexpected delays, the atomic weapon test yesterday morning was the first major detonation seen by observers near the site, but faintly heard and felt by residents throughout southern Nevada.

Reports from AEC officials explained that some radiation was detected in an area between Beatty and Lathrop Wells, but the quantity "was so infinitesmal that it is harmless."

There was no indication there would be another detonation this morning, although the weatherman forecast clear and cloudless skies, perfect weather for the scientists.

One of the observers with AEC scientists was Congressman Walter Baring. "I'd like to tell you what happened, but I can't talk about it," said the Nevada congressman when interviewed.

An atomic weapon apparently dropped by a red-tailed B-29 bomber went off with a greenish flash at the desolated Frenchman's Flat testing ground yesterday and sent a purple toadstool shaped cloud mushrooming 30,000 feet into the sky.

The explosion, which sounded like a thunderclap, was the second atomic detonation of the Atomic Energy Commission's current series of atomic tests. It was the AEC's seventh blast here.

The sky was clear and the cloud was visible from roof tops in Las Vegas, 90 miles to the southeast. Most of the city's residents appeared to be unaware that an atomic test had been held, although the shock waves were felt in Henderson, Boulder City, Overton and on Lake Mead.

No troops participated in the test and the AEC refused to comment on it except to say there had been an explosion. The ex-

(Continued on Page 2)

BUSTER BAKER SHOT

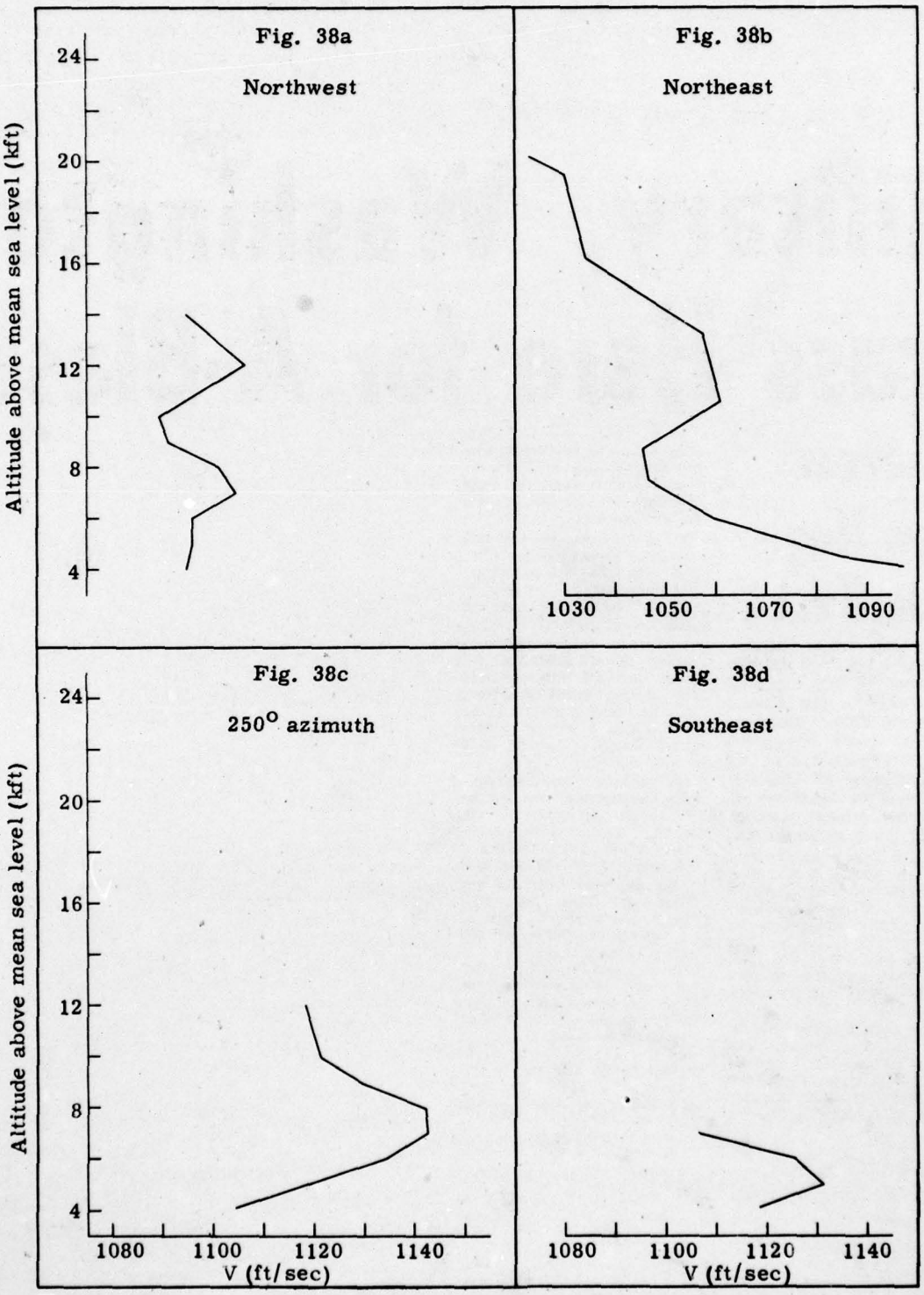


Fig. 38. -- Meteorological conditions and sound ray paths, October 28, 1950, at 0720 PST

BUSTER BAKER SHOT

Buster Baker, the first air drop of the Buster series, was scheduled for 0700 PST on October 28, 1951, but an additional aiming run of the dropping aircraft delayed the shot until 0720:09.5. Figures 38a-e show the meteorological situation at the time of this fission bomb explosion. Figures 38a, c, f, and h show that moderate amounts of energy would be transmitted toward Goldfield and Beatty. Energy transmission toward the south and southeast would be small, and none would be transmitted toward the northeast. The situation looked far more favorable on this date than it had on October 22, 1951, except for the fact that from the 1.2-ton advance shot an ozone signal greater than 38 microbars peak-to-peak pressure had knocked the Boulder City microbarograph off scale. The strength of the ozone signal that the fission bomb might impose upon Boulder City was a great concern.

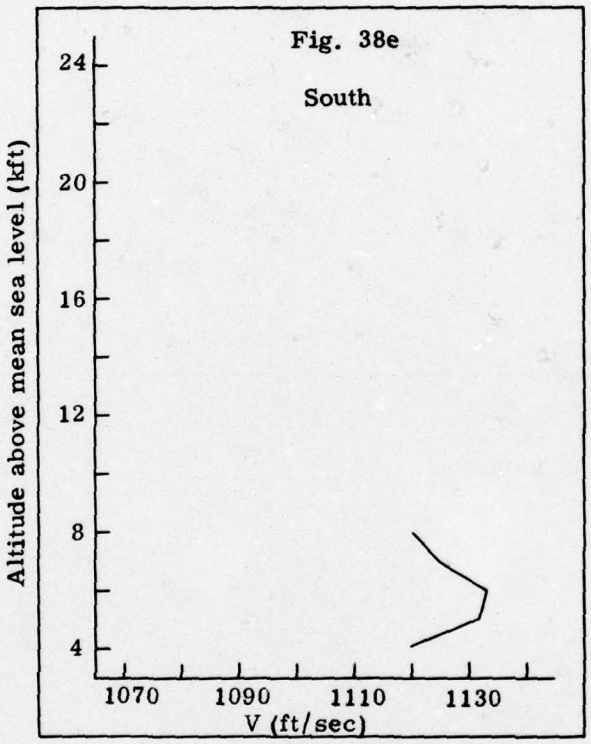


Fig. 38 (cont)

Figure 21b shows peak-to-peak signal strengths for the advance shot and the Buster Baker shot.

As predicted, Goldfield, northwest of the shot point, reported the largest troposphere signal, 936 microbars. Residents of Goldfield heard the noise distinctly. The sound was also heard in Indian Springs where the signal strength was 520 microbars and was barely audible in Beatty where 65 microbars peak-to-peak pressure was registered. Excellent ozonosphere signals were recorded in Las Vegas, Henderson, Boulder City, Caliente, and St. George, and were heard in all these except Las Vegas where the recorded ozone signal strength was only 132 microbars. The largest ozonosphere signal was that received by Boulder City, 420 microbars. No damage was reported from any inhabited locality.

Fig. 38f

Northwest

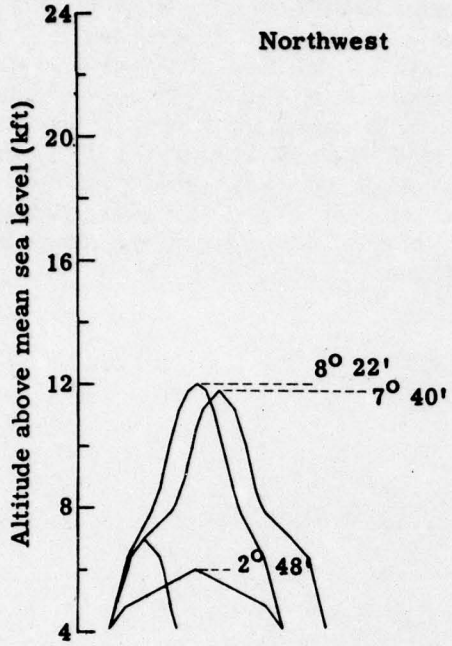


Fig. 38g

Southeast

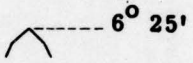


Fig. 38h

250° azimuth

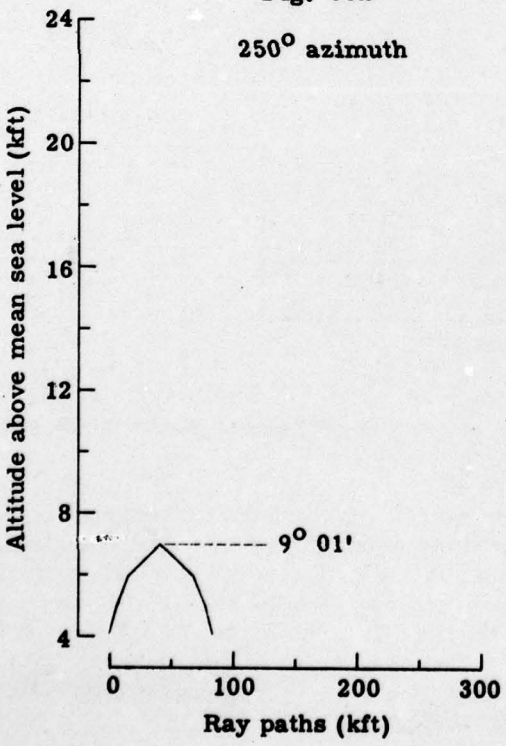


Fig. 38i

South

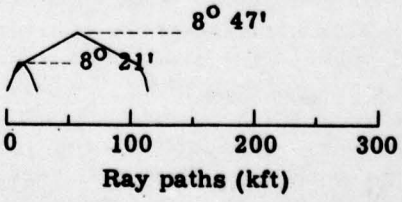


Fig. 38 (cont)

BUSTER CHARLIE SHOT

Meteorological predictions at the time of the Buster Charlie Shot called for essentially equal sound propagation in all directions from the shot point, as shown by Figs. 39a-39d. The advance 1.2-ton TNT shot produced no very large troposphere or ozonosphere signals. Only Indian Springs and Goldfield observed troposphere signals from the advance shot, 26 and 2.0 microbars, respectively. Las Vegas, Henderson, Boulder City, Caliente, and St. George recorded distinct ozonosphere signals, but the greatest strength was only 18 microbars. There appeared to be little likelihood of damage to any locality by the fission bomb to follow.

Excellent microbarograph records were obtained at all eight stations. With the exception of the Beatty instrument, all microbarographs remained on scale. Figure 21c shows recorded peak-to-peak pressures. Troposphere signals reached Indian Springs, Beatty, Goldfield, Las Vegas, and Caliente, and ozonosphere signals struck Las Vegas, Henderson, Boulder City, Caliente, and St. George. The shot was audible in Indian Springs, Henderson, Boulder City, Caliente, Beatty, and Goldfield, and was especially loud in St. George. Even the Weather Bureau barometer at Prescott, Arizona, recorded a pip which was undoubtedly the second cycle of the ozonosphere signal.

Two distinct shocks having a separation between shocks of approximately 1/2 second were heard at the Control Point.

Las Vegas Review - Journal, October 30, 1951

Only Puny Blast Wave Felt Here

By JOE McCLAIN

The atomic energy commission this morning detonated its third nuclear test of this series and old man weather played ping-pong with the resulting blast waves.

Las Vegas residents who saw the brilliant flash light up the sky at 7 AM waited fruitlessly for the blast wave they felt must be coming because of magnitude of the explosion.

And today's mild one wasn't felt by customers in Georgia Carpenters grocery store at Indian Springs, 30 miles south of the test site.

But residents of Henderson both saw the flash and felt their homes tremble from the blast waves. It will be recalled that they also felt the blast in the second test Sunday morning, while Las Vegas residents failed to get any reaction.

Boulder City residents also reported they saw the explosion and some reported hearing two distinct booms, several seconds apart.

And several residents of southern Utah claimed they heard and felt today's nuclear detonation.

In Cedar City, about 100 miles east of the blast, Mrs. Helen Simkins, city recorder, said she felt the blast wave distinctly.

Max Whitney, Cedar City airport worker, felt the blast and told newsmen he could see the top of the atomic cloud forming over the sage and pine covered mountains along the Utah-Nevada border to the west.

In Kanarraville, 12 miles southwest of Cedar City, Mrs. Glade Barry described the blast wave as being "as violent as an earthquake," adding she detected the effects for "about 90 seconds while I was walking across the kitchen."

But in Las Vegas, the city that during last winter's test series had homes shaken, windows damaged and coolers rattled, atom-watchers only saw the explosion and the towering atomic cloud that erupted from Frenchman flat following the explosion.

Today's was by far the most spectacular of any of the Nevada tests—and for brilliance and color probably butclassed the first test in continental United States—at Alamagordo, New Mexico in 1944.

And in Sunday's test, two minutes or more elapsed before the cloud was seen in Las Vegas. This time the ascent was speedy.

Atomic scientists at the headquarters here were delighted by the perfect mushroom shape the cloud took as it shot upward. They termed it the "classical atomic cloud" shape, indicating it was a perfect test.

It's central stem was a grey purple spread with a pinkish-

(Continued on Page 2)

Radiological safety unit of the AEC test organization has issued the following summary, based on 11 AM report to the Nevada test site:

"No measurable radiation above normal background has been reported from any point in the region adjacent to the test site."

BUSTER CHARLIE SHOT

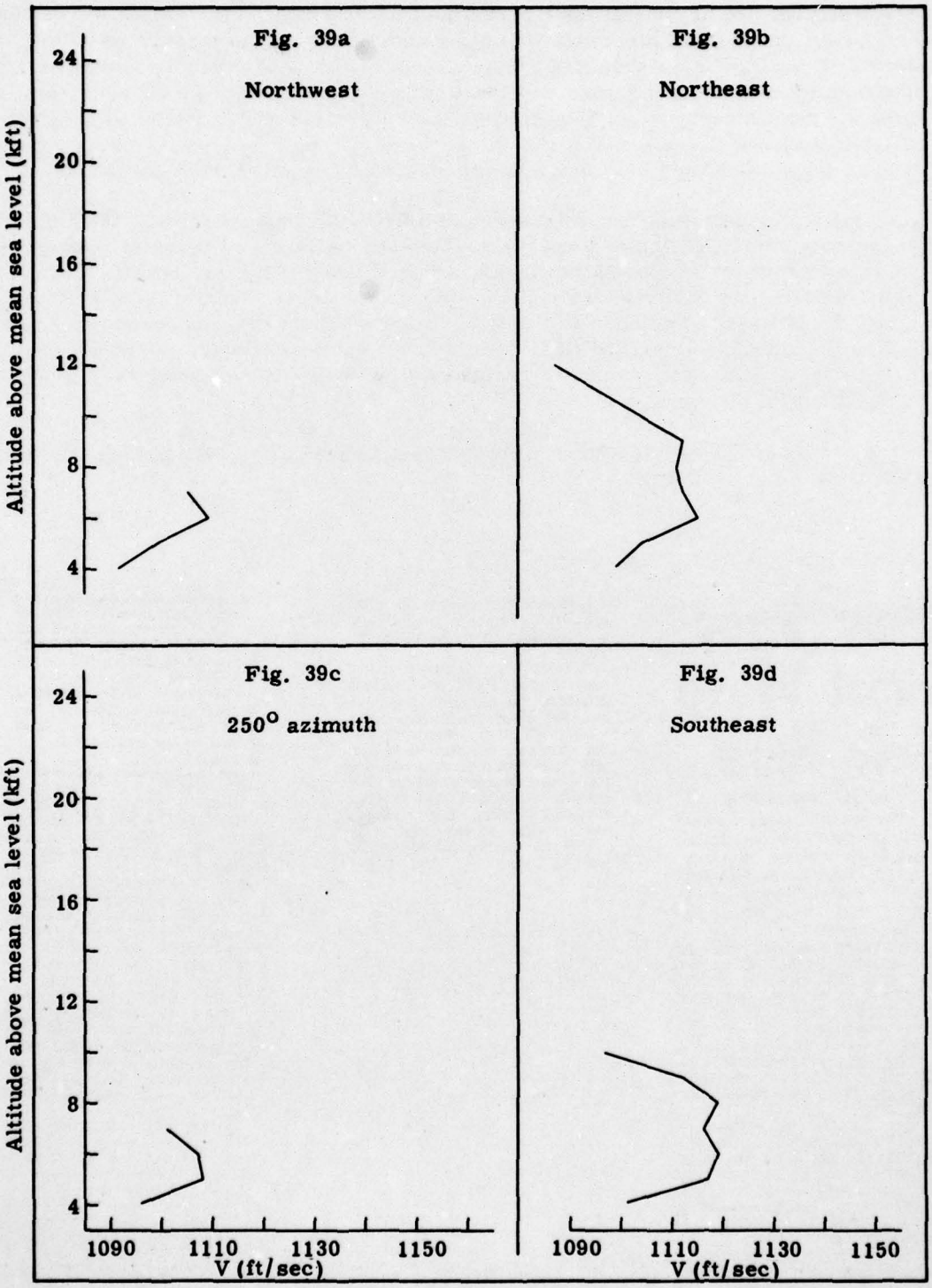


Fig. 39. -- Meteorological conditions and sound ray paths, October 30, 1951, at 0700 PST

BUSTER CHARLIE SHOT

Fig. 39e

Northwest

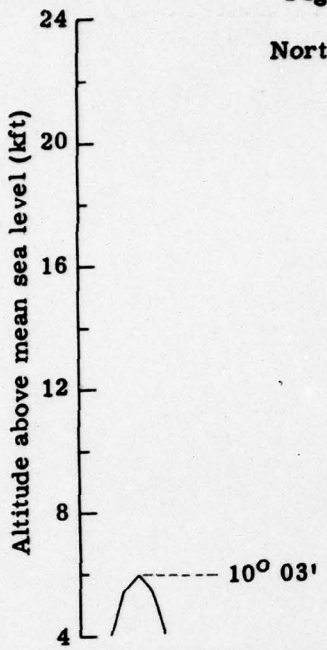


Fig. 39f

Northeast

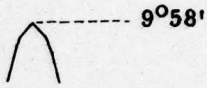


Fig. 39g

250° azimuth

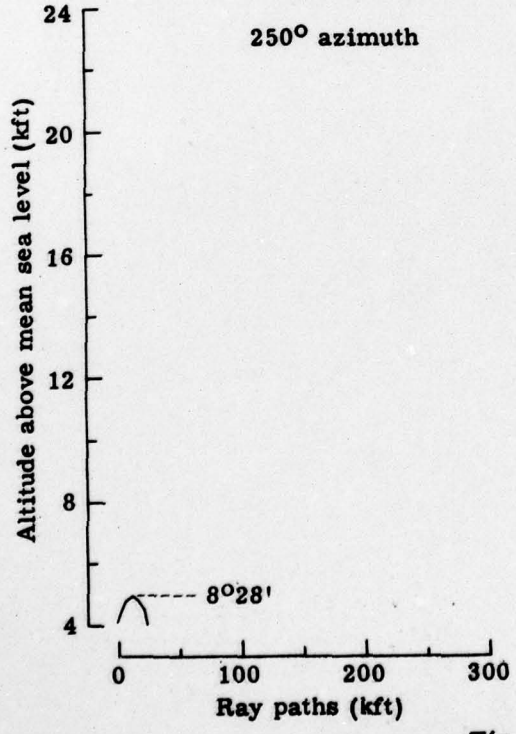


Fig. 39h

Southeast

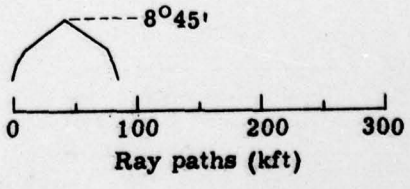


Fig. 39 (cont)

BUSTER CHARLIE SHOT

Fig. 39i

East

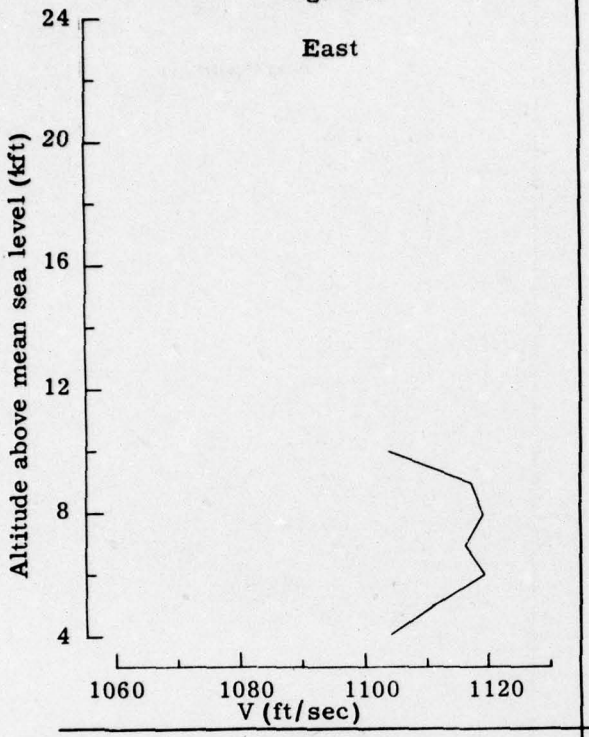


Fig. 39j

South



Fig. 39k

East

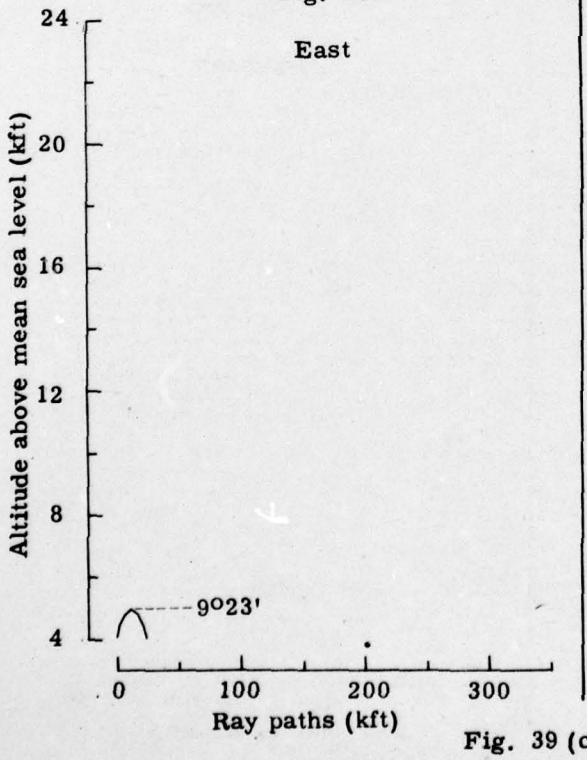


Fig. 39l

South

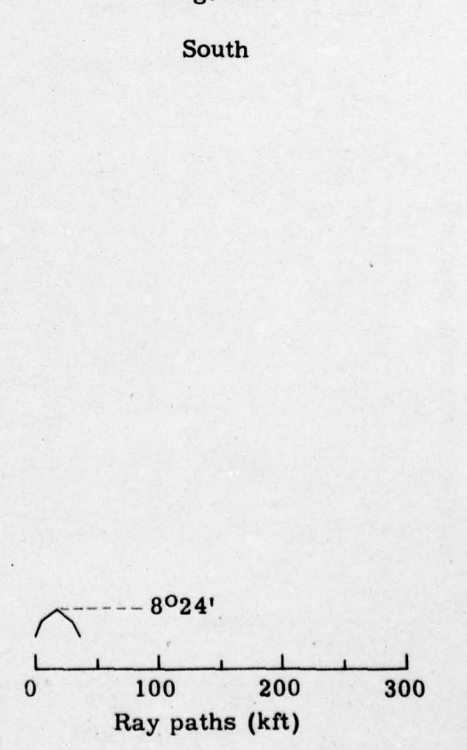
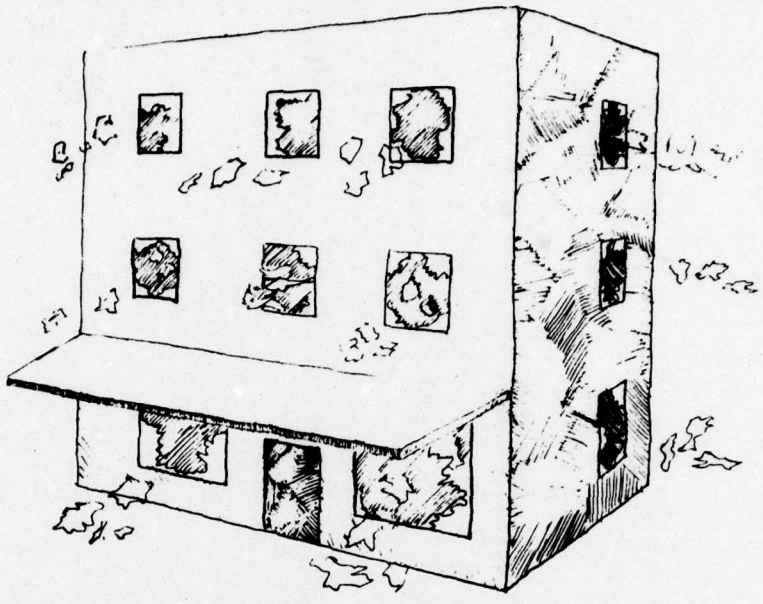


Fig. 39 (cont)

BUSTER DOG SHOT



Las Vegas Morning Sun, November 2, 1951

Congress Trio Hails War Games

By ADAM YACENDA

America's military might has a new "beach-head" of experience in tactical atomic uses which will help win a war without fear of world destruction.

Atom bombs, while the most destructive weapon known today, will not end wars, nor end the world.

This was the conclusion drawn by congressional witnesses as a result of the history-making atomic war maneuver staged at the improvised Yucca Pass battlefield yesterday.

The bomb exploded at 7:30 a. m. It shot a huge fireball and a mushrooming cloud of deadly smoke into the sky. Six and a half minutes later a jarring, earthquake-like concussion hit Las Vegas. It shattered four plate glass windows in downtown stores and dumped boxes of China off warehouse shelves at a resort hotel.

Doors swung open, window curtains and venetian blinds billowed out and buildings shook.

The blast shattered windows at Sears-Roebuck, Allan and Hanson, Rose, Ltd., and Western Auto Supply stores, and cracked plate glass windows at others.

The AEC announced shortly after the blast that the General Adjustment Bureau of Las Vegas will handle all damage claims resulting from the test.

A few residents were alarmed an hour after the blast when the huge radioactive cloud was caught by a stiff wind at 40,000 feet and was carried swiftly and directly over the city. However, AEC radiation monitors tested the atmosphere here and found that it was a harmless dose.

The rumble of the explosion was reported at Prescott, Ariz., 260 miles away, and at Salt Lake City, 450 miles away. Residents at Eureka, Nev., and St. George, Utah ,reported it as a thunder-like roar. Windows rattled in Cedar City, Utah, 100 miles east of the firing site.

In the interview at the Morning Sun office yesterday, Congressman Price said the history-making operation undoubtedly "has successfully answered the question posed by the military on the tactical use of the atom bomb.

"It has shown to the troops that atomic fire-power can be used in a tactical way and followed up without fear of radiation," he added.

Representative Price, who witnessed the huge "Greenhouse" and "Sandstone" atomic detonations at Eniwetok, said yesterday's epoch experiment "established a beach-head of experience in tactical atomic uses."

"It was a beautiful shot. The Army maneuvers were very interesting and important."

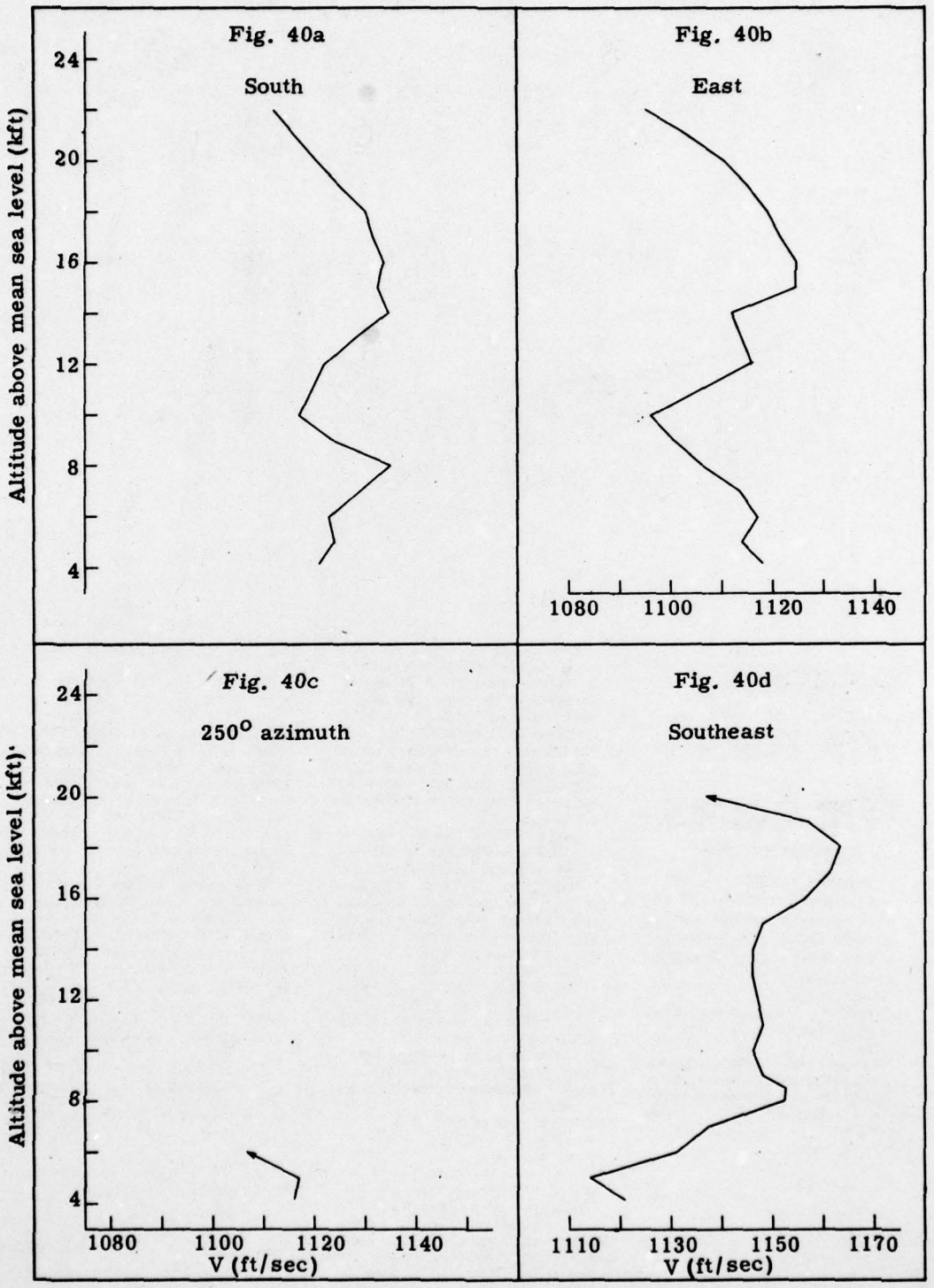


Fig. 40. -- Meteorological conditions and sound ray paths, November 1, 1951, at 0800 PST

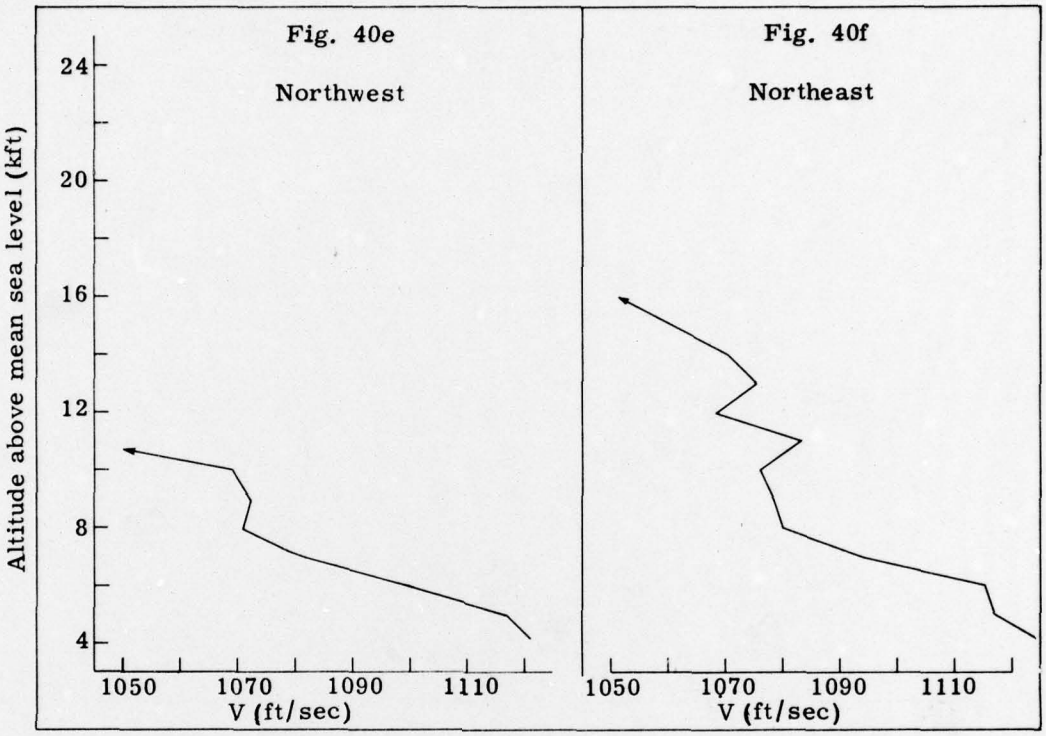


Fig. 40 (cont)

Weather predictions, then RAOB soundings, and finally the 1.2-ton TNT shot fired 1/2 hour prior to the scheduled firing time of the Buster Dog Shot gave real cause for concern. Figures 40c, e, and f show that very little energy would be transmitted toward Beatty, and that no troposphere signal need be expected northwest and northeast from the firing site. On the other hand, focusing conditions existed toward the south, toward the east, and especially toward the southeast. The advance shot produced very strong troposphere signals at all our stations to the southeast and quite strong ozonosphere signals at both Caliente and St. George. Figure 21d shows the magnitudes of the signals, where they remained on scale; the Test Director was warned that damage would likely occur southeast from the blast point.

Figure 40j shows some of the sound ray tracks toward the southeast. The distribution of energy bounded by rays having incidence angles between 0^{o} and $13^{o}32'$ is similar to that shown in Fig. 7a. An extremely heavy concentration of energy would therefore occur about 35 kilofeet southeast of ground zero. The dip in the V vs h curve between 8 and 18 kilofeet would produce a second, more distant focus. Its heavy concentration of energy would land very near the half-way point to Las Vegas and one bounce would send it smashing into that city.

In spite of the fact that we predicted that damage would be done on this date if the fission weapon were fired, the Test Director felt compelled to go ahead with the operation since thousands of visitors were present for Exercise Desert Rock. Unfortunately all results were as predicted. Measured signal strengths are shown in Fig. 21d. The noise was heard at all our stations except Beatty and Goldfield, and in Prescott, Arizona. It is believed that in Las Vegas the signal strength was about 5 pounds per square foot. Since the other inhabited areas reported no significant damage, their signal strengths must have been somewhat less.

Fig. 40g

South

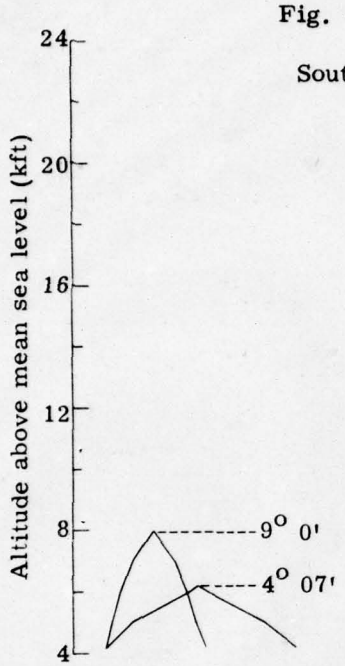


Fig. 40h

East

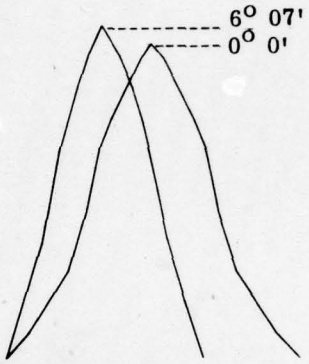


Fig. 40i

250° azimuth

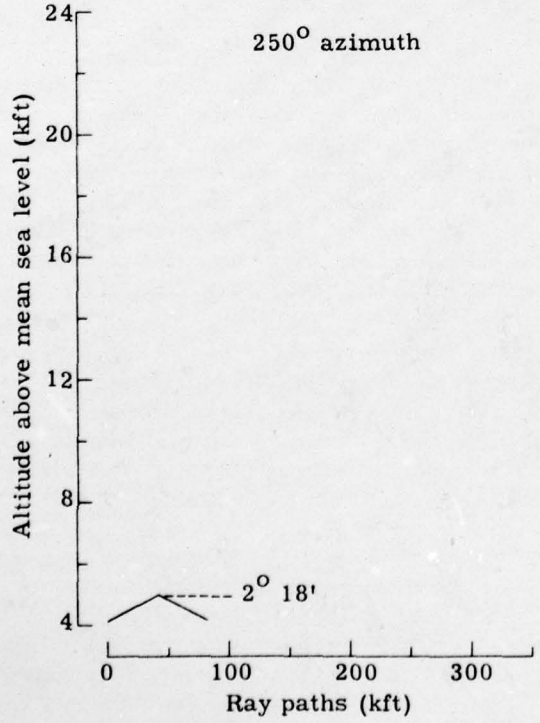


Fig. 40j

Southeast

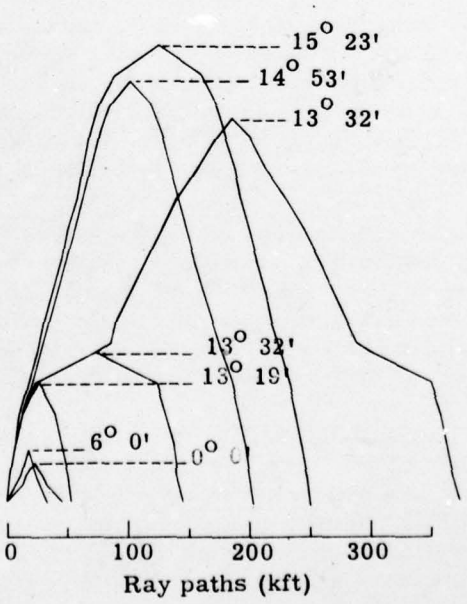
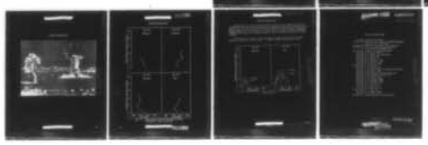


Fig. 40 (cont)

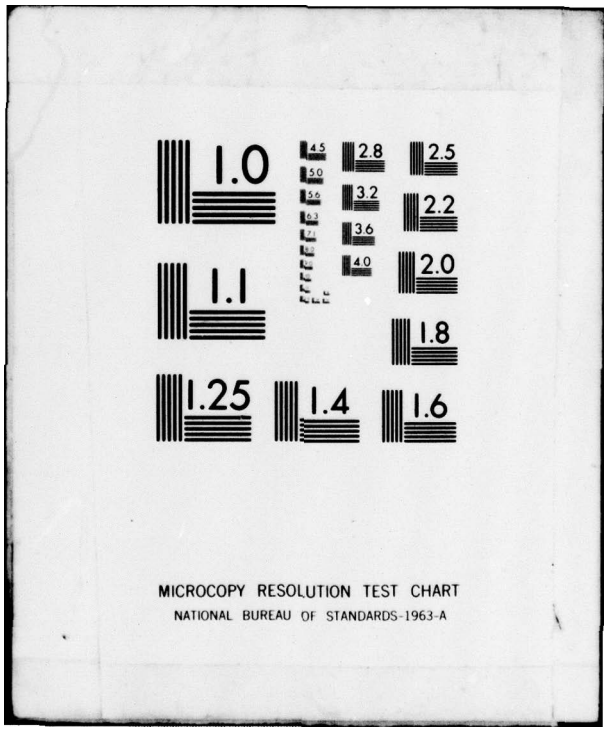
AD-A074 621 SANDIA CORP ALBUQUERQUE N MEX F/G 18/3
DAMAGING AIR SHOCKS AT LARGE DISTANCES FROM EXPLOSIONS.(U)
APR 52 E F COX, H J PLAGGE, J W REED
UNCLASSIFIED AEC-WT-303 NL

2 OF 2
AD
A074621





END
DATE FILMED
11-79
DDC


1.0
1.1
1.25
1.4
1.6
1.8
2.0
2.2
2.5
2.8
3.2
3.6
4.0
4.5
5.0
5.6
6.3
MICROCOPY RESOLUTION TEST CHART
NATIONAL BUREAU OF STANDARDS-1963-A

BUSTER DOG SHOT

Las Vegas Review - Journal, November 1, 1951

US Troops Participate First Time

"Trick or treat" came to Las Vegas about 12 hours late when the atomic energy commission detonated its fourth nuclear explosion in the current test series this morning, with troops stationed at Camp Desert Rock taking part in the first atomic maneuvers in history.

Major General William B. Kean, in charge of army operations, reported shortly after the maneuvers that the operation was "most successful."

For most Las Vegans and residents of nearby communities, the test this morning was a "treat." It gave them the long-awaited thrill of hearing windows rattle, the sound of rushing air from the blast wave, and the sight of a beautiful atomic cloud forming after the explosion.

A tail of that cloud, incidentally, reportedly wafted over Las Vegas but there was no indication that it was dangerous to local residents because of radioactivity.

But for some merchants along Fremont street, and a few local homeowners, there was a "trick" wrapped up in the explosion.

Plate glass windows at Sears-Roebuck store, Rose Limited, Allen and Hanson and Western Auto store were broken. Residents reported that cracks in walls resulted from the blast wave.

Officials at the Desert Inn reported that cases of china stored in their warehouse toppled and dishes were broken.

The AEC, when advised that there was some damage, announced that reports of damaged property should be made to General Adjustment Bureau, incorporated, 214 Stewart street, for evaluation.

The blast was seen and felt elsewhere:

In Henderson, residents felt and heard the blast. Boulder City residents reported that they "heard a prolonged rumble."

The rumble was also heard in Caliente, Prescott, Arizona; Cedar City and St. George, Utah. Eureka, Nevada, 180 miles north of the test site also noted blast effects.

An unnamed motorist driving to Las Vegas from Searchlight reported that the blast broke the windshield in his car.

AEC spokesman said that blast waves have been reported in communities near the site during previous tests in this series, but no reports of damage had been made to responsible officials.

The nuclear explosion believed an air drop, that touched off the maneuver came at 7:30 AM. Seven and a half minutes later a wave of rushing air hit Las Vegas like an earthquake.

Residents said the blast hit harder than that from any of eight previous tests held at the atomic energy commission's Frenchman's flat proving grounds.

An hour after the explosion, General Kean, commander of "Operation Desert Rock," released a terse statement on the troop phase of the maneuver.

He said there were no injuries of any kind to military personnel.

"An appreciable step forward has been taken toward relating military tactics to the employment of atomic weapons," General Kean said.

The operation "has every indication of producing effective results which when evaluated will be greater than anticipated," he added.

The army disclosed no details of the troop participation, however.

"Army combat troops and service troops with a large number of military observers representing the army, navy and marine corps participated today in a nuclear detonation," said the general's statement.

He said the troops' part in the test "involved observation of the detonation, observation of the effects on test items and equipment and observation of psychological and physiological reactions."

It was indicated this statement would be all that the army intends to say at present regarding the test.

General Kean said reporters will be permitted to interview some troops here tomorrow, but that the soldiers will not be allowed to discuss military, technical or scientific phases of the test.

In addition to the participating troops, numerous high-ranking military observers and congressmen were on hand for the display.

If the maneuver followed previously reported plans, the troops advanced toward the scorched area after the blast as rapidly as radioactivity would permit.

The maneuver is expected to determine how fast attacking ground troops can move into an area swept by an atomic blast, the reaction of GIs to this unique experience and to answer hundreds of questions posed to military planners by the prospect of adding atomic weapons to the rifle, the mortar, the bazooka, the artillery piece and other fighting tools of the foot soldier.

At least 4500 observers, including the tactical troops, witnessed today's awesome display.

They included General Mark Clark, chief of US army ground forces, and Secretary of the Army Frank Pace.

Also watching the much-ballyhooed "big show" were AEC Commissioners Keith T. Glennan and Dr. H. D. Smyth, Chairman John Small of the national munitions board and Blay Bedford, assistant director of US military defense, plus a handfull of congressmen.

The atomic cloud itself first resembled a head of cauliflower, moving steadily upward for two minutes before it assumed the perfect mushroom-shaped atomic cloud.

Its head, wrinkled like the exposed surface of a human brain, continued to boil violently and to expand steadily.

Five minutes after the blast, it still was boiling furiously.

A reddish spot appeared in the upper left portion of the cloud, which did not break up immediately but continued to rise as it grew larger.

By 7:35 AM, the cloud had assumed a clover-leaf shape and tinges of reddish pink appeared throughout its upper folds. Later, the lower portion assumed an orange hue.

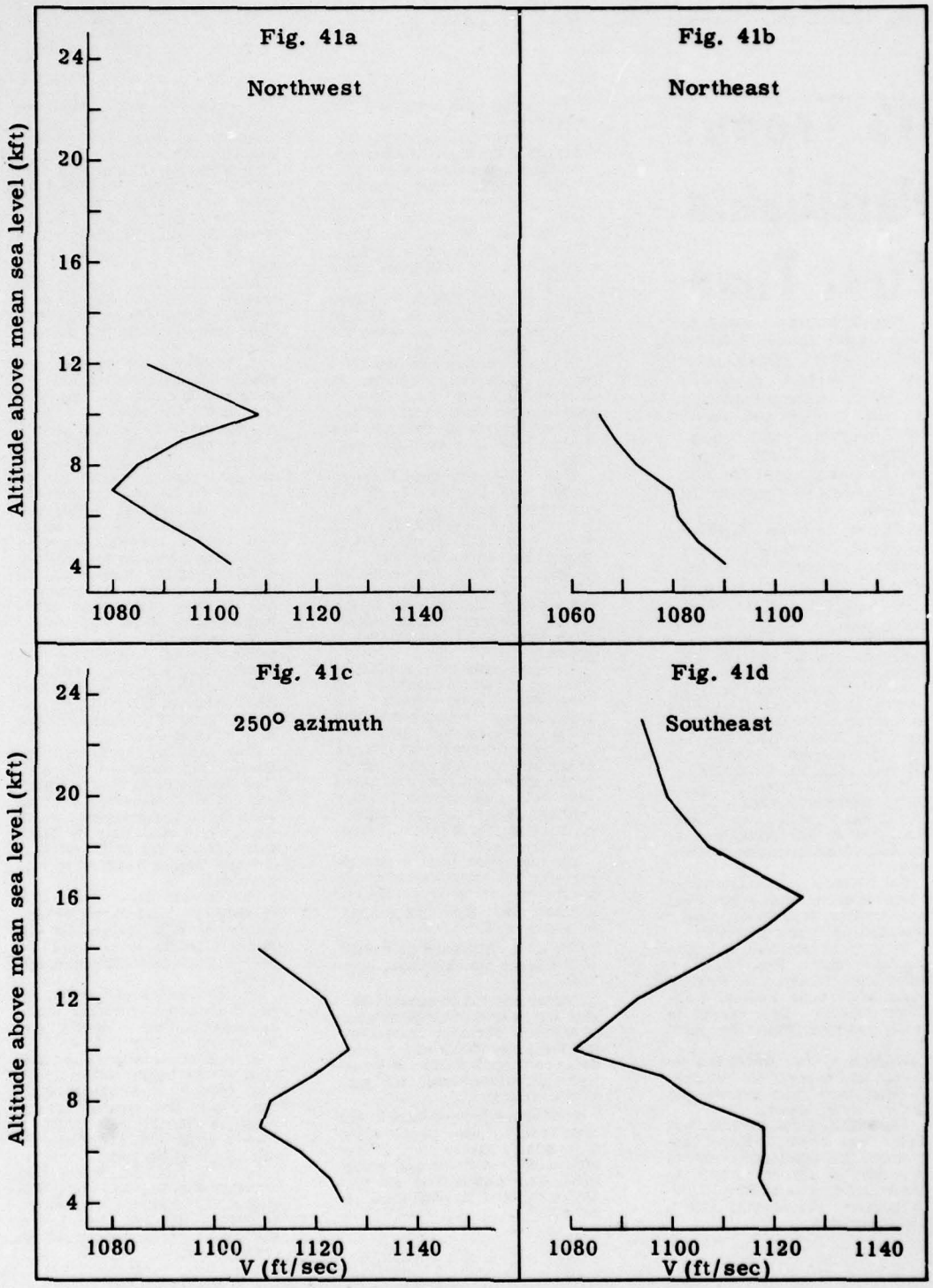


Fig. 41. -- Meteorological conditions and sound ray paths, November 5, 1951, at 0900 PST

BUSTER EASY SHOT

The meteorological situation on the morning of November 5, 1951, as depicted in Figs. 41a-f, is quite unusual in that an acoustic focus would exist in all directions except east and northeast from the shot point. The peak values of the V vs h curves are only slightly above V_0 values, however, so no large amounts of blast energy would be held in the troposphere in any direction.

Figure 21e shows signal strengths from the Easy Shot recorded at all stations. From the advance 1.2-ton TNT shot fired at 0730 PST, Caliente received an ozonosphere signal of 55 microbars peak-to-peak value. We had some concern as to what the Easy Shot signal strength via the ozonosphere might do to Caliente, so that village was warned by the AEC. No damage was done to Caliente although the blast was heard and felt strongly there.

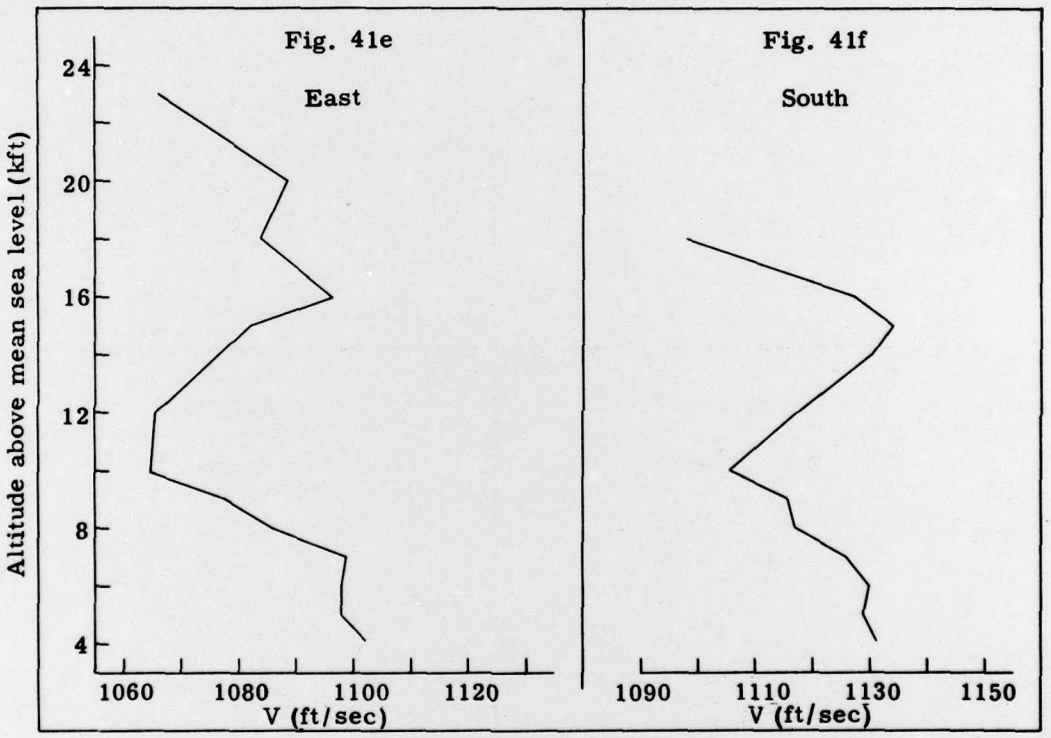


Fig. 41 (cont)

The shot was heard and felt at all stations except Boulder City. Once again the Prescott, Arizona, barograph recorded a pip at a time consistent with the second cycle of the ozonosphere signal.

The first shock from the Easy Shot reached the Control Point in 48.2 seconds. A second weak shock followed, perhaps 0.3 second after the first, and then a strong third shock struck the observers. All data shown in Figs. 41a-f reproduce the meteorological RAOB results obtained at 0900 PST, 1/2 hour after the fission weapon was fired. It is quite probable that the value of V_0 increased between the time of the shot and the time of RAOB balloon release. If V_0 in the south direction is reduced to 1,125 fps, then Fig. 41f resembles Fig. 8, and page 28. of this report shows how three distinct booms might result for an airburst occurring under these meteorological conditions.

Fig. 41g

Northwest

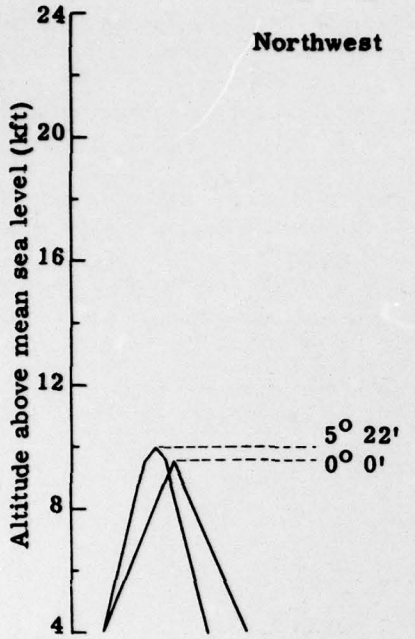


Fig. 41h

Southeast

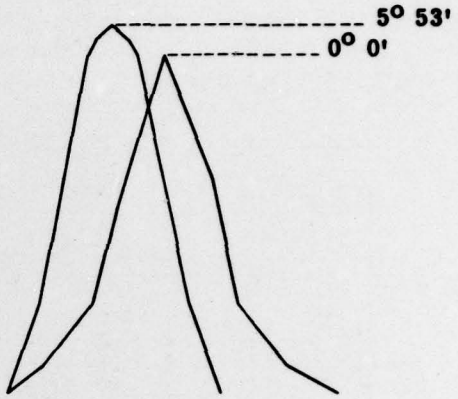


Fig. 41i

250° azimuth

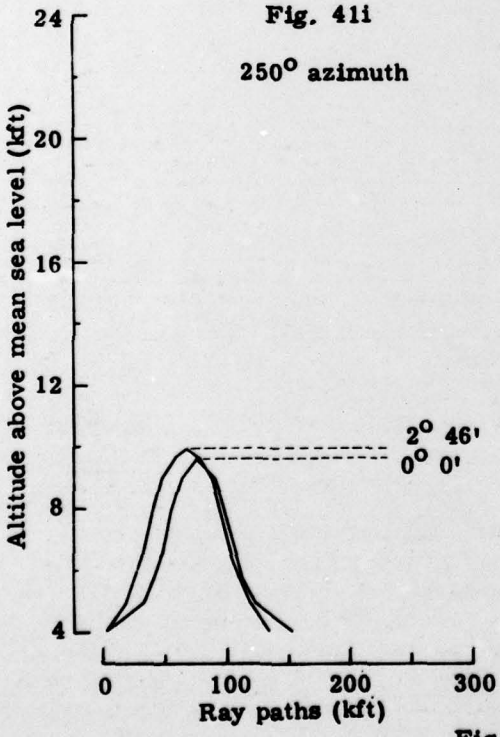


Fig. 41j

South

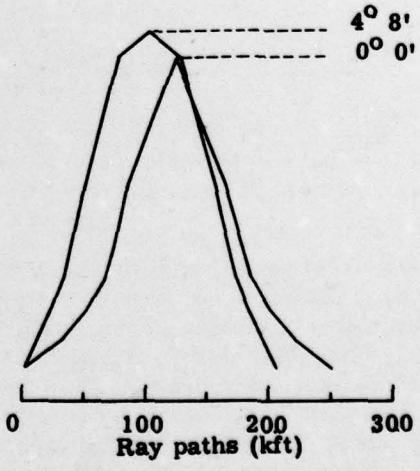
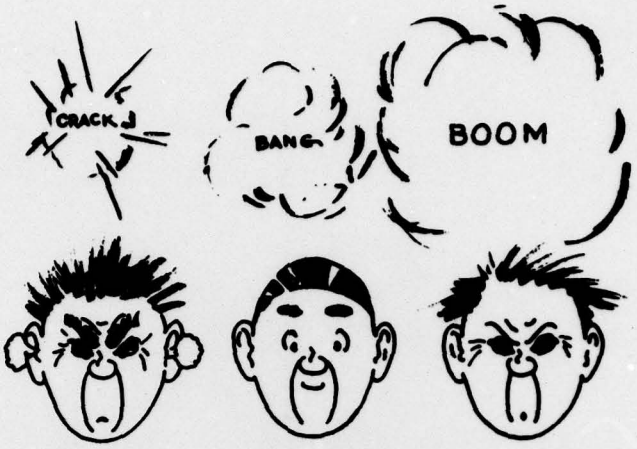


Fig. 41 (cont)

BUSTER EASY SHOT



Las Vegas Morning Sun, November 6, 1951

Atom Tests End; New Series Soon

Blast Strong In Utah

The Atomic Energy Commission last night announced that yesterday's nuclear detonation — the fifth in the current series and one which rattled windows up to 350 miles away —concluded the first phase of the tests and that a lapse of several days will occur before the next phase is ready to start.

After the "rest period" AEC test manager Carroll L. Tyler announced, a second series of blasts will be started to study the effects of nuclear detonations on military equipment. It was indicated the new phase may be underway in about 10 days.

Yesterday's A-bomb blast was carried out at the latest hour in the day of any since the Nevada proving grounds was activated almost a year ago. All prior tests were held at dawn or shortly after the sun came up. But in the current series, they have been staged later with each detonation, until yesterday's drop from a B-29 at 8:30 a.m.

The bomb lit the daylight sky with a flash more brilliant than any of its four immediate predecessors and its rumble was the longest and loudest yet heard by observers in the vicinity of the site. However, it was not heard so loudly in Las Vegas, and the AEC said atmospheric and weather conditions made the explosion felt more strongly east and northeast.

Observers on Mt. Charleston, 45 miles south of the test site and at an elevation of 10,000 feet, saw a brilliant, fiery-red fireball which lasted five or six seconds before the traditional mushroom-shaped cloud shot out of the flaming mass into the sky, boiling furiously up to 35,000 feet.

Six and one-half minutes after the burst, a low rumble like faraway thunder was heard in Las Vegas, but only slight shock waves were felt and there were only scattered reports of minor damage.

Mrs. Fora Mitchell, telephone operator at Caliente, 90 air miles northeast of the proving ground, said the AEC called her shortly before 8 a.m. and told her to warn the townspeople that an atomic explosion within 15 or 20 minutes would shake the town. A similar warning went to Goldfield, 100 miles north of the test site.

Mrs. Mitchell said she called police officers and every person she could in the short time and "told them to stay away from window panes."

However, the blast did not cause any damage in the town and although the flash was seen and the noise was audible, there was very little shaking, Mrs. Mitchell told reporters.

The detonation was clearly felt in most southern Utah towns in addition to the reports from Caliente and Goldfield. At Cedar City, Mrs. Gertrude Barton said that the A-bomb rattling of houses is distinctly different from that of the wind. She heard a nuclear detonation Monday for the first time.

A special investigator for the Union Pacific Railroad, A. W. Woody, heard the blast for the first time in Cedar City yesterday. He said it was like someone pushing in on a door and then releasing it suddenly.

At Parowan, north of Cedar City, the rattle was audible. It came in three blasts, according to reports. The last was less audible. than the first and second, with the second giving a definite shake to the houses which made doors and windows rattle.

Monday's A-bomb blast was recorded also in Richfield, Utah and there it was believed stronger than any blast of the present series. Observers there said it was felt and heard more distinct than any in the past. Richfield is about 350 airline miles from the testing ground.

Workers at the Telluride Power Co. operations reported they "heard the blast inside the building as a rumble." Large plate glass windows in business houses on Main St. shook and rattled for several seconds.

A similar story was told by residents of Beaver, Utah where the houses there shook for the first time on Monday. The vibrations were felt repeatedly in houses at Beaver but the noise was much less audible than those noticed last January and February when first blasts took place.

Ellis Larson, cattleman of Washington County, Utah, said that Monday's blast didn't last as long as the others heard in that area but the rumbling seemed louder.

RESTRICTED UNCLASSIFIED

Las Vegas Morning Journal, November 6, 1951

AEC Concludes 'King-Size' Blasts; Next to be Smaller

★ ★ ★ ★ ★ ★ ★ ★ ★ ★ ★ ★ ★ ★ ★

New Experiments Will Not be Heard in Vegas

Atomic energy commission developmental tests were concluded with yesterday morning's nuclear blast and southern Nevada residents will have at least a week before the second phase of the current test series will start.

At the same time qualified observers report that an army unit under command of a brigadier general will continue to staff Camp Desert Rock at the outskirts of the AEC's test site.

The next phase of the operations will "deal primarily with weapons effects data," Carroll L. Tyler, AEC test manager, reported in announcing conclusion of the developmental series. When the weapons effects tests are conducted, Las Vegans probably will not see or feel atomic blasts used during the studies.

It was indicated the civilian defense officials also will be interested in the weapons effects tests.

"The test organization which conducted the first phase will also conduct the second phase," Tyler said.

"This organization is a composite of technical, supply and administrative units which draws its personnel largely from the commission's Santa Fe operations office, the Los Alamos scientific laboratory, the San Dia laboratory at Albuquerque, New Mexico, and the armed forces." Tyler said.

"It is supported by units and individuals from the armed forces, AEC national laboratories, industrial and research organization's and from other governmental agencies," Tyler continued.

"The job of permanentizing the site is continuing," he said, "considerable construction still remains to be done at Camp Mercury. Other construction is continuing in the technical areas."

The radiological safety unit of the test organization issued the following summary yesterday afternoon from reports from air and ground patrols following the fifth atomic blast in the current series; "The main cloud traveling in a south east direction passed west of Las Vegas at an altitude of about 40,000 feet. A small piece of the cloud passed over Las Vegas. An intermediate altitude cloud traveled directly south from Nevada test site and a low altitude cloud passed south, southwest. Both were dispersed rapidly."

"Measureable radiation above normal background level has been detected by very sensitive instruments along the ground path of the intermediate altitude cloud only. The amounts measured are of no significance and are far below levels considered harmful in any way to humans, animals, crops or water supply."

RESTRICTED UNCLASSIFIED

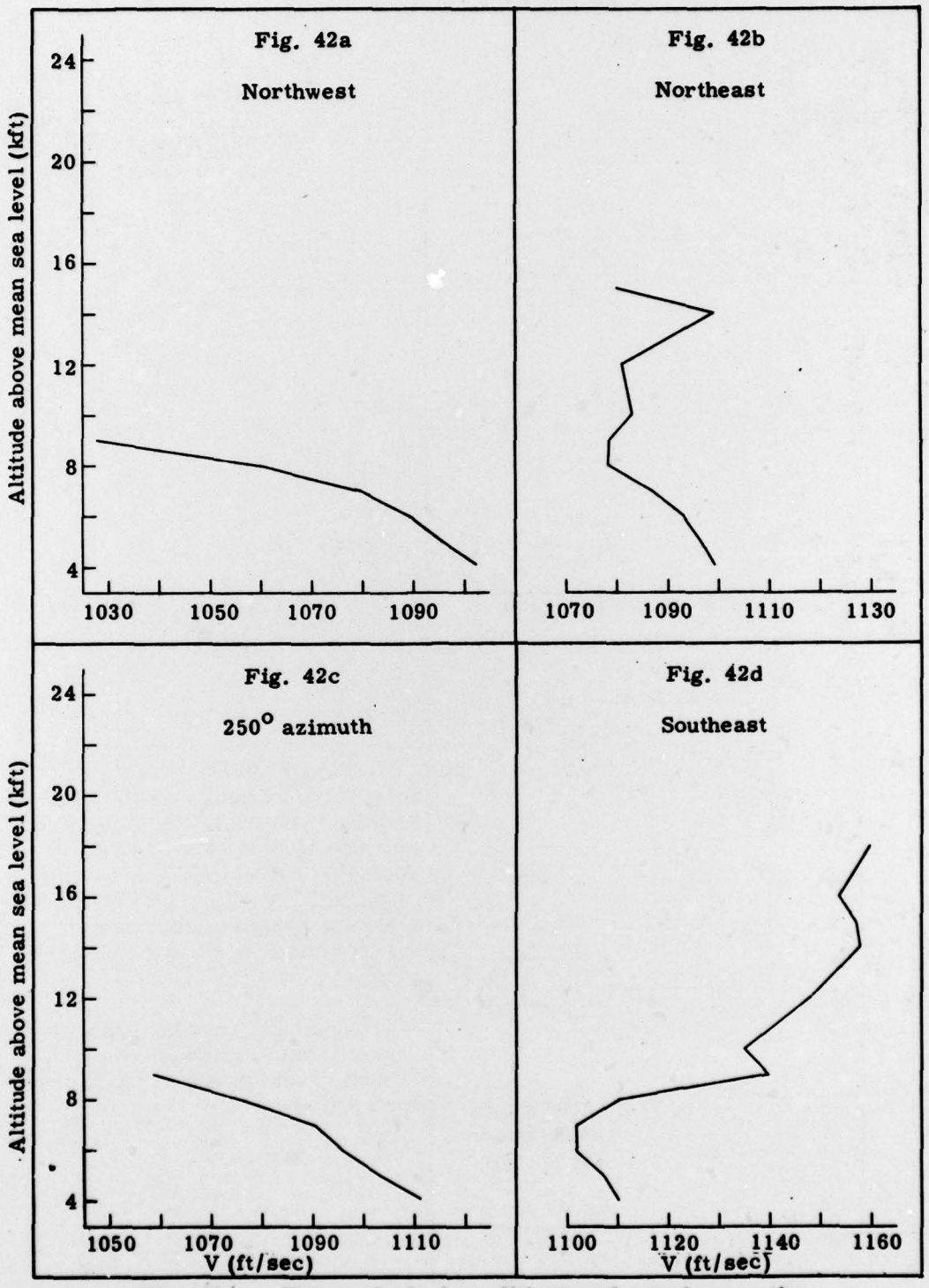


Fig. 42. -- Meteorological conditions and sound ray paths, November 13, 1951, at 0800 PST

TNT SHOT

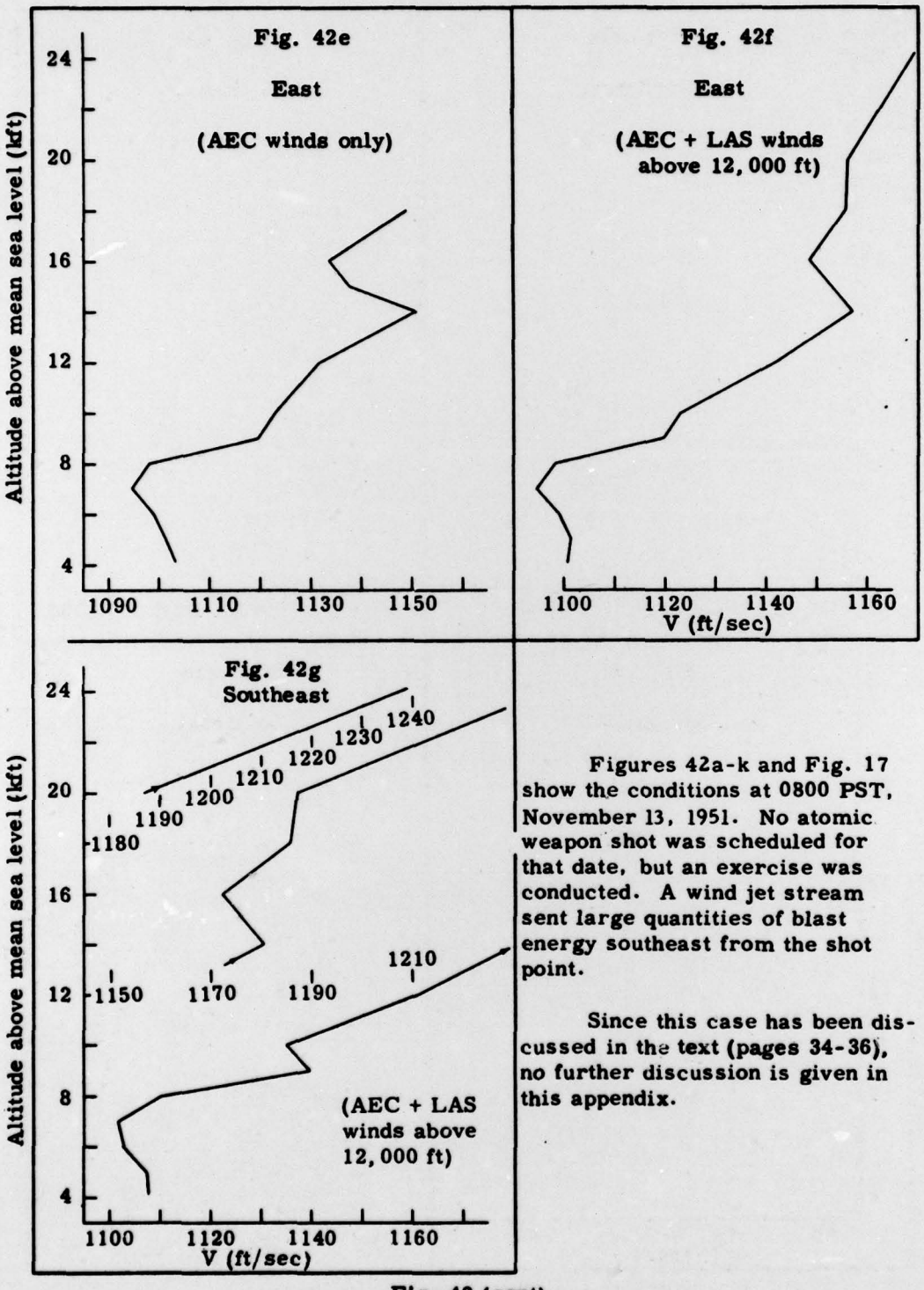


Fig. 42 (cont)

Figures 42a-k and Fig. 17 show the conditions at 0800 PST, November 13, 1951. No atomic weapon shot was scheduled for that date, but an exercise was conducted. A wind jet stream sent large quantities of blast energy southeast from the shot point.

Since this case has been discussed in the text (pages 34-36), no further discussion is given in this appendix.

TNT SHOT

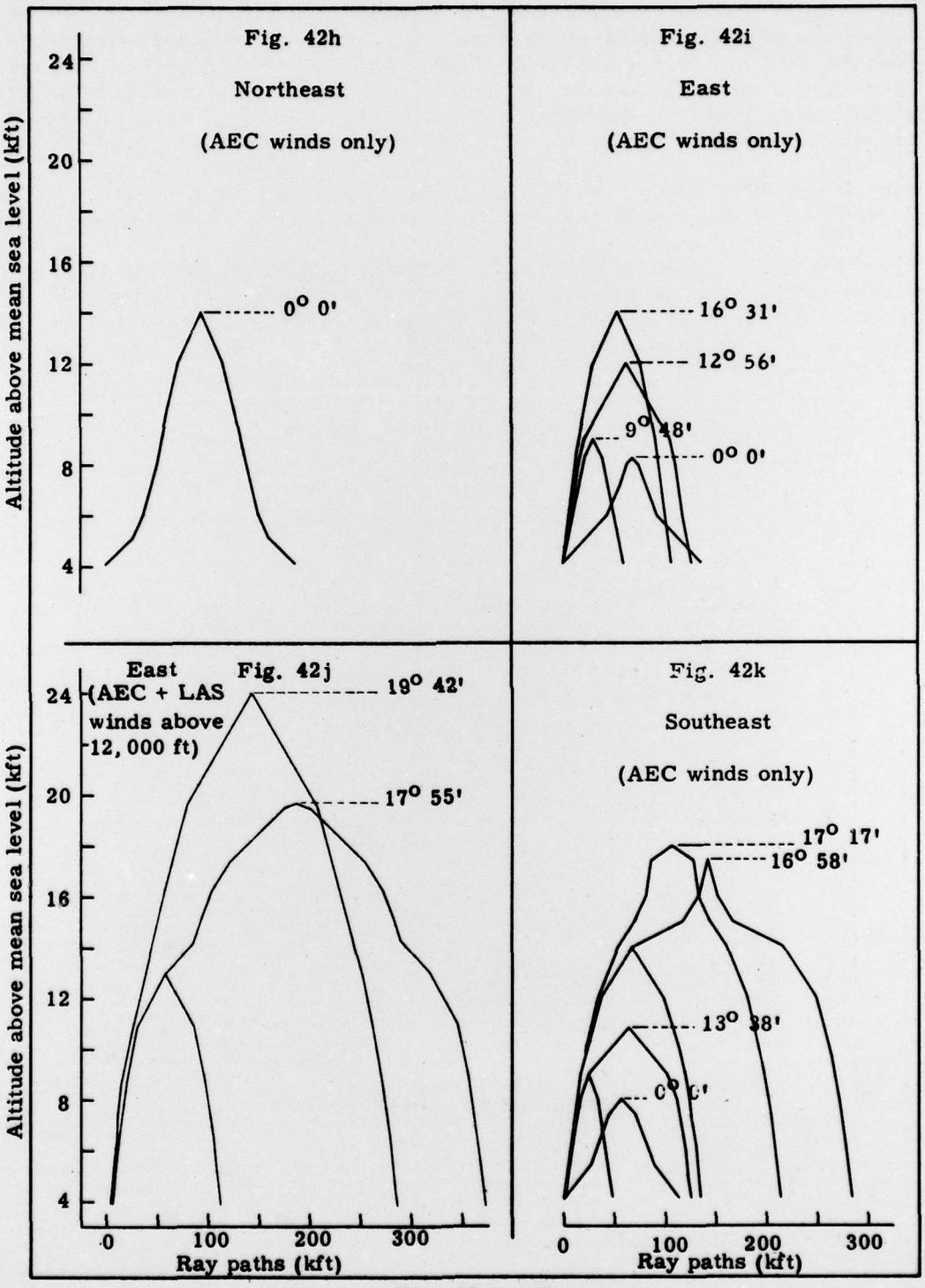


Fig. 42 (cont)

FIRST JANGLE SHOT

For all directions except northeast, the situation for firing the first shot of Operation Jangle was quite excellent, as can be seen from Figs. 43a-d and 43g. Although the meteorological data in Fig. 43d, obtained from an RAOB sounding at 0930 PST, shows that no troposphere signal would travel to the southeast, yet a small signal (2.1 microbars) was recorded at Indian Springs from the advance shot at 0800 PST and from the nuclear shot (43 microbars) at 0900 PST.

The largest troposphere signal recorded from the advance shot was at Caliente, 17.2 microbars, so it was believed that no damage would result from the nuclear shot to follow.

From the advance shot, St. George recorded an ozonosphere signal of 42 microbars, and from the nuclear shot, an ozonosphere signal of 154 microbars. All signal strengths from this shot are shown in Fig. 21f. The noise heard at the Control Point on the occasion of this shot, 13.6 miles away, was just barely audible. That such would be the case is evident from Figs. 43c and d.

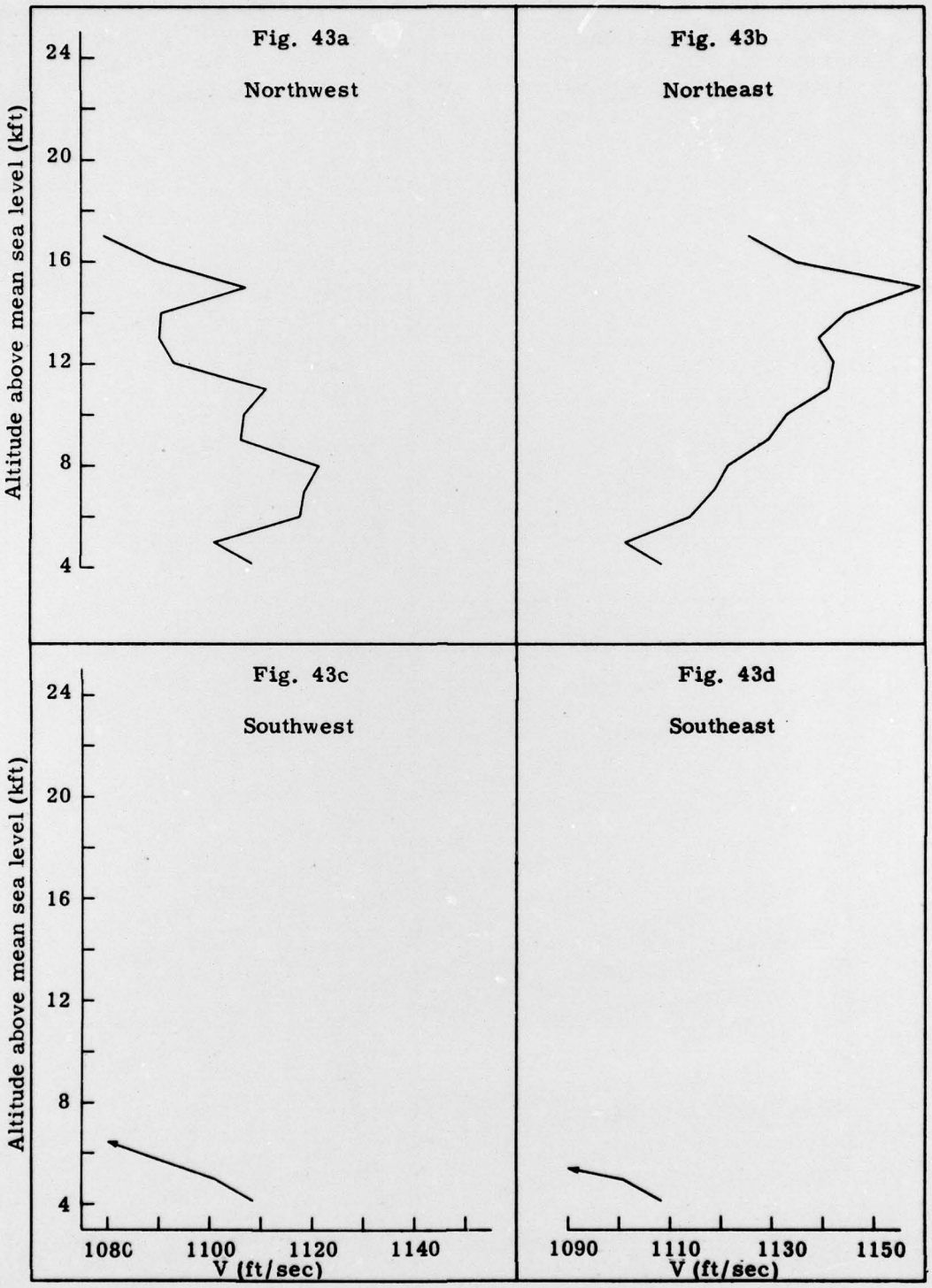


Fig. 43. -- Meteorological conditions and sound ray paths, November 19, 1951, at 0930 PST

FIRST JANGLE SHOT

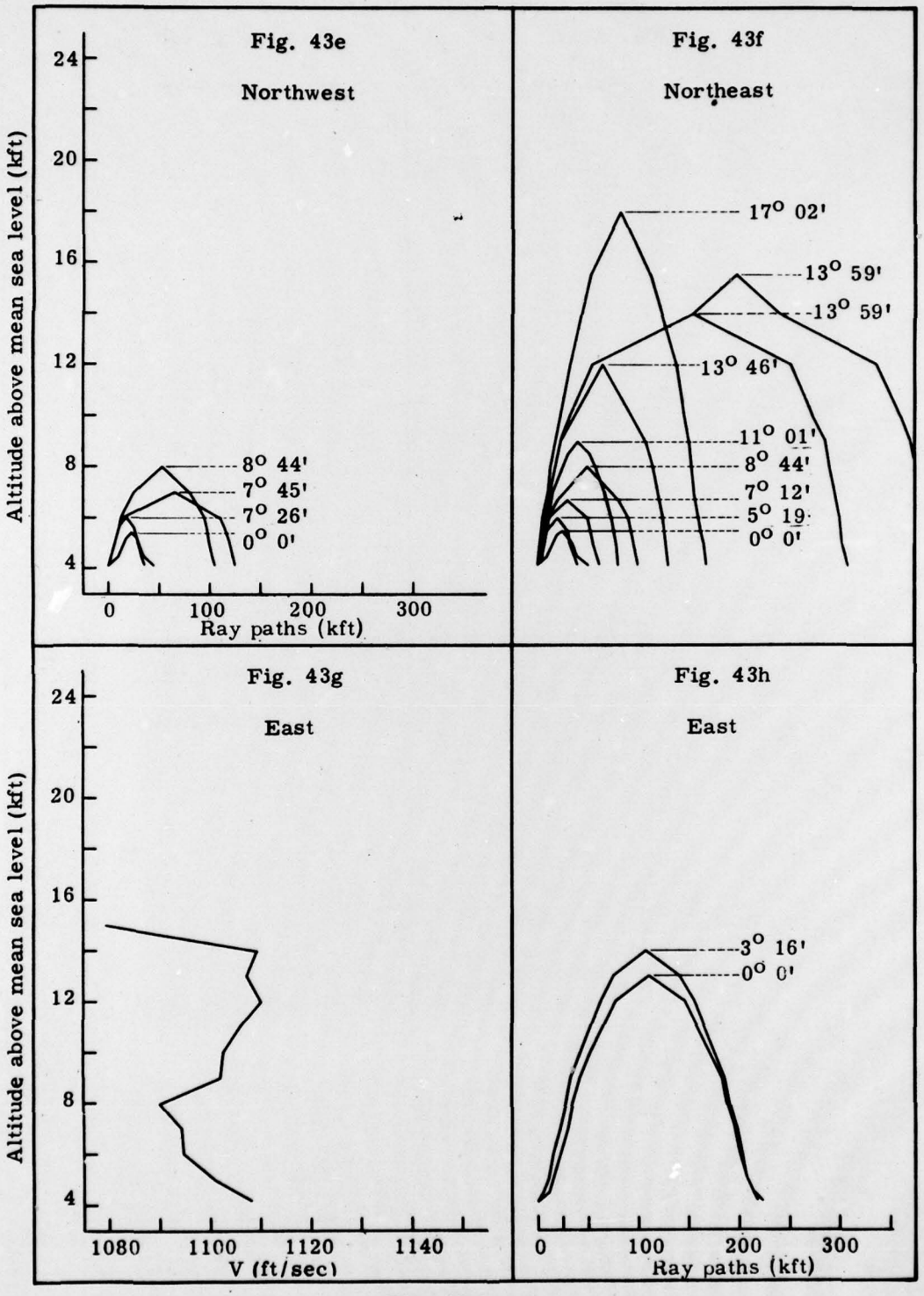
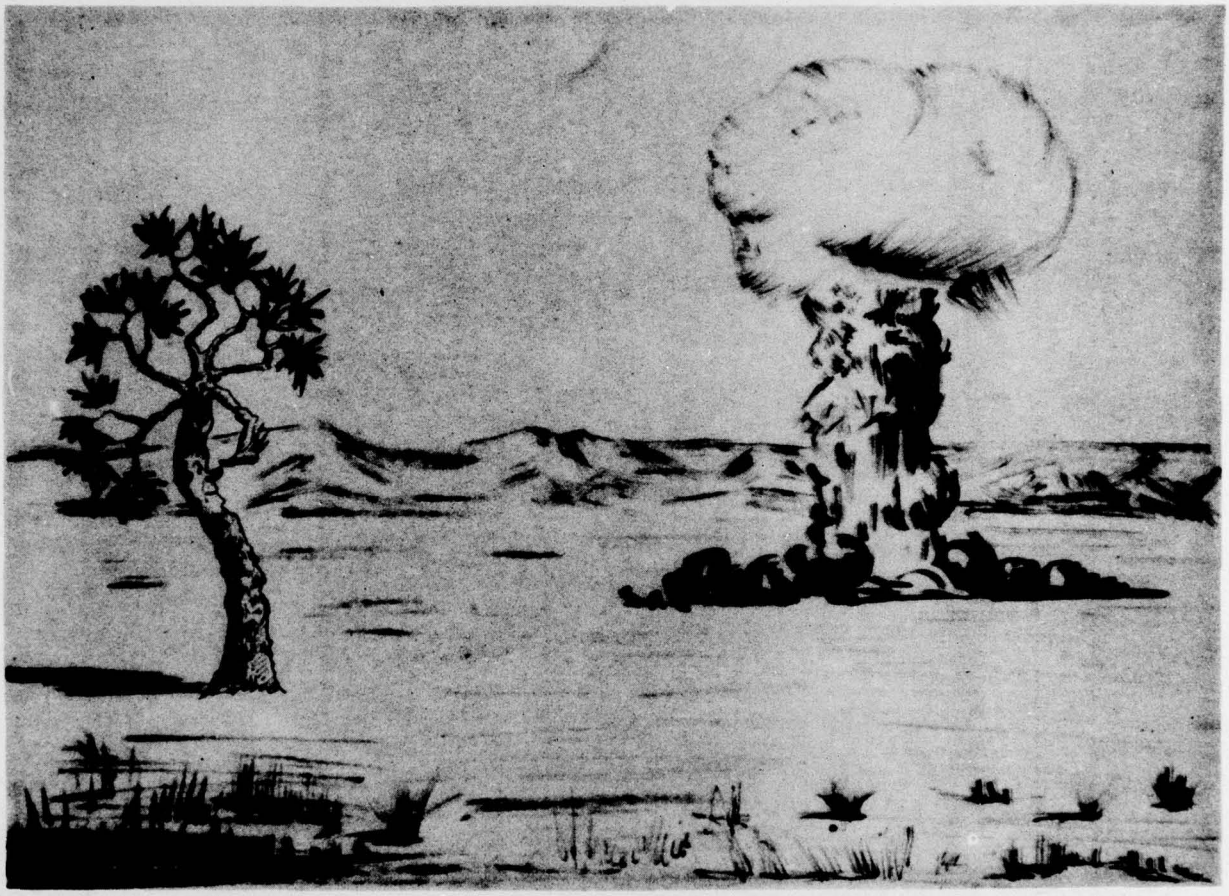


Fig. 43 (cont)

SECOND JANGLE SHOT



SECOND JANGLE SHOT

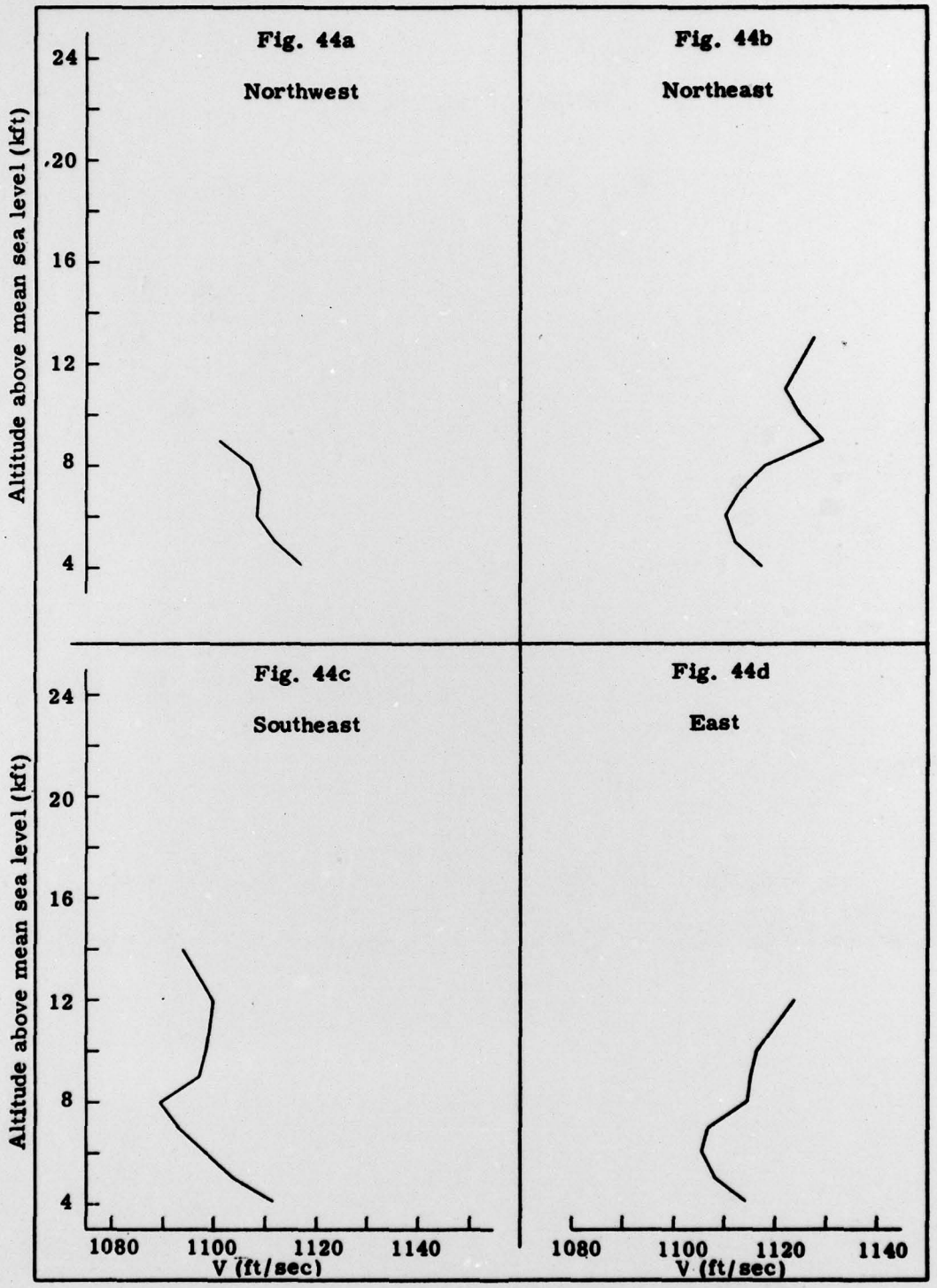


Fig. 44. -- Meteorological conditions and sound ray paths, November 29, 1951, at 1245 PST

SECOND JANGLE SHOT

Although Fig. 44C, drawn from meteorological data taken from a RAOB at 1245 PST on November 29, 1951, shows that no sound should be propagated southeast via a troposphere route, yet the advance shot fired at 1000 PST and the nuclear shot fired at noon both gave troposphere signals southeast from the shot point. It is obvious that meteorological conditions had changed somewhat between shot times and RAOB soundings. Only a trivial boom was heard at the Control Point.

Of most interest on this date were the ozonosphere signals which were quite strong at Henderson, Boulder City, and St. George. All signal strengths are shown in Fig. 21g.

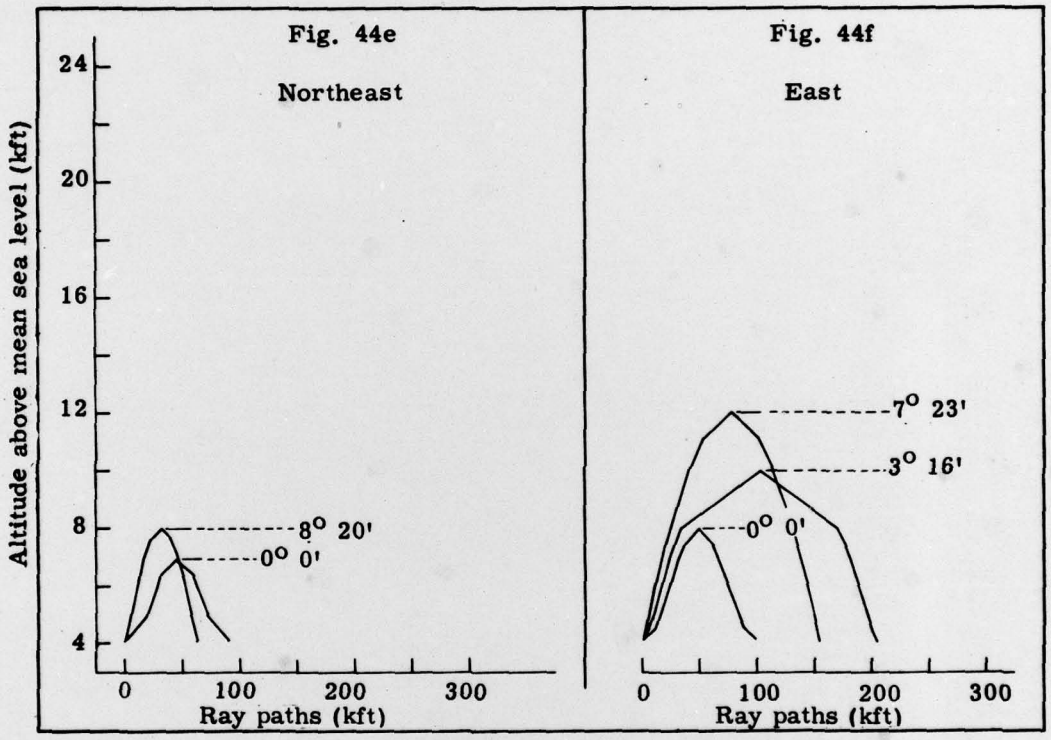


Fig. 44 (cont)

INITIAL DISTRIBUTION

1-21/270A	LASL Document Room
22-221/270A	Technical Library Branch, AFSWP Washington, Attn: Lt. Col. J. H. Veyette
222-226/270A	DMA/AEC, Washington, Attn: Paul Fine
227-228/270A	Special Weapons Command, Kirtland, Attn: Lt. Col. E. H. Karstens
229-230/270A	AFSWP Test Command, Kirtland
231/270A	C. L. Tyler, SFOO
232/270A	D. F. Worth, Jr., AEC Sandia
233/270A	M. J. Kelly, BTL
234/270A	D. A. Quarles, 1
235/270A	W. A. MacNair, 5000
236/270A	R. P. Petersen, 5100
237/270A	G. A. Fowler, 5200
238-239/270A	G. B. Olmsted
240/270A	A. B. Focke, NEL
241/270A	J. A. Peoples, USAF Cambridge Field Station
242/270A	J. W. Smith, ONR
243/270A	Walker Bleakney, Princeton University
244/270A	J. von Neumann, Princeton IAS
245/270A	R. F. Bacher, CIT
246/270A	C. W. Lampson, BRL
247/270A	G. K. Hartmann, NOL
248/270A	H. E. Lenander, 5230
249/270A	G. T. Pelsor, 5121
250/270A	E. B. Doll, SRI
251/270A	M. L. Merritt, 5112
252-253/270A	E. F. Cox, 5110
254/270A	H. J. Plagge, 5242-3
255/270A	J. W. Reed, 5242-3
256-270/270A	Sandia Corporation Document Room